FINAL REPORT

DEVELOPMENT OF A SMEAR PROOF HORIZONTAL AND VERTICAL PERMEABILITY PROBE
(Vertical and Horizontal In Situ Permeameter)
V.A.H.I.P.

FDOT Contract No. BDK75 977-35
UF Contract No. 00088338

Submitted by:

Raphael W. Crowley, Ph.D., P.E.
David Bloomquist, Ph.D., P.E.
Michael Rodgers, E.I.

Department of Civil and Coastal Engineering
University of Florida
Gainesville, Florida 32611

Developed for the

David Horhota, Ph.D., P.E., Project Manager

January 2013

DISCLAIMER

The opinions, findings, and conclusions expressed in this publication are those of the authors and not necessarily those of the State of Florida Department of Transportation.

SI (MODERN METRIC) CONVERSION FACTORS (from FHWA)

APPROXIMATE CONVERSIONS TO SI UNITS

SYMBOL	WHEN YOU KNOW	MULTIPLY BY	TO FIND	SYMBOL
LENGTH				
in	inches	25.4	millimeters	mm
ft	feet	0.305	meters	m
yd	yards	0.914	meters	m
mi	miles	1.61	kilometers	km
SYMBOL	**WHEN YOU KNOW**	**MULTIPLY BY**	**TO FIND**	**SYMBOL**
AREA				
in^2	square inches	645.2	square millimeters	mm^2
ft^2	square feet	0.093	square meters	m^2
yd^2	square yard	0.836	square meters	m^2
ac	acres	0.405	hectares	ha
mi^2	square miles	2.59	square kilometers	km^2
SYMBOL	**WHEN YOU KNOW**	**MULTIPLY BY**	**TO FIND**	**SYMBOL**
VOLUME				
fl oz	fluid ounces	29.57	milliliters	mL
gal	gallons	3.785	liters	L
ft^3	cubic feet	0.028	cubic meters	m^3
yd^3	cubic yards	0.765	cubic meters	m^3
NOTE: volumes greater than 1000 L shall be shown in m^3				
SYMBOL	**WHEN YOU KNOW**	**MULTIPLY BY**	**TO FIND**	**SYMBOL**
MASS				
oz	ounces	28.35	grams	g
lb	pounds	0.454	kilograms	kg
T	short tons (2000 lb)	0.907	megagrams (or "metric ton")	Mg (or "t")
SYMBOL	**WHEN YOU KNOW**	**MULTIPLY BY**	**TO FIND**	**SYMBOL**
TEMPERATURE (exact degrees)				
^oF	Fahrenheit	5 (F-32)/9 or (F-32)/1.8	Celsius	^oC
SYMBOL	**WHEN YOU KNOW**	**MULTIPLY BY**	**TO FIND**	**SYMBOL**
ILLUMINATION				
fc	foot-candles	10.76	lux	lx
fl	foot-Lamberts	3.426	$candela/m^2$	cd/m^2
SYMBOL	**WHEN YOU KNOW**	**MULTIPLY BY**	**TO FIND**	**SYMBOL**
FORCE and PRESSURE or STRESS				
lbf	pound force	4.45	newtons	N
lbf/in^2	pound force per square inch	6.89	kilopascals	kPa

APPROXIMATE CONVERSIONS TO ENGLISH UNITS

SYMBOL	WHEN YOU KNOW	MULTIPLY BY	TO FIND	SYMBOL
LENGTH				
mm	millimeters	0.039	inches	in
m	meters	3.28	feet	ft
m	meters	1.09	yards	yd
km	kilometers	0.621	miles	mi
SYMBOL	**WHEN YOU KNOW**	**MULTIPLY BY**	**TO FIND**	**SYMBOL**
AREA				
mm^2	square millimeters	0.0016	square inches	in^2
m^2	square meters	10.764	square feet	ft^2
m^2	square meters	1.195	square yards	yd^2
ha	hectares	2.47	acres	ac
km^2	square kilometers	0.386	square miles	mi^2
SYMBOL	**WHEN YOU KNOW**	**MULTIPLY BY**	**TO FIND**	**SYMBOL**
VOLUME				
mL	milliliters	0.034	fluid ounces	fl oz
L	liters	0.264	gallons	gal
m^3	cubic meters	35.314	cubic feet	ft^3
m^3	cubic meters	1.307	cubic yards	yd^3
SYMBOL	**WHEN YOU KNOW**	**MULTIPLY BY**	**TO FIND**	**SYMBOL**
MASS				
g	grams	0.035	ounces	oz
kg	kilograms	2.202	pounds	lb
Mg (or "t")	megagrams (or "metric ton")	1.103	short tons (2000 lb)	T
SYMBOL	**WHEN YOU KNOW**	**MULTIPLY BY**	**TO FIND**	**SYMBOL**
TEMPERATURE (exact degrees)				
^oC	Celsius	1.8C+32	Fahrenheit	^oF
SYMBOL	**WHEN YOU KNOW**	**MULTIPLY BY**	**TO FIND**	**SYMBOL**
ILLUMINATION				
lx	lux	0.0929	foot-candles	fc
cd/m^2	$candela/m^2$	0.2919	foot-Lamberts	fl
SYMBOL	**WHEN YOU KNOW**	**MULTIPLY BY**	**TO FIND**	**SYMBOL**
FORCE and PRESSURE or STRESS				
N	newtons	0.225	pound force	lbf
kPa	kilopascals	0.145	pound force per square inch	lbf/in^2

*SI is the symbol for the International System of Units. Appropriate rounding should be made to comply with Section 4 of ASTM E380.(Revised March 2003)

TECHNICAL REPORT DOCUMENTATION PAGE

<table>
<tr><td>1. Report No.</td><td>2. Government Accession No.</td><td colspan="2">3. Recipient's Catalog No.</td></tr>
<tr><td colspan="2" rowspan="2">4. Title and Subtitle
DEVELOPMENT OF A SMEAR PROOF HORIZONTAL AND VERTICAL PERMEABILITY PROBE
(Vertical and Horizontal In Situ Permeameter)
V.A.H.I.P.</td><td colspan="2">5. Report Date
January 2013</td></tr>
<tr><td colspan="2">6. Performing Organization
University of Florida</td></tr>
<tr><td colspan="2">7. Author(s)
Raphael Crowley, Dave Bloomquist, Mike Rodgers</td><td colspan="2">8. Performing Organization Report No.
00088338</td></tr>
<tr><td colspan="2" rowspan="2">9. Performing Organization Name and Address
Department of Civil and Coastal Engineering
365 Weil Hall
University of Florida
Gainesville, Florida 32611</td><td colspan="2">10. Work Unit No.</td></tr>
<tr><td colspan="2">11. Contract or Grant No.
BDK75 977-35</td></tr>
<tr><td colspan="2" rowspan="2">12. Sponsoring Agency Name and Address
Florida Department of Transportation
605 Suwannee Street, MS 30
Tallahassee, FL 32399</td><td colspan="2">13. Type of Report and Period Covered
Draft Report
09/01/10 – 11/30/2012</td></tr>
<tr><td colspan="2">14. Sponsoring Agency Code</td></tr>
<tr><td colspan="4">15. Supplementary Notes</td></tr>
<tr><td colspan="4">16. Abstract
Under a previous FDOT sponsored project (BD545-15), the PI developed a probe (the VAHIP) to measure both horizontal and vertical permeabilities. The VAHIP worked well in the field trials except that if it penetrated a weak clay layer, the soil would smear its side screens. Then, if the probe was pushed into sand, its water flow rate would not be measured accurately because of the smeared clay. This research was aimed at designing a probe where smearing was minimized. Field and laboratory tests were conducted with the instrument. Results appeared to indicate that smearing was reduced. A smaller probe (the VIP) was designed and built because there was some question as to whether or not the VAHIP would truly give different horizontal and vertical permeability values. Some believed that water would flow through the path of least resistance regardless of the fluid’s original orientation. Analysis of Hvorslev’s equations indicated that it was unclear how one would use horizontal flow rate to estimate orientation-dependent permeability. Field testing with the VIP indicated that it needs to be modified if it is to be deployed regularly in the field. Specifically, a “locking” mechanism must be added to the instrument similar to the mechanism currently used with the VAHIP. Or testing procedures should be modified so that predrilling a borehole is no longer allowable.</td></tr>
<tr><td colspan="2">17. Key Word
Permeability, field testing, geotechnical probe</td><td colspan="2">18. Distribution Statement
No restrictions.</td></tr>
<tr><td>19. Security Classif. (of this report):
Unclassified</td><td>20. Security Classif. (of this page):
Unclassified</td><td>21. No. of Pages
179</td><td>22. Price</td></tr>
</table>

EXECUTIVE SUMMARY

Hydraulic conductivity (permeability) in soils is one of the most important parameters that controls the performance of several civil engineering structures and facilities (reservoirs, retention ponds, consolidation, seepage, etc.); however, it is also one of the most difficult to measure. Spatial variability usually associated with geological formations of soils, orientation of soil particles, and discontinuities all contribute to a soil's anisotropy, which makes it difficult to relate an individual test result to the actual field conditions.

In situ methods for determining a soil's permeability (versus laboratory tests) appear to be the best solution from a technical standpoint. However, current methodologies available for such field tests are both time consuming and expensive. Research in this report focuses on fabricating a simple, inexpensive (from test-to-test) device to measure both vertical and horizontal permeability at various depths within a soil deposit (a feature not possible with conventional methods; Bloomquist, 2007).

Under a previous FDOT sponsored project, the PI developed a probe (the VAHIP) that measures both horizontal and vertical water flow rates. The VAHIP worked well in the field trials except that if it penetrated a weak clay layer, the soil would smear the probe's side screens. Then, if the probe was pushed into a sand layer, its flow rate would not be measured accurately. The goal of this research was to improve upon the previous design.

A new probe was developed to be "smear-proof." Laboratory and field testing results appeared to indicate a reduction in "smearing." However, it remained unclear whether or not differing "vertical" and "horizontal" permeabilities could be measured with the device or if during a field test water followed the path of least resistance and a

scalar “permeability number” was all that data indicated. Analysis was conducted to explore this question, and results were inconclusive. Future testing may reveal that the vertical probe components alone may be sufficient to compute field permeability.

A smaller, vertical-only probe was also tested. This device did not remain closed properly when pushed to depth. As a result, sand penetrated its tip and prevented it from opening. A slight modification with a locking mechanism and/or a slight modification to the testing procedure would probably be sufficient to allow the device to function properly. However, before mass production of either device begins, investigators strongly recommend conducting research to determine if flow from the VAHIP is truly both vertical and horizontal or if a vertical probe alone will be sufficient.

TABLE OF CONTENTS

LIST OF TABLES

LIST OF FIGURES

CHAPTER 1
INTRODUCTION

Permeability is defined as the ability to transmit fluid through a network of void spaces contained within a material or porous medium. Permeability is typically referred to as hydraulic conductivity when water is used as the fluid transmitted through a network of voids. Many engineering designs are heavily influenced by the degree of hydraulic conductivity associated with surrounding soils and strata.

The measure of hydraulic conductivity is essential for projects involving earthen dams, retention ponds, dewatering systems, hydraulic structures, wells, landfills, and many other engineered facilities. Retention ponds are particularly of interest because in these basins, water exits in two stages: an initial stage which is due to vertical infiltration; followed by a second stage consisting of predominately horizontal flow. The accuracy of determining hydraulic conductivity is critical and plays a pivotal role in determining the economy and effectiveness of the resulting design.

1.1 Background

Hydraulic conductivity values generally vary throughout soil formations, making a generalized characterization of the overall permeability difficult to quantify. Due to the nature of these stratified sedimentary soils, they usually have anisotropic properties even when homogenous. In other words, the properties of most soils differ with the direction of measurement. The vertical component of the saturated hydraulic conductivity is usually lower than the horizontal component by one or more orders of magnitude.

Often, the method used in measuring hydraulic conductivity directly affects measured results. In general, there are two techniques used in the measurement of hydraulic conductivity: laboratory and field tests. Each method has its strengths and weaknesses as outlined in Table 1-1. To summarize, field data provide a better

representation of actual in situ conditions when compared to laboratory methods. Lab testing is used when actual representation of field conditions is not of fundamental importance in design. Field testing is usually more costly than lab testing.

The Florida Department of Transportation (FDOT) conducts on-site permeability testing for a variety of projects and sites. Field testing using conventional methods has proven expensive and time consuming. A simple and fast-paced field method for assessing in situ permeability could save time and money.

The VAHIP (Vertical and Horizontal In Situ Permeameter) was built by the University of Florida through a previous FDOT funded research project (Project No. BD-545, RPWO #15) to measure horizontal and vertical in situ permeability. However, during field testing, the probe was found to have several weaknesses, and modifications to the original design were required.

Table 1-1. Advantages and disadvantages of laboratory and in situ testing techniques*

Laboratory Methods		In situ Methods	
Advantages	Disadvantages	Advantages	Disadvantages
Results are relatively easy to reproduce	Highly disturbed samples	Avoid disturbance effects	Larger variation in results
Variety of test can be performed on same sample	Sample may not be representative of actual in situ	Provide a profile of permeability with depth	Difficult to reproduce results
Some in situ properties can be modeled	Test conditions may not be representative of actual site conditions	Larger test area thus more representative.	Unknown influences can exist (i.e., cavities) and contribute to results.

*The table is for the general case. Specific tests may have different qualities.

1.2 Scope

The objective of this research was to modify the previous probe to make it "smear-proof," because testing with the previous device showed that when pushed through a clay layer, the previous probe's side screens often "smeared" with clay. The goal of the redesign required the device to still be easy to use and durable under rugged field testing conditions. Also, results obtained from field testing needed to be verified and must be consistent with values obtained using other methods.

The direct push technique used in the previous method would again be used for the new model. This technique was chosen because it reduces time, increases safety, allows for multiple permeability results for different depths, and integrates well with other data obtained from the similar processes (i.e., traditional soil borings). FDOT already uses standard penetration test (SPT)/cone penetration test (CPT) rigs in most of its subsurface analyses. The new probe was to be designed to work with these existing rigs so that permeability data could supplement test results from SPT borings and/or CPT data.

Originally, researchers developed a control panel that measured flow rates that accompanied the probe. However, the control panel was too large and inconvenient to be transported in the field. Hence, a new, simpler system for recording data was created. A computer analysis program was developed to analyze results.

CHAPTER 2
LITERATURE REVIEW

The permeability coefficient, *k*, is defined as the discharge velocity of a fluid through a unit area driven by a unit hydraulic gradient within the material. Relevant literature about measuring in situ permeability was reviewed by Bloomquist (2007); a summary is provided in this chapter.

2.1 Hydraulic Conductivity

As discussed, hydraulic conductivity is a property of the soil or rock that describes the ease with which water flows through its pore spaces. For design, the desired soil permeability is a function of the project's objectives. In a landfill, permeability of the liner should be low so that contaminants are restrained from entering the ground water supply. In a retention pond, the opposite is true; high soil permeability is desired so that the storage areas do not fail due to overloading.

In general, water flowing through a saturated soil mass experiences a resistance to its flow as a result of the presence of solid soil matter in accordance with the laws of fluid mechanics. Darcy (1856) derived an empirical formula for the behavior of flow through saturated soils under steady state conditions. He concluded that the quantity of water per second (*q*) flowing through a cross-sectional area (*A)* of soil normal to the direction of flow under hydraulic gradient (*i)* can be expressed by the formula,

$$q = kiA \tag{2-1}$$

where: *k* is termed the hydraulic conductivity of the soil. The hydraulic conductivity of soils depends largely on the following parameters:

- Size and continuity of the pore spaces through which the fluid flows
- Particle-size distribution, particle shape and texture
- Discontinuities within the soil mass

- Degree of saturation
- Viscosity of water.

Darcy's law is limited to the laminar flow regime and begins to break down in materials such as clean gravel and open graded rock fills where turbulent flow occurs (Das, 2004). Reynolds (1883) found from experiments on flow in pipes that flow remains laminar as long as the velocity of flow is less than a critical velocity. Fancher et al. (1933) demonstrated the validity of Darcy's law for soils with respect to particle size, velocity of flow and hydraulic gradient. They observed that Darcy's law was valid as long as the Reynolds number expressed in the form of the equation below is equal to or less than unity.

$$\frac{vD_a\gamma_w}{\eta g} \leq 1 \qquad (2\text{-}2)$$

where:

- v = velocity of flow (cm/s)
- Da = diameter of the average particle, assumed spherical (cm)
- γ_w = unit weight of water (g/cm^3)
- η = viscosity of water (g/s/cm^2)
- g = acceleration due to gravity (cm/s^2).

Equation 2-2 was observed to suffice well for sands, silts and clays; however, Scheidegger (1960) showed that this critical Reynolds number may vary from 0.1 to 75 (Shroff and Shah, 2003).

2.1.1 Hydraulic Conductivity in Sands

Sands are naturally occurring sedimentary materials ranging in size from 0.06 mm to 2.0 mm. As a result of their granular nature and high porosity, sands have a high permeability and consequently high hydraulic conductivity. Generally sands drain relatively quickly and are employed in situations where quick drainage is required (i.e.,

retention ponds). Well-graded sands are generally more stable but less permeable than those which are poorly graded (Lambe and Whitman, 1969).

In general, the smaller the particle size the less permeable the soil media. Values of hydraulic conductivity measured for sands typically range from 10^{-1} cm/sec to 10^{-3} cm/sec for coarse to fine sands; and 10^{-3} cm/sec to 10^{-5} cm/sec for fine to silty sands. As the sand particles approach the size of silt particles, the sand will exhibit properties of silt, including silt-like permeability (Lambe and Whitman, 1969).

2.1.2 Hydraulic Conductivity in Clays

Clays may be defined as soil particles that develop plasticity with the addition of water (Grim, 1953). On the basis of size and shape, clay is typically a fine flake-shaped particle with diameters less than 0.002mm. In general, clays have a higher affinity for water than sands and silt due to unbalanced surface charges of the clay particle and/or hydrogen bonding (Das, 2002). As a result of their particle size, structure, cohesiveness, and presence of hydroxides clays have a low hydraulic conductivity. It is common for clays even with high porosity to generally have low hydraulic conductivities. In other words, clays can hold a large volume of water per unit bulk material, but they may not release water easily. The hydraulic conductivity of clays is important in the analysis of consolidation settlement of clay layers. Clays typically have a hydraulic conductivity on the order of 10^{-7} cm/sec or less.

2.1.3 Typical Range of Hydraulic Conductivity for Various Soils

In general the permeability can be categorized by soil type. Table 2-2 through Table 2-4 shows ranges of permeability and drainage characteristics for various soil types:

Table 2-1. Hydraulic conductivity of some soils (from Casagrande and Fadum, 1939, as cited in Lambe and Whitman, 1969)

k (cm/sec)	Soils type	Drainage conditions
10^{1} to 10^{2}	Clean gravels	Good
10^{1}	Clean sand	Good
10^{-1} to 10^{-4}	Clean sand and gravel mixtures	Good
10^{-5}	Very fine sand	Poor
10^{-6}	Silt	Poor
10^{-7} to 10^{-9}	Clayey soils	Practically impervious

Table 2-2. Classification of soils according to their coefficients of permeability (Terzaghi and Peck, as cited in Lambe and Whitman, 1969)

Degree of Permeability	Value of *k* (cm/sec)
High	Over 10^{-1}
Medium	10^{-1} – 10^{-3}
Low	10^{-3} – 10^{-5}
Very low	10^{-5} – 10^{-7}
Practically impermeable	Less than 10^{-7}

Table 2-3. Ranges of hydraulic conductivities for unconsolidated sediments (from Fetter, 2001 as cited in Murthy, 2003)*

Material	*Intrinsic Permeability (Darcy's)	Hydraulic Conductivity (cm/sec)
Clay	10^{-6} – 10^{-3}	10^{-9} – 10^{-6}
Silt, sandy silts, clayey sands, till	10^{-3} – 10^{-1}	10^{-6} – 10^{-4}
Silty sands, fine sands	10^{-2} – 1	10^{-5} – 10^{-3}
Well-sorted sands, glacial outwash	10^{0} – 10^{1}	10^{-3} – 10^{-1}
Well-sorted gravel	10^{1} – 10^{2}	10^{-2} – 10^{0}

* Portion of hydraulic conductivity which is representative of the properties of the porous medium and is a function of the openings through which the fluid moves.

Table 2-4. Typical values of permeability for sands (Leonards, 1962)

Type of sand (U.S. Army Engineer classification)	Value of $k \times 10^{-4}$ (cm/sec)
Very fine sand	50
Fine sand	200
Fine to medium sand	500
Medium sand	1000
Medium to coarse sand	1500
Gravel and coarse sand	3000

2.2 Vertical and Horizontal Permeability

Natural soil deposits and compacted embankments are almost always stratified to some degree and are rarely isotropic. Soil stratification and discontinuities provide flow channels within the soil matrix which are less resistive to flow. Also, under field conditions, both vertical and horizontal hydraulic gradients exist to induce the flow of water either in the vertical or horizontal direction.

The culminating effect of these factors means that soils usually possess anisotropic permeability, with differing permeability in the vertical and horizontal directions. The natural orientation of particles in soils which have been consolidated vertically, and discontinuities on stratum bedding planes ensures that the average permeability parallel to the planes of stratification is greater than the permeability perpendicular to these planes. The inclusion of thin horizontal layers of coarse-grained soil in a mass of fine-grained soil may increase the horizontal permeability while having little effect on the vertical permeability.

Also, it is possible to increase the drainage rate of a soil layer without changing the permeability of the bulk soil by introducing layer drains (sand wicks) or fracturing the soil. These examples reveal that soil permeability in the horizontal and vertical directions are affected by the sizes and orientation of soil particles and discontinuities.

Thus it can be inferred that the coefficient of permeability in horizontal and vertical directions in soil is not always be the same. Horizontal values are often greater than vertical values.

2.2.1 Mean Coefficient of Permeability

In seepage analysis for most soils, permeability is determined in terms of the average rate of water movement through the soil mass, regardless of direction. To obtain such an isotropic representative value of the coefficient of permeability, it is usually common to transform and express the overall average coefficient of permeability of a soil mass and the degree of anisotropy (respectively) as:

$$k_m = \sqrt{k_v k_h} \quad \text{and} \quad m = \frac{k_h}{k_v} \tag{2-3}$$

where:

- k_m is the mean coefficient of permeability for the soil mass
- k_v is the coefficient of permeability in the vertical direction
- k_h is the coefficient of permeability in the horizontal direction
- m is the degree of anisotropy.

The mathematical basis of this transformation is outlined as follows. Plane flow in an anisotropic material having a horizontal permeability, k_h , and a vertical permeability, k_v , is governed by the equation:

$$k_h \frac{\partial^2 h}{\partial x^2} + k_v \frac{\partial^2 h}{\partial z^2} = 0 \tag{2-4}$$

where h is the hydraulic head, and x, y, and z are standard coordinates. Averaging with respect to x and z such that $x = m\overline{x}$ and $z = \overline{z}$ the seepage equation then becomes:

$$\frac{k_h}{m^2 k_v}\frac{\partial^2 h}{\partial x^2} + \frac{\partial^2 h}{\partial z^2} = 0 \tag{2-5}$$

Substituting $m = \sqrt{\frac{k_h}{k_v}}$ (Equation 2-3), which represents flow in anisotropic medium,

converts Equation 2-5 to a relationship for isotropic conditions given by:

$$\frac{\partial^2 h}{\partial x^2} + \frac{\partial^2 h}{\partial z^2} = 0 \tag{2-6}$$

Considering an element of soil in the x direction, having a length, *l,* and cross-sectional area, *A*, under a hydraulic head, Δh, the flow rate in the untransformed state is given by:

$$q_v = k_v A \frac{\Delta h}{l} \tag{2-7}$$

Substituting the coefficient of permeability into the transformed state equation and solving yields:

$$q_v = k_m A \frac{\Delta h}{l\sqrt{\frac{k_h}{k_v}}} = \sqrt{k_v k_h} A \frac{\Delta h}{l\sqrt{\frac{k_h}{k_v}}} = k_v A \frac{\Delta h}{l} = q_v \tag{2-8}$$

Hence a mean coefficient of permeability defined by $k_m = \sqrt{k_v k_h}$ can then be

introduced under this transformed isotropic condition for seepage analysis.

2.3 Retention Ponds

Retention ponds are used to store storm water run-off and allow it to percolate through the permeable soil layer into the underlying aquifer. It is essential that the soil in the retention pond has the desired permeability properties to allow efficient water flow through the medium. A high permeability and favorable ground water table are preferred.

2.3.1 Infiltration in Retention Ponds

The process by which water exits a retention pond takes place in two stages. In the first stage, only vertical infiltration through the bottom of the pond (unsaturated flow) occurs. In the second, the water migrates horizontally through the side slopes. This fills the voids of the unsaturated soil on the slope above the bottom of the basin.

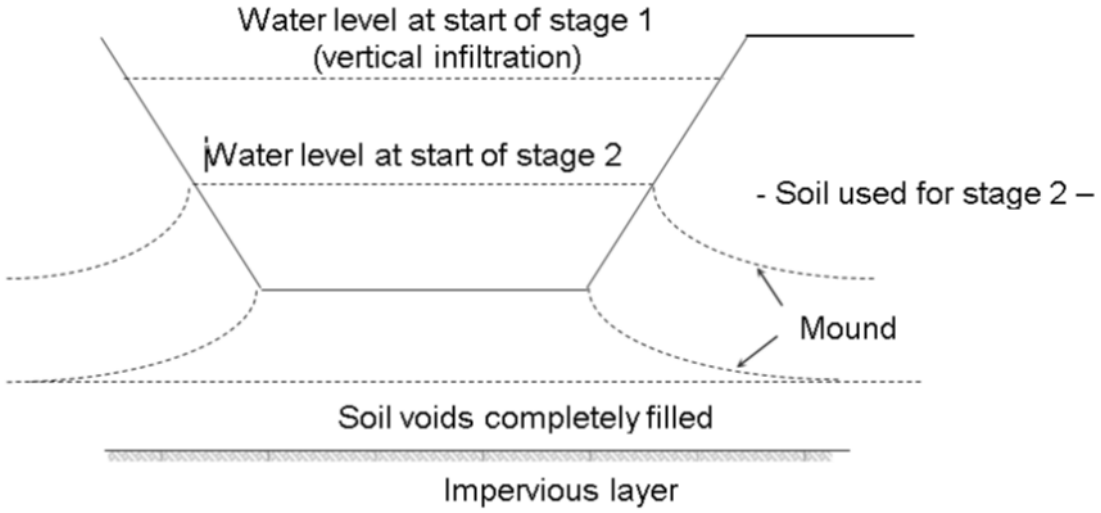

Figure 2-1. Infiltration stages in retention ponds

2.3.2 Vertical Unsaturated Flow Analysis

Vertical unsaturated flow occurs when there is only vertical infiltration. This occurs when either of the following two conditions is satisfied:

1. The volume retained is less than the volume required to saturate the underlying soil at the bottom of a pond.
2. The height of the retained water in a basin is less than the height of water required to saturate the underlying soil at the bottom of the pond.

The volume (V_u) required to saturate the soil below the basin is given by:

$$V_u = A_b \cdot H_b \cdot f \tag{2-9}$$

where:

- A_b = Area of basin bottom
- H_b = Height of basin bottom above the ground water table
- f = Fillable porosity

For unsaturated vertical flow, the recovery time T_{sat} is given by:

$$T_{sat} = \frac{f \cdot H_b}{I_d} \tag{2-10}$$

where I_d is design infiltration rate. According to the modified Green and Ampt infiltration equation:

$$I_d = \frac{k_v}{FS} \tag{2-11}$$

where k_v is the unsaturated vertical hydraulic conductivity and FS is the factor of safety introduced to account for flow losses due to the basin bottom silting or clogging. It is usually given a recommended value of 2.0.

2.3.3 Lateral Saturated Flow

When the volume of storm water retained in a basin is such that it does not percolate through the unsaturated soil beneath the basin, lateral flow occurs when the basin's underlying soil becomes saturated. The rate of lateral flow depends on the horizontal permeability of the soil on the side slopes of the retention pond.

Andreyev and Wiseman (1989) proposed a methodology to calculate the recovery time of a pond under lateral saturated flow using the following dimensionless parameters:

$$F_x = \left[\frac{W^2}{A \cdot H_T \cdot D \cdot \alpha}\right]^{0.33} \tag{2-12}$$

$$F_y = \frac{h_0}{H_T} \tag{2-13}$$

where:

- F_x = Dimensionless parameter representing the physical and hydraulic characteristics of the retention basin and effective aquifer system.
- F_y = Dimensionless parameter representing the percent of water level decline below a maximum level.
- W = Average width of the pond midway between basin bottom and water level at time, t.
- K_H = Average horizontal hydraulic conductivity (ft/day).
- D = Average thickness of aquifer (ft.) given by $D = H + \frac{h_c}{2}$
- h_c = Height of water (ft.) in the basin above the initial ground water table time t.
- H = Initial saturation thickness of the aquifer (ft.).
- t = Cumulative time space (days) since the saturated lateral (stage two) flow started.
- h_t = Height of water (ft.) in the basin above the initial ground water table at the start of the saturated flow (stage two) given by $H_T = H_b + h_2$.
- h_2 = Height of water (ft.) in the basin above the basin bottom at the start of saturated lateral flow (stage two).

2.4 Determination of Hydraulic Conductivity

Determination of hydraulic conductivity is usually conducted by laboratory methods, field methods, empirical correlations, or indirect methods. Some of these methodologies are discussed below.

2.4.1 Laboratory Methods

One of the main advantages of laboratory methods is result reproduction. In a laboratory, conditions (hydraulic head, for example) can be better monitored and controlled; however, it is very difficult to obtain an undisturbed sample. Because of this,

laboratory tests on these materials are typically conducted on samples which are reconstructed or remolded to best simulate field conditions of the soil.

The test method usually involves a cylindrical soil specimen with a length (*L*) and surface area (*A*) being placed into the testing device. A difference in head between the top and bottom of the specimen is created resulting in a hydraulic gradient, *i*, which in turn forces the water to flow though the specimen. The hydraulic conductivity during steady state conditions is then calculated using Darcy's law. Three types of laboratory methods used to determine the hydraulic conductivity of soils are discussed below.

2.4.1.1 Constant Head Method

This test is particularly suited for granular soils with a coefficient of permeability on the order of 10^{-3} or greater (Terzaghi and Peck, 1969). This method may not be well-suited for low permeability soils because of the length of time required for a sufficient quantity of water to flow through a sample and the possibility of evaporation (Davidson, 2002).

The apparatus, depicted in Figure 2-2, consists of a vertical cylindrical tube containing the soil specimen. The sample of length, *L,* and cross-sectional area, *A*, is submersed with water with a constant head, *H*. This total head is held constant throughout the test by using overflow reservoirs to maintain headwater and tailwater levels. Under steady state and fully saturated conditions, the volume of water, *Q* collected in a given time, *t,* is measured. The value of the permeability coefficient can then be determined directly from Darcy's law as expressed below.

$$k = \frac{QL}{\Delta H A t} \qquad (2\text{-}14)$$

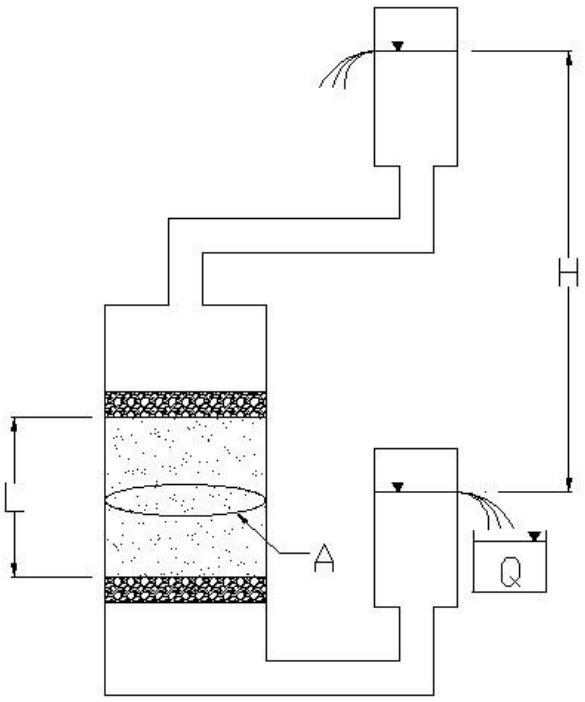

Figure 2-2. Constant head test laboratory setup.

2.4.1.2 Falling Head Method

Terzaghi and Peck (1969) suggest using the falling head method for soils that have a permeability coefficient less than 1 cm/s. However, if the permeability of a soil is too high (e.g., coarse grained sands) accurate timing measurements of the falling water column may be too difficult (Davidson, 2002). This method is well-suited for fine grained soils such as silts and clays with low hydraulic conductivities.

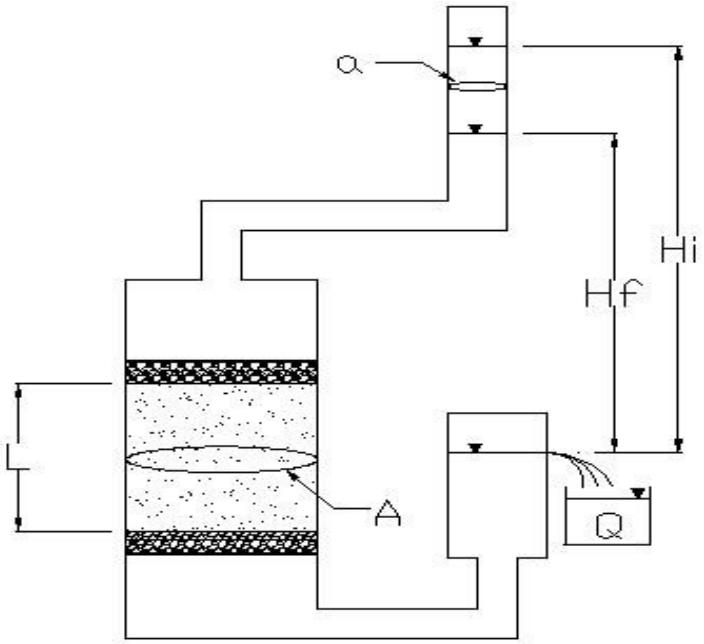

Figure 2-3. Falling head laboratory test set up.

Figure 2-3 shows a schematic of a falling head permeability apparatus. The soil sample is placed in a vertical cylinder with a cross-sectional area, *A*. A transparent standpipe of cross- sectional area, *a*, is attached to the test cylinder. During the test, the tailwater is held consent by an overflow reservoir while the elevation of the headwater is allowed to change. Under steady state and fully saturated conditions, the change in head ($H_i - H_f$) with respect to time, *t*, is measured. The flow rate, *q*, through the specimen is computed by:

$$q = k\frac{H}{L}A = -a\frac{dH}{dt} \tag{2-15}$$

where *q* = flow rate and *a* = area of standpipe. Rearranging (2-15) to solve for *dt* gives

$$dt = \frac{aL}{Ak}\left(-\frac{dH}{H}\right) \tag{2-16}$$

Integrating both sides yields:

$$\int_0^t dt = \frac{aL}{Ak}\int_{H_i}^{H_f} -\frac{dH}{H} \tag{2-17}$$

$$t = \frac{aL}{Ak} ln \frac{H_i}{H_f} \tag{2-18}$$

Solving for k produces the following equation:

$$k = \frac{aL}{At} ln \frac{H_i}{H_f} \tag{2-19}$$

2.4.1.3 Flexible Walled Permeability Device

For a rigid wall permeability test apparatus, the interface between the soil specimen and fixed wall may act as a flow channel. Hence water may bypass the specimen. This phenomenon which is termed “flow short-circuiting” occurs because water flows along the path of least resistance. Short-circuiting mostly occurs in soils with low permeability.

A flexible walled permeability apparatus may be employed to reduce the possibility of flow short-circuiting. In a flexible walled device, the rigid cylinder containing the specimen is replaced by a rubber membrane. The specimen in then placed into the chamber where the pressure can be adjusted. By increasing the pressure, the flexible membrane takes the shape of the soil specimen and hinders the development of flow paths around the specimen (2-4B). Other advantages of this device include:

1. Low permeability soil may be tested ($k < 1 \times 10^{-4}$ cm/sec)
2. Hydraulic gradient is easily varied
3. Confining pressure may also be varied
4. Back pressure causes adequate saturation

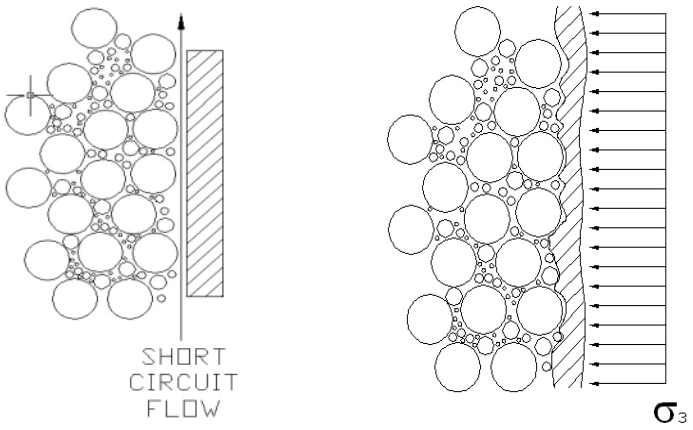

A B

Figure 2-4. Short-circuit flow: (A) short-circuiting of water flow along fixed wall permeability testing device; (B) flexible walled permeability testing device reduces chances of short circuiting.

2.4.1.4 Limitations of Laboratory Methods

Some limitations of laboratory methods are:

- **Disturbance.** It is not possible to obtain a truly undisturbed sample. Careful sampling may reduce the disturbance but cannot eliminate it completely. Factors that affect the permeability include anisotropy, confining pressures, particle orientation, and void ratio.

- **Sample size.** The soil sample size obtained for a given site is very small relative to the site itself. Thus the samples may not reflect the effects of non-homogeneity that may exist on the site.

- **Test Duration.** During long testing hours, water losses due to evaporation may result in errors in the calculated total head.

2.4.2 Empirical Methods

Other soil parameters appear to be related to permeability. Soil properties such as void ratio and grain size distribution have been used to estimate permeability. Smaller soil grains results in smaller voids or flow channels, subsequently lowering the material's permeability. Various empirical correlations have been obtained between such properties and hydraulic conductivity. Some empirical correlations are discussed below.

2.4.2.1 Hansen's Empirical Formula (1892)

Extensive investigations by Hansen on fine uniform sand with sizes varying up to 3 mm and uniformity coefficients less than 5 resulted in the correlation:

$$k = CD_e^2 \tag{2-20}$$

The term D_e (cm) is the characteristic effective grain size which was determined to be equal to D_{10} where:

- D_{10} corresponds to the grain size at which 10 percent of the particles are finer.
- k is the coefficient of permeability (cm/s)
- C is a constant

The magnitude of C varies and is based upon soil type. Published values for C may range from 1 to 1,000 (Carrier, 2003).

2.4.2.2 Kozeny-Carman Formula

A more accurate equation for estimating permeability was developed by Kozeny and Carman. Their expression is a semi-empirical/semi-theoretical prediction of permeability in porous media. It is defined below for water:

$$k = (\gamma_w/\mu_w)(1/C_{K-C})(1/S_0^2)[e^3(1+e)] \tag{2-21}$$

where:

- γ_w = unit weight of water.
- μ_w = viscosity of water.
- C_{K-C} = Kozeny-Carman empirical coefficient
- S_0 = specific surface area per unit volume of particles.
- e = void ratio.

The coefficient C_{K-C} is usually taken to be 5.0 for uniform spheres (sands). The specific storage, S_0, may be calculated by

$$S_0 = 6/D_{eff} \tag{2-22}$$

where effective diameter, D_{eff} is given by:

$$D_{eff} = 100\% / [\Sigma f_i / D_{avgi}] \quad (2\text{-}23)$$

and f_i is the ratio of particles larger and smaller than two (2) sieve sizes; and D_{avg} is average particle size between the two sieves.

As mentioned, the Kozeny-Carman formula is a better predictor of permeability for clean sands when compared to the Hansen equation. However, more computations are required when compared to the Hansen method. This may be why the method is not as popular as Hansen's. With advances in computer technology since the development of the Kozeny-Carman equation in the 1950s, a program may be written with relatively few inputs.

2.4.2.3 Hagen-Poiseuille Formula

Analysis of hydraulic conductivity, *k*, of granular soils, based on Hagen-Poiseuille's equation leads to correlations between *k* and void ratio, *e*. The hydraulic conductivity of a granular soil may be expressed as:

$$k = k' F(e) \quad (2\text{-}24)$$

where *k'* is a soil constant depending on temperature and void ratio. The term *F(e)* is an empirical function of the void ratio. Experimental data appear to indicate that *F(e)* may be approximated as:

$$F(e) = \frac{e^3}{1+e} \quad (2\text{-}25)$$

2.4.2.4 Limitations and Assumptions of Empirical Methods

The empirical formulas discussed above were derived by performing various experiments which may not be fully representative of in situ conditions. These expressions must be used as approximations. The above formulas for predicting permeability had the following assumptions and/or constraints:

1. They assumed no ionic attraction between water and soil particles. Therefore these methods should not be used for clayey material.
2. They assumed laminar flow. Large particles that have large void spaces will allow greater pore velocities. If void channels become too large and allow high pore velocities, the laminar flow assumption would not be valid.
3. They assumed soil particles were compact (round). Plate shaped particles (i.e., clay, mica, etc.) would make this assumption invalid.
4. They assumed soil is isotropic.
5. These formulas are not valid for soils with long, flat soil distribution curves.

In general, the above methods are only applicable for uniform sands. Due to the variability of permeability predictions, empirical methods should not be relied upon for permeability-dependent design.

2.4.3 Indirect Testing Methods

Indirect testing methods are usually performed to provide an approximation of the coefficient of hydraulic conductivity that can be used for preliminary analysis. The most common indirect method makes use of an extension of the one-dimensional consolidation test.

2.4.3.1 CRS Test Permeability Theory

This test determines the coefficient of permeability indirectly from the constant rate of strain (CRS) test for clays using a method developed by Yoshikuni et al. (1995). This method assumes that compressibility and permeability of clays are nonlinear, flow

is one dimensional, the fluid is incompressible, the soil homogenous, and Darcy's Law applies. By applying the latter assumption, the consolidation equation may be written:

$$\frac{k}{\gamma_w}\frac{\partial^2 u}{\partial z} = \frac{1}{1+e}\frac{\partial e}{\partial t} \tag{2-26}$$

The volumetric strain ratio can be computed by

$$\frac{1}{1+e}\frac{\partial e}{\partial t} = \frac{\Delta e}{1+e}\frac{1}{\Delta t} = \frac{1}{H}\frac{\Delta H}{\Delta t} = \frac{1}{V}\frac{\Delta V}{\Delta t} = \frac{\Delta \dot{V}}{V} \tag{2-27}$$

$$\frac{k}{\gamma_w}\frac{\partial^2 u}{\partial z} = \frac{\Delta \dot{V}}{V} \tag{2-28}$$

where:

- V = Volume
- e = void ratio
- H = height of specimen
- u = pore pressure
- $\Delta \dot{V}$ = volumetric strain rate

Assuming the following boundary conditions:

- Top drainage: $u(0,t) = 0$
- Impervious base: $\frac{\partial u}{\partial z}(H,t) = 0$

Integrating twice using the above boundary conditions and solving for k yields

$$k = -\frac{1}{2}\frac{\gamma_w}{u_b}\frac{\Delta \dot{V}}{V}H^2 \tag{2-29}$$

$$k = \frac{1}{2}\frac{\gamma_w}{u_b}\frac{\Delta H}{(H\cdot\Delta t)}H^2 \tag{2-30}$$

where:

$$\frac{\Delta H}{\Delta t} = \dot{\delta} = \text{strain rate} \tag{2-31}$$

Therefore:

$$k = -\frac{1}{2}\frac{\gamma_w}{w_b}\dot{\varepsilon}H \qquad (2\text{-}32)$$

Since the strain rate is constant for the CRS test, Equation 2-32 is solvable.

2.4.3.2 CRS Test Limitations and Assumptions

As discussed, the CRS test hinges upon a number of assumptions. The Darcy's Law assumption merits particular discussion. Consolidation is a function of excess pore pressure applied to vertical stress. According to ASTM D4044, the ratio between pore pressure and vertical stress must remain within a predefined range. If this ratio exceeds a certain limit, particle migration may occur. This would render the Darcy's Law assumption invalid.

2.4.4 In Situ Methods

Accurate and reliable information on hydraulic conductivity of soils may be obtained by conducting in situ tests. The advantages of these methods are: (1) that the soil is tested in place; and (2) the "specimen" size is substantially larger. This appears to yield results that are more representative of the site. Various types of in situ tests have been developed and are discussed below.

2.4.4.1 Infiltrometers

Infiltrometers (Figure 2-5) are devices used to measure the infiltration rate of water through soils. If additional soil parameters are measured, permeability can be calculated. The procedure involves placing water in the infiltrometer and allowing it to percolate into the soil. A measured quantity of water is added to maintain a constant head. Infiltrometers are an economical way to determine the infiltration rate of a

localized surface layer of soil. There is a wide variety available. The type of infiltrometer setup and test method is determined by:

1. Soil type
2. Required accuracy of results
3. Expected conditions which will be modeled
4. Direction of flow (vertical or horizontal)
5. Ground water table (GWT) location

The most common types of infiltrometer are discussed below.

Open single ring

An open single ring infiltrometer is the simplest of the infiltrometers. It consists of a steel ring approximately 8 inches in diameter. A test is run by embedding the infiltrometer into the soil and sealing it, usually with a bentonite based grout. The ring is filled with water, which is maintained at a constant measured height. The flow rate is also monitored. With the use of the Green-Ampt model for unsaturated soil flow and measured flow rate, the vertical hydraulic conductivity can be calculated.

Closed single ring

The closed single ring functions in the same fashion as the open single ring infiltrometer previously discussed. The advantage with a closed ring is that evaporation effects become negligible. However, only a limited head can be applied, rendering the closed single ring infiltrometer ineffective for very permeable materials.

Open double ring

The open double ring infiltrometer is similar to the open single ring infiltrometer with the addition of a second inner ring. The equipment consists of two concentric rings and a driving plate, with handles for both the inner and outer rings. The outer ring is

24 inch diameter and the inner ring 12 inches. The two rings are driven into the ground and partially filled with water. The double ring design helps prevent divergent flow in layered soils. The outer ring acts as a barrier to encourage only vertical flow into the inner ring. The water-level is maintained for a specific period of time, depending on the type of soil and permeability. Permeability is computed by using measurements of the volume of water needed to maintain a specified level and a time factor.

Closed double ring

The closed double ring infiltrometer is similar to the open double ring infiltrometer with the inner ring sealed to prevent evaporation. Like the closed single ring type, the closed double ring is used primarily for soils with low permeability. It was designed primarily to calculate the vertical permeability in a clay liner.

Cylinder Permeameter

The cylinder permeameter method was developed by Boersma in 1965 and improved by Moulton and Seals in 1979. To perform the test, a large diameter borehole is drilled and a cylindrical sleeve is place in its center (Birgisson and Solseng, 1996). The bottom of the sleeve is made to penetrate the soil at the bottom of the borehole. Water is then pumped into the borehole/casing, and an approximately equal and constant head is maintained. Only the flow into the casing is measured. A tensiometer is placed at the bottom of the casing to measure pressure. When the tensiometer indicates a zero tension reading, saturation is assumed and the vertical hydraulic conductivity may be calculated.

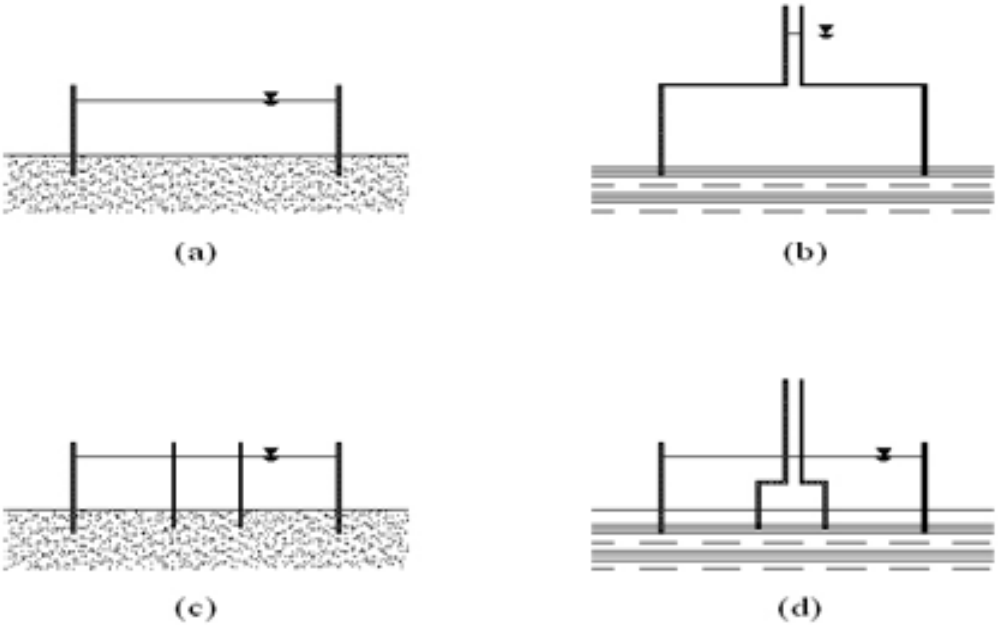

Figure 2-5. Ring Infiltrometers Profile View; (A) open single ring (B) closed single ring (C) open double ring (D) closed double ring

Other Infiltrometers

Other infiltrometers available but not discussed include:

- Gradient intake
- Seepage meter
- Technical University of Munich infiltration test
- Australian Road research board permeameter
- Mid-slab constant head permeability test
- Mid-slab falling head permeability test
- Edge of slab constant head permeability test

Limitations

Infiltrometers are economical and are relatively easy to use. However, they are limited to shallow soils above the groundwater table. An estimate of soil moisture content from the wetting front suction head, lateral spreading, and evaporation may be required depending on the test method (Birgisson and Solseng 1996). Testing time and disturbances (usually medium to high) are also a function of soil type and test method.

2.4.4.2 Tracer Dilution Tests

A tracer dilution test is a method of determining the permeability of soil around a borehole by measuring the concentration of a tracer with time. The tracer (i.e., salt, bromide) is mixed in the water present in a borehole until a nearly uniform mixture is produced. An initial concentration reading is taken followed by additional readings. The change in tracer concentration is measured as a function of time. Readings may be taken with ion-specific electrode probes placed vertically in the borehole. The decline in the measured concentration with time can be correlated to determine seepage velocities.

2.4.4.3 Slug Test

A slug test (Figure 2-6) is an in situ method commonly used to measure the permeability of soils. In this test, an element of known volume (slug) is added to or removed from a well. The recovery of head verses time is then measured. The response of head in the well is used to estimate soil permeability parameters.

Procedure

To perform this test a borehole must be drilled to the desired depth, and a well must be developed. The procedure with which a well is developed will determine the effectiveness of collecting accurate data (Butler, 1998). An approximately instantaneous change in head is applied to the borehole by the addition or withdrawal of a measured quantity of water. The recovery time (time it takes water to return to its static state) is measured and can be correlated to the permeability of the surrounding soil. The slug test design, performance, and analysis are detailed by Butler (1998).

The test procedure for a slug test depends on the properties of the aquifer, especially its transmissivity. If the surrounding soil has low transmissivity, then a bail-

down method (removing a measured volume) works well. However, in soils where transmissivity is high, it may be more accurate to add a measured volume (slug). The use of a pressure transducer is recommended during these tests.

Slug test analysis

The analysis of a slug test is highly dependent upon site conditions. Butler (1998) stresses the importance of well development, test design, and appropriate analysis procedures to produce accurate results. Selecting the proper analysis model requires the following (Butler, 1998):

- Relative permeability
- Confined or unconfined aquifer
- Fully or partially penetrating well
- Reproducible dependence on the distance between an aquifer's water-level and the water level in the well hole at the start of the test (H_0)
- Dependence on flow direction
- Implausibility on dimensionless storage parameter (α)f
- Noise in data.

Commonly accepted analysis methods are shown in Table 2-5. The proper method is dependent upon conditions listed above.

Table 2-5. Typical slug test analysis methods

Method	Permeability Equation	General Use Conditions
Cooper et al.	$K_r = \frac{r_c^2}{2Lt_{3.0}}$	1. CA, PPW, FPW 2. UCA, plausible a 3. Low conductivity 4. Multi well w/ packer
Peres et al. Approximate Deconvolution	$K_r = \frac{2.30r_c^2}{4BA\beta}$	CA, PPW
KGS model	$K_r = \frac{r_c^2}{bt_{3.0}}$	1. CA, PPW 2. UCA, below WT 3. Low conductivity 4. Multi well w/ packer
Bouwer and Rice	$K_r = \frac{r_c^2 \ln\left(\frac{R_e}{r_w\sqrt{(K_z/K_r)}}\right)}{2LT_0}$	UCA, no skin effects
Dagan	$K_r = \frac{r_c^2(1/P)}{2bT_0}$ Where P = dimensionless parameter	UCA, no skin effects
Chu and Grader	$K_r = \frac{\left(\frac{4L}{\sqrt{K_z/K_r}}\right)r_c^2}{2Lr_D^2r_w^2}$	FPW, CA, Multi well tests
Hvorslev	$K_r = \frac{r_c^2 \ln(R_e/r_w)}{2LT_0}$ where T = 0.368	FPW, CA, no skin effects

Note: Some of the above equations rely on the use of curves not presented in this report. Other factors such as noise in the data, skin effects, and the plausibility α, may influence which method should be used. Key: FPW: Fully penetrating well, PPW: partially penetrating well, CA: confined aquifer, UCA: unconfined aquifer

Slug test theory

Using Horslev's Theory, the permeability from a slug test may be determined. For a cased, uncased, or perforated extension into an aquifer of finite thickness for $L > 8r$, the empirical F-factor is given as

$$F = \frac{2\pi L}{\ln\left(\frac{L}{r}\right)} \tag{2-33}$$

where L is the length of the intake; and *r* is the radius of the borehole. Substituting into Hvorslev's Equations:

$$t_2 - t_1 = T\left(\ln\frac{H_2}{H_3} - \ln\frac{H_2}{H_4}\right) = \frac{A}{Fk}\ln\frac{H_4}{H_3} \tag{2-34}$$

Solving for *k*:

$$k = \frac{r^2 \ln(L/r)}{2L}\frac{\ln(H_4/H_3)}{(t_1 - t_2)} \tag{2-35}$$

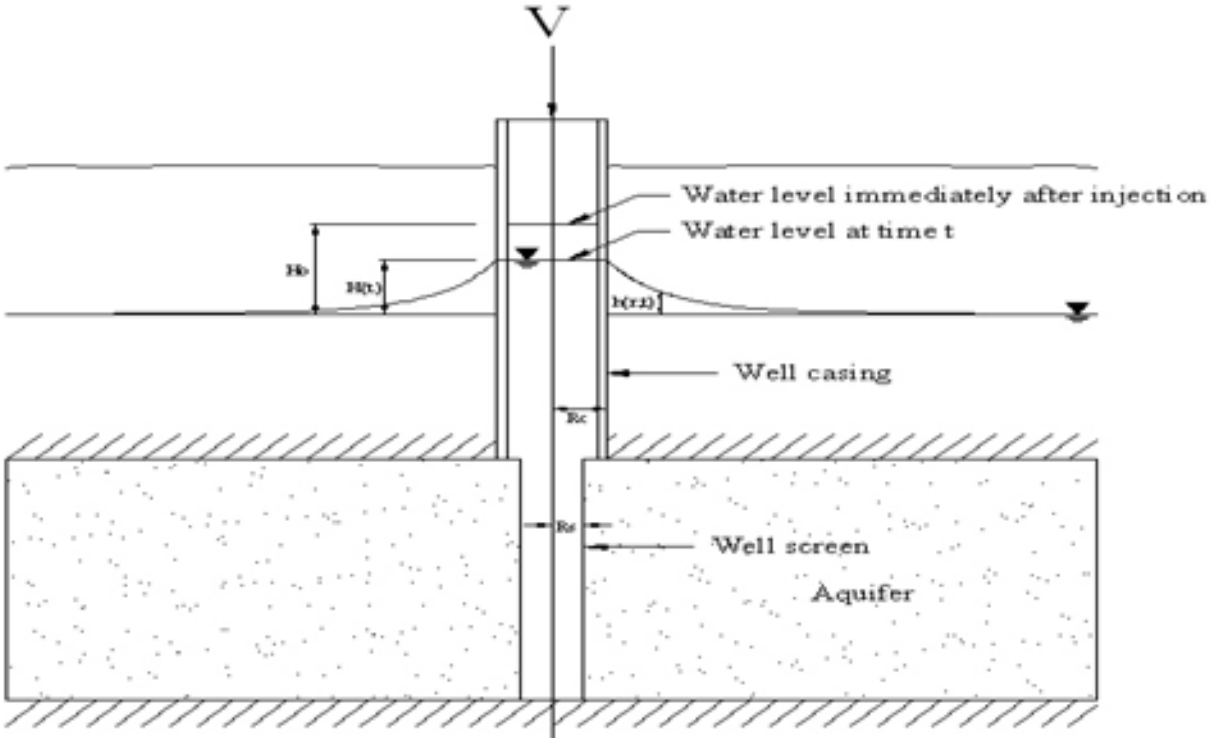

Figure 2-6. Slug test schematic

The field data in Hvorslev's method (h/h_0 verses t) is plotted on a semi-log plot with h/h_0 on the log scale (Domenico and Schwartz, 1990). Using a best-fit regression

line to fit the data and defining a T_0 value when h/h_0 = 0.368, the permeability coefficient can be calculated by:

$$k = \frac{r^2 \ln(L/r)}{2L T_0} \quad (2\text{-}36)$$

For confined aquifers with fully penetrating wells, the Cooper et al. method is valid in most cases. It is based upon the mathematical model for radial flow:

$$\frac{\partial^2 h}{\partial r^2} \frac{1}{r} \frac{\partial h}{\partial r} = \frac{S_s}{K_r} \frac{\partial h}{\partial t} \quad (2\text{-}37)$$

By applying the following conditions:

- No drawdown in well at $t = 0$ $h(r,0) = 0$
- Instantaneous change in head at $t = 0$ $H(0) = H_0$
- No drawdown effects at an infinite distance from well $h(\infty,t) = 0$
- Drawdown is equal to head difference in well screen $h(r_w,t) = H(t)$

The differential becomes:

$$2\pi r_w K_r B \frac{\partial h(r_w,t)}{\partial r} = \pi r_c^2 \frac{dH(t)}{dt} \quad (2\text{-}38)$$

By matching the data to type-curves, an estimate of permeability may be calculated by:

$$K_r = \frac{r_c^2}{b t_{1.0}} \quad (2\text{-}39)$$

The KGS model assumptions are the same as those used in the Cooper et al. model. But, the KGS model allows the well to be partially penetrating and it allows for the possibility of a vertical flow component. The set of calibration curves for the KGS model is different than those of Cooper et al. However, the curves do converge to the Cooper et al.-type at large α values.

Strengths and limitations

Butler (1998) outlined the advantages and disadvantages of the slug test. These are presented in Table 2-6. It is important to note that the advantages and disadvantages are based upon the comparison between the slug test and the well test (discussed in the Section 2.4.4.3).

Table 2-6. Typical slug test analysis methods (Butler, 1998)

Advantages	**Disadvantages**
Manpower and equipment requirements result in low costs	Poor field procedures and/or improperly developed observation wells may cause accuracy errors
Procedure is simple	Only a relatively small volume of aquifer is tested
Test can be performed relatively quickly	
Useful for low permeability formations	
Use of a solid slug precludes pumping and contaminated waste disposal	Values of k may reflect the presence of the gravel pack around well screen and/or drilling mud left in borehole
Large number of large scale tests may characterize spatial variability	

2.4.4.4 Well tests

In a pump test, water is extracted at a constant rate for a specified time. By measuring the drawdown in wells and flow rate, the transmissivity and specific yield may be extrapolated, and the permeability estimated. Pump tests may be performed in a well which already exists.

General Procedure

For accuracy, it is important that the well screen be fully submerged below the water table. It is recommended that controllable activities which may affect the aquifer (i.e., pumping, drilling, etc.) should be halted at least 48 hours prior to the test. Diurnal fluctuations due to tidal influences should be noted and compared with water level readings after the test(s). Static fluctuations should be measured until a trend is established. Typically the length of a pumping test is 72 hours for a non-confined aquifer and 24 hours for a confined situation. This testing time may be reduced for low-capacity tests.

Data collection should be completed at all available points including points outside the radius of influence. Observation wells should be placed as uniformly as practical around the pumped well. A minimum of 3 wells is recommended. The diameter of the observation well is dependent upon the type of measuring equipment to be used. The pumping well should be equipped with a flow rate recording device and a flow rate regulator. Recovery measurements may be recorded at the end of the test or in the event of pump failure.

Fluids pumped from the well should not be discharged where they will affect measurements. It should be noted that pumped water may be hazardous. If so, it must be pumped into holding facilities to await proper disposal. The frequency of measurements recorded is shown in Table 2-7. Measurements must be recorded more frequently at the beginning of the test because when a test first begins, data tend to change more quickly.

Table 2-7. Typical pump test measurement recording frequency

Time Interval (min)	Time Between Recordings
0 - 2	30 seconds
2 - 5	1 minutes
5 - 10	2 minutes
10 - 30	5 minutes
30 - 60	10 minutes
60 – 120	20 minutes
120 - end	1 hour

Theory

Flow in a phreatic aquifer is 3-dimensional and difficult to solve. Therefore, simplifying assumptions must be made. Dupuit assumed that flow is horizontal. Therefore, the equipotentials are vertical. For radial flow in an unconfined aquifer in a fully penetrating well (refer to Figure 2-7), Boussinesq's Equation (Bear, 1979) is:

$$\frac{\partial}{\partial x}\left(k\frac{\partial h}{\partial x}\right)+\frac{\partial}{\partial y}\left(k\frac{\partial h}{\partial y}\right)+\frac{N}{k}=\frac{S_y}{k}\frac{\partial h}{\partial t} \qquad (2\text{-}40)$$

Assuming steady state conditions, and a homogeneous/isotropic soil, Equation 2-40 in radial coordinates yields:

$$\frac{d^2h^2}{dr^2}+\frac{1}{r}\frac{dh^2}{dr}+\frac{2N}{k}=0 \qquad (2\text{-}41)$$

Rewritten:

$$\frac{1}{r}\frac{d}{dr}\left(r\frac{dh^2}{dr}\right)+\frac{2N}{k}=0 \qquad (2\text{-}42)$$

where r = the radial distance from well. Two boundary conditions exist: $h = h_w$ at $r = r_w$ and $h = H_0$ at $r = R$. Integrating twice, applying the boundary conditions, and applying Darcy's equation gives:

$$Q = -\pi r^2 N + \frac{\pi\left[2K(H_0 - h_w) + NR^2\right]}{2\ln\left(R/r_w\right)} \tag{2-43}$$

If there is no recharge (N=0) then Equation 2-42 reduces to the Dupuit-Forcheimer well discharge equation:

$$Q = \frac{\pi K\left(H_0^2 - h_w^2\right)}{\ln\left(R/r_w\right)} \tag{2-44}$$

Solving for the coefficient of permeability for $N \neq 0$ and N=0 yields Equations 2-45 and 2-46, respectively:

$$K = \frac{\ln\left(R/r_w\right)\left(Q + \pi r^2 N\right) - NR^2}{\pi\left(H_0^2 - h_w^2\right)} \tag{2-45}$$

$$K = \frac{Q \cdot \ln\left(R/r_w\right)}{\pi\left(H_0^2 - h_w^2\right)} \tag{2-46}$$

The variable R is the effective radius of influence. Dimensionally constant equations (Bear, 1979) include:

Lembke (1886):

$$R = H\sqrt{\frac{K}{2N}} \tag{2-47}$$

Schultze, (1924):

$$R = 2.45\sqrt{\frac{HKt}{n_e}} \tag{2-48}$$

Aravin and Numerov (1953):

$$R = 1.9\sqrt{\frac{HKe}{\eta_e}} \tag{2-49}$$

where η_e is dimensionless. Empirical equations for R include:

Chertousov (1962):

$$R = 3000 s_w K^{1/2} \tag{2-50}$$

Chertousov (1949):

$$R = 575 s_w (HK)^{1/2} \tag{2-51}$$

where H, R and S_w are expressed in meters and K is expressed in m/s.

Equation 2-45 may be transposed to account for monitoring wells placed at radial distances (r_i) from the pumping well with heads, h_i. The new equation becomes:

$$K = \frac{Q \cdot \ln\left(r_2/r_1\right)}{\pi\left(h_2^2 - h_1^2\right)} \tag{2-52}$$

For the pump test described above, steady state conditions must be established within reasonable boundaries. This may require pumping times ranging between hours and days. Duration is largely dependent upon permeability. The advantage of the pump test is that it accounts for relatively large areas, and it may include effects of channeling.

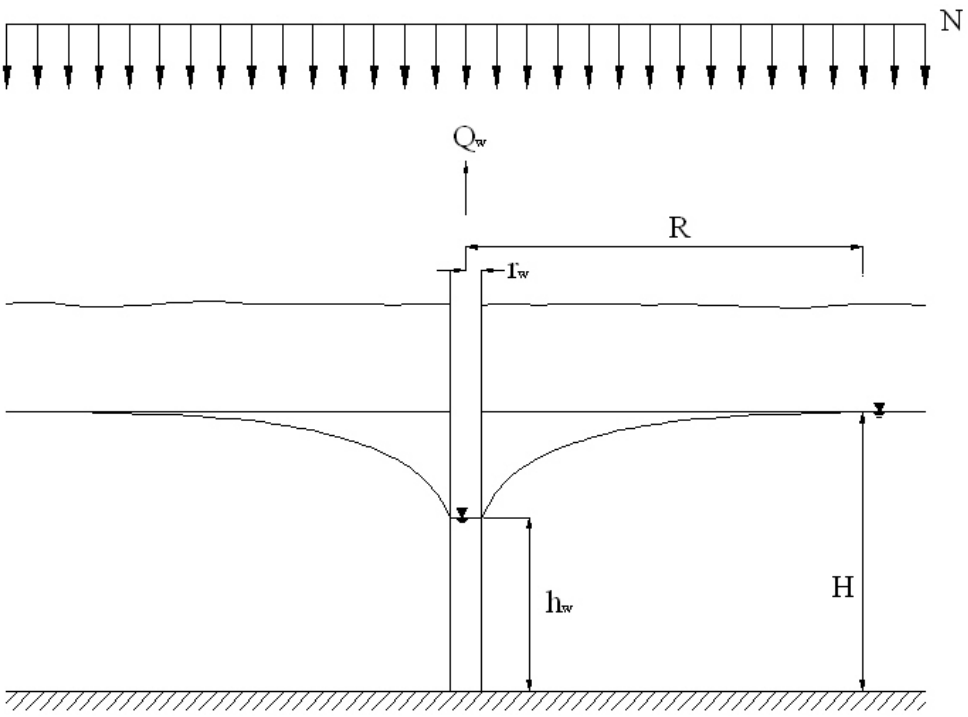

Figure 2-7. Pump test schematic

CHAPTER 3
DEVELOPMENT OF THE VAHIP

A Vertical and Horizontal In situ Permeameter (VAHIP) prototype was developed, and preliminary testing of the permeameter was performed by J. Sandoval in the summer of 2004. The purpose of the tests was to determine:

- A proper procedure for field tests
- If the VAHIP functioned according to the intended design.
- If testing data could be replicated.
- If permeability results using the VAHIP were similar to those from other conventional tests.

This chapter will discuss the history of the device and development of a new version.

3.1 Description of Prototype

The 2004 prototype is depicted in Figure 3-1. A brief description of the device is presented below.

3.1.1 Basic Design

The VAHIP was designed as a probe that could be connected to a SPT rig, advanced to the desired depth within a soil formation using the SPT rig, and measure vertical and horizontal permeability in two stages. During Stage I, water was designed to flow vertically from the tip of the probe so that permeability in the vertical direction was measured. Once stage I testing was complete, the Stage II test was to begin. Water was to be directed to flow through a horizontal screen to measure horizontal permeability. An O-ring inside the tip directed the water to flow in the appropriate direction during each stage. To toggle between stages, the periphery parts moved along the probe's shaft by mechanical means. As seen in Figure 3-1 the compressed position and extended position is Stage I and Stage II, respectively. In the field, Stage I was achieved by pushing on the rod and Stage II achieved by pulling up on the rod.

3.1.2 Assembly

As shown in Figure 3-1, the probe consisted of its core and its periphery members (collar, well screen, shoulder stops, and tip):

- **Core**. The VAHIP consists of a hollow steel core, threaded to fit an AWJ rod. The core allowed water to pass through the probe and exit horizontally or at the tip via flow ports. The core also secured the 0.0625 inch tubing used to estimate the hydrostatic pressure in the soil.

- **Screen.** The screen, used to force water horizontally, was made from a 1.25 inch PVC well screen. It has a total open area of 12.5 in^2 per foot of screen. The screen was backed with non-woven filter paper to prevent soil particles from entering the interior of the probe. Eight machine screws attached the screen to the collar and tip.

- **Tip**. The leading edge of the probe consisted of a steel 45^o cone tip. Eight 0.25 inch diameter flow ports were drilled symmetrically about its axis. Sintered steel, with a 0.0625 inch diameter hole was placed inside each flow port. Four machine screws fasten the cone tip to the probe.

The tip was allowed to slide along the core. Within the tip was an O-ring which directed flow for Stage I or Stage II measurements. The position of the O-ring with respect to the flow ports in the core determined flow direction.

Other Components. The other two components of the original VAHIP probe were its collar and shoulder. The steel collar fit securely around the 0.875 inch diameter core and was allowed to slide along it in the axial direction. The collar's range of motion is limited by a section of the core and a steel shoulder. The steel shoulder consisted of two cylindrical halves which fit around the 0.75 inch diameter section of the core. Once assembled, the collar could not be separated from the core. The core served two purposes: (1), it held an O-ring inside the collar to prevent water from flowing up the probe during Stage II testing; and (2), it served as the link to connect the screen and tip to the core.

A B

Figure 3-1. VAHIP probe (2004). (A) stage I (vertical permeability); (B) stage II (horizontal permeability)

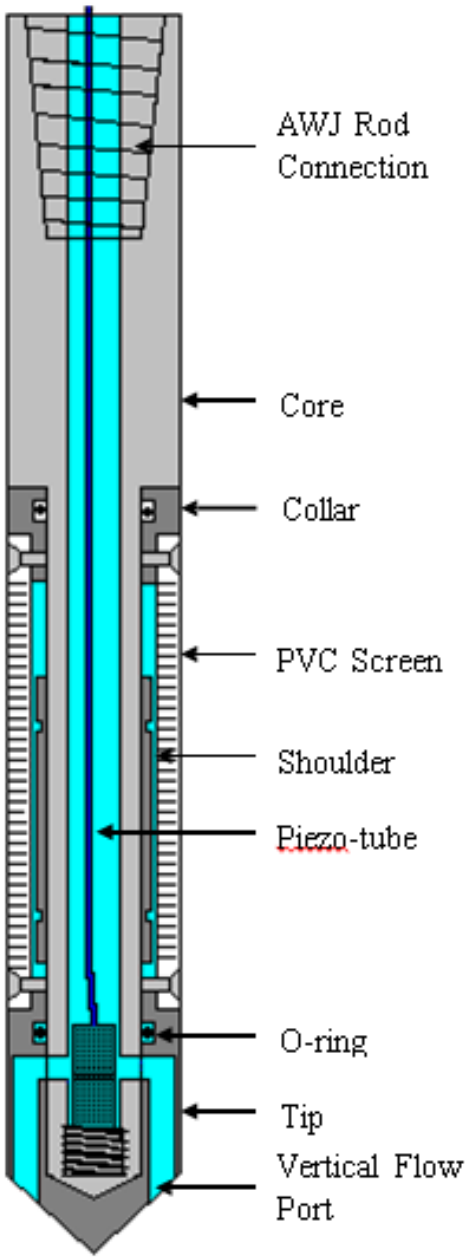

Figure 3-2. Schematic of 2004 VAHIP

3.2 Issues with Design

The preliminary testing of the probe both in the laboratory and in the field showed that it offered advantages over other, more established methods. However, some issues were evident. These are outlined below.

3.2.1 Full Flow Condition

When measuring Stage II (horizontal) permeability, the equations assumed water was flowing out of the entire screen area. This is called full flow condition (FFC). FFC could not be achieved when gradients were low. To correct this, a reduction in screen area was recommended.

3.2.2 Area Correction

A correction to account for non-FFC needed to be made. This would reduce the calculated permeability except during the falling head test for lateral flow. Under such conditions, an American Society for Testing and Materials (ASTM) equation that was not sensitive to the actual flow area of the screen was used.

3.2.3 Equation Limitations

Several theoretical permeability equations used to reduce the data had limitations. The United States Bureau of Reclamation (USBR) equation ($k=V*ln(L_{eff}/R)$) used to calculate permeability in the constant head lateral flow tests tended to fail because the effective length of the horizontal flow area was typically less than the radius of the probe. Thus L_{eff}/R was often 1.0, and the natural log term in the equation produced a negative number, resulting in a negative permeability computation.

3.2.4 Mechanical Issues

Some complications experienced were due to the limitations of the probe and the test media. These are outlined below.

3.2.4.1 Sand Intrusion

Stage I testing of the VAHIP involved compressing the device by pushing on it. To switch to Stage II testing the rod needed to be pulled upward thereby exposing a small gap between the collar and the core. During Stage II testing, material often spilled into this gap and sometimes prevented the VAHIP from returning to its Stage I position.

3.2.4.2 Piezotube Connection

The 0.0625 inch tube used to measure head was attached to the core using a quick connect. This connection sometimes did not allow high enough flow rates into the core during testing with highly permeable soil. This issue was exacerbated during Stage II testing because FFC could not be established.

3.2.4.3 Assembling and Disassembling

The 2004 VAHIP probe prototype was assembled using machine screws to attach the screen to the tip and collar. This arrangement was not practical when performing multiple tests in multiple locations. Because of sand infiltration, the probe had to be disassembled and cleaned between tests, but the machine screws made quick disassembly impossible.

3.2.5 Rigidity

The screen of the 2004 VAHIP was made from a 1.25 inch diameter PVC well screen. The advantage of using the PVC well screen was that it is easily replaceable and it was successful in the preliminary testing phase. However, the screen is the link between the collar and the tip. Though the screen was easily replaceable the tip was not. If the screen were to fail structurally during field testing the tip would be lost.

3.3 Description of 2005 VAHIP Probe

By observing the wear after preliminary testing with the 2004 probe and reviewing the complications previously discussed, a series of modifications were made in 2005. The modifications were intended to allow for easier assembly, improved workability, and improved rigidity. A discussion of these enhancements, their associated deficiencies, and some "quick fixes" to these issues is presented below:

1. A threaded steel plug was screwed into the tip of the core. The purpose of the plug was to secure the piezotube inside the core. However, the extent of the threads inside the core would not allow the plug to be fully inserted. This caused the plug to become deformed by the tip while advancing the VAHIP into the ground. The threads were extended into the core to compensate.

2. The quick connect used to hold the piezotube to the plug at the bottom of the core hindered the flow of water from the exit ports. Rather than change the locations of the exit ports, the connection was shortened. The piezotube quick connect assembly was replaced with a shorter "C-hold" setup. This setup consisted of a tube cap attached to the piezotube. A 0.0625 inch hole was drilled into the cap to allow the tube to function. The threaded steel plug was machined to secure the cap to the plug to prevent the piezotube from changing elevation during testing. This setup allowed for functionality of the piezotube without obstructing the water flow through the exit ports.

3. The head of the core would deform (mushroom) due to stress induced when pushing probe into ground. The sharp edges would slice O-shaped grooves in the tip and collar when assembling and disassembling the probe. This section of the core was beveled to allow the stresses to be distributed over a larger area.

4. In previous tests, horizontal permeability tests could not be performed because the water could not be supplied fast enough to establish a FFC. The slits on the outer shaft were modified to reduce the flow area. The new flow area was also designed such that the *F*-factor would be a round number to allow easier calculations in the field.

5. Due to the limited strength of PVC, a stronger material was required for the screen. The material of the outer shaft was changed from PVC to steel.

6. Assembly and disassembly in the field required too much time. To remedy this, the tip, outer ring, and collar were tapped so the sections could be threaded together.

7. During field testing, soil entered into spaces created by the moving parts. Therefore, a PVC sand shield was placed on the collar to hinder sand from entering the void between moving pieces on the probe.

8. During the preliminary testing, various components of the VAHIP were spread out in no particular order. Testing using this “loose” setup proved to be time consuming. To remedy this, a control panel to hold measuring devices was built. This allowed data to be read more easily and allowed for a more efficient setup.

9. Tools were placed in a 5-gallon bucket and needed a place to be stored. Extra parts were also needed in case a problem occurred in the field. Storage boxes were required to keep tools and parts organized. Two toolboxes were purchased to remedy this.

10. Flow measurement was difficult to perform in the field. The flow meter used for constant head did not function as well as intended. Falling head tests were difficult to perform due to the various components used at the time of testing. To address these issues, a Plexiglas pipette was designed. The pipette could be pressurized to apply a greater head when mounted directly atop of the AWJ rod. A different type of flow meter was purchased to record flow rate.

11. The infiltration of sand between moving parts on the permeameter caused an increase in friction. It was feared that the soil pressure required to toggle from Stage I to II would not be great enough to overcome the internal frictional forces. The probe was modified to include a spring between the collar and the large diameter section of the core. The spring would allow the probe to be compressed (Stage I) under pressure from the SPT rig but stiff enough to overcome friction when switching to Stage II testing. The collar and core were counter-bored so that the spring would not reduce the range of motion of the apparatus.

The 2005 prototype was more rigid than its predecessor because for the first time, the VAHIP’s screen was steel. The addition of the spring exerted a force of approximately 25 pounds, which significantly increased the VAHIP’s ability to toggle between stages. Figure 3-3 through Figure 3-5 shows the 2005 VAHIP prototype.

Figure 3-3. 2005 VAHIP prototype

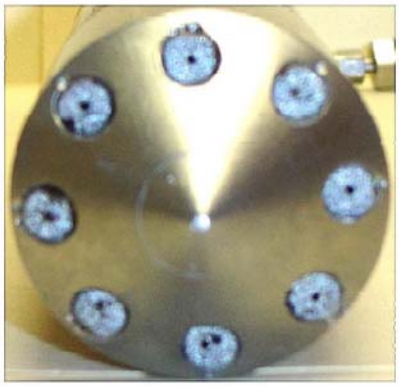

Figure 3-4. VAHIP probe tip.

Figure 3-5. 2005 disassembled VAHIP

3.4 Field Testing of 2005 VAHIP Probe

Field tests using the 2005 VAHIP were performed at two test sites: Hawthorne and Newberry. A 5-acre retention pond existed at the Newberry site while a retention pond was proposed at the Hawthorne site.

At the Hawthorne site, the VAHIP was advanced 7 feet into the soil via an automatic hammer on a SPT rig. Hand auger borings revealed that the soil was fine sand. Vertical and horizontal tests were performed and data collected. The constant head test for the vertical direction could not be performed due to low flow rates. A

borehole test was performed at the site by the FDOT technician so that the result could be compared with those of the VAHIP.

The testing performed at the Newberry site was performed in conjunction with another UF/FDOT project. Testing at this site occurred at only one location because the SPT rig was owned and operated by a private engineering firm that charged a setup fee when the rig was moved. Two depths were tested at the Newberry site. Two soil samples were obtained at the Newberry site using a hand auger. They revealed that the soil was sand. Borehole permeability tests were performed on these samples to compare to the VAHIP results.

During the field testing of the 2005 probe, the vertical flow ports at the probe's top often clogged during pushing (Figure 3-6). Consequently it became necessary again to redesign the probe to address this problem.

Figure 3-6. Potentially clogged flow ports (2005 probe)

3.5 Description of 2006 VAHIP Probe

The main design feature of the 2006 probe (Figure 3-7) was the development of a new tip. Overall, the mechanical basis of the 2005 design was not significantly altered. The eight small flow ports of the 2005 prototype were replaced by one large vertical flow port. The total area of the eight flow ports was approximately 0.025 square inches. The single flow port designed for the new probe had a diameter of 0.75 inches, which appeared to generate the required flow rates.

Because the new probe was closed when it was pushed to testing depth, the testing procedure needed to be modified. The horizontal slots remained open during pushing. Instead of toggling the probe from a vertical to a horizontal test, the new probe toggled from a horizontal to a vertical test. In other words, the side-screens remained open during pushing.

To close the vertical flow ports during the pushing process, the 2006 prototype was designed to have a core (central shaft) with a pointed end that extended through the 0.75 inch opening at its tip. This cone was flush with the tip when pushed, thereby closing the probe. During a test, the top was lifted upward so that vertical flow could be initiated. This core was fixed to an SPT union connector on the probe to which an SPT rod could be attached. Photographs of the 2006 probe are presented in Figure 3-8 through Figure 3-10.

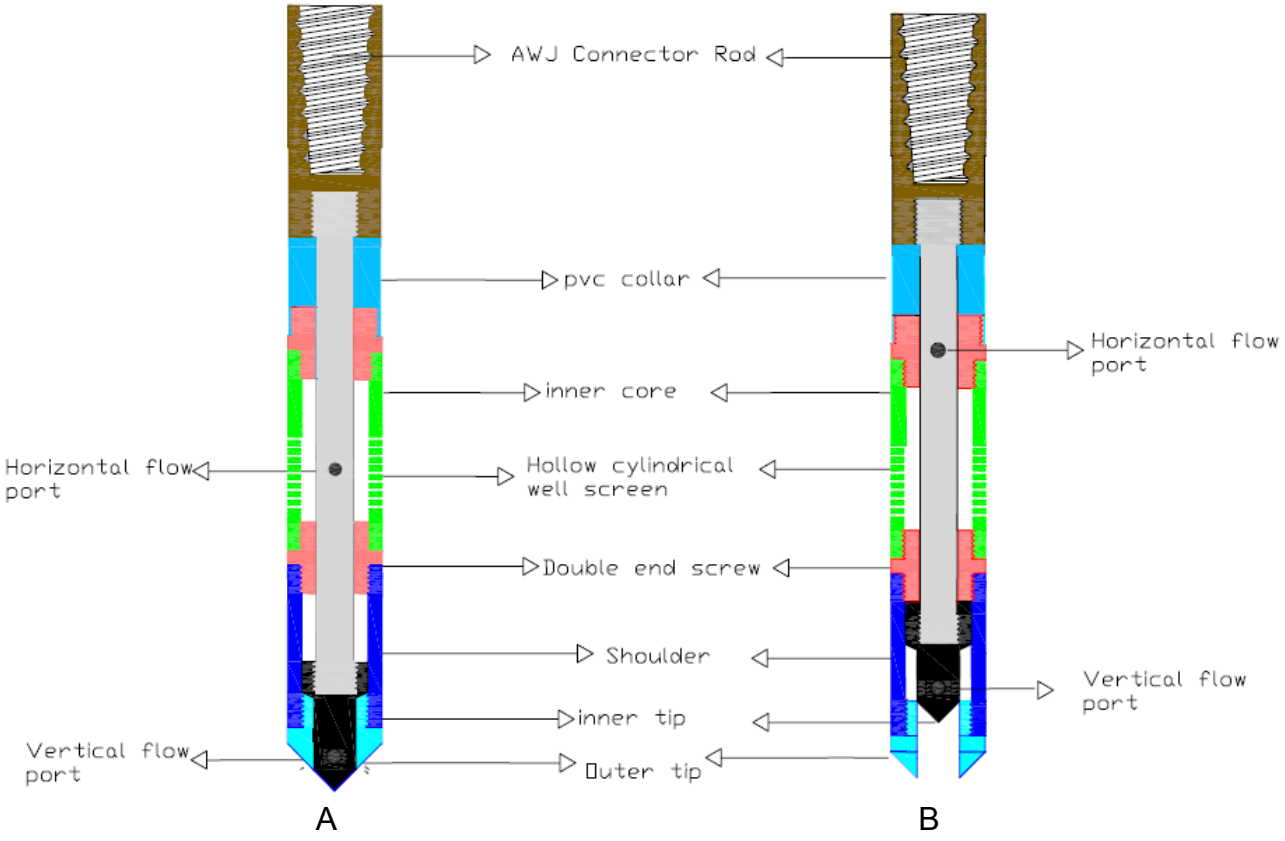

Figure 3-7. Schematic representation of 2006 probe: (A) tip closed for horizontal flow (B) Tip opened for vertical flow.

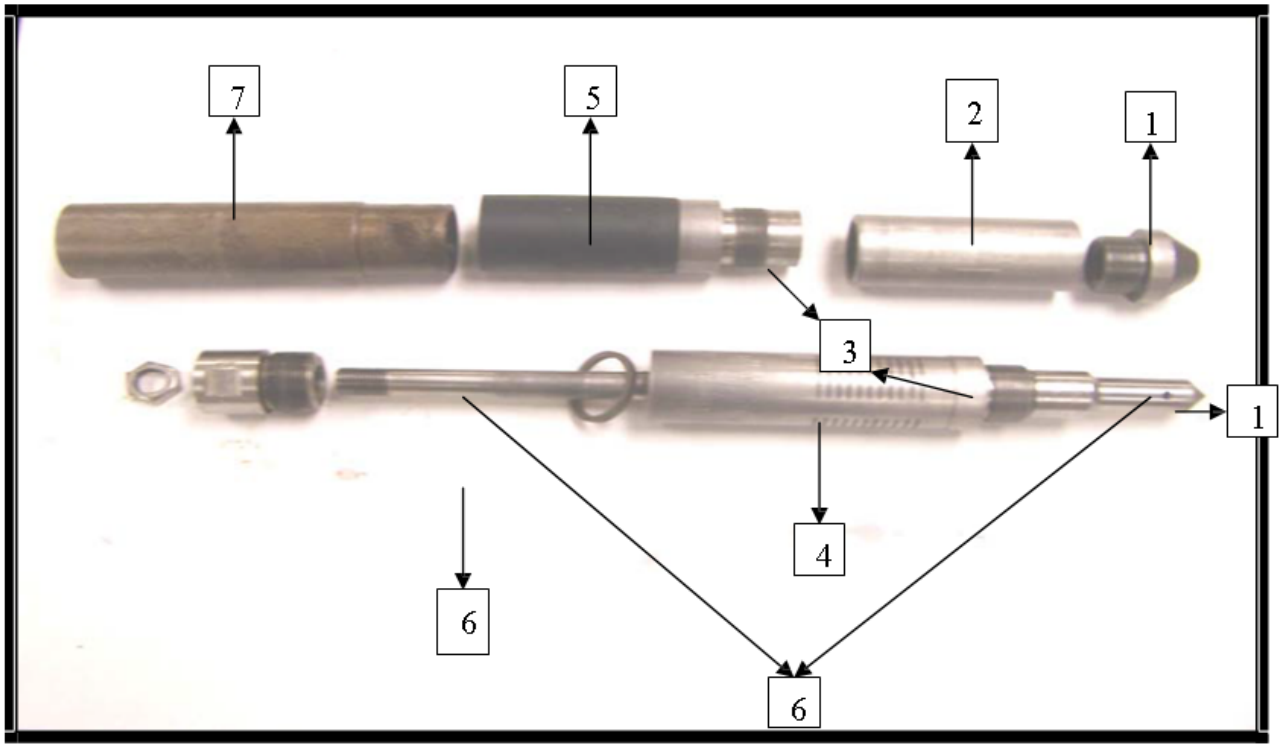

Figure 3-8. Dismantled 2006 VAHIP probe showing components

The probe components:

1. Outer tip with 0.75 inch diameter tip opening
2. Hollow cylindrical shoulder
3. Double-end threaded connection screw
4. Hollow cylindrical screen with horizontal slots
5. PVC collar connected to a double-end threaded screw
6. Hollow inner core with tip
7. AWJ connector rod.

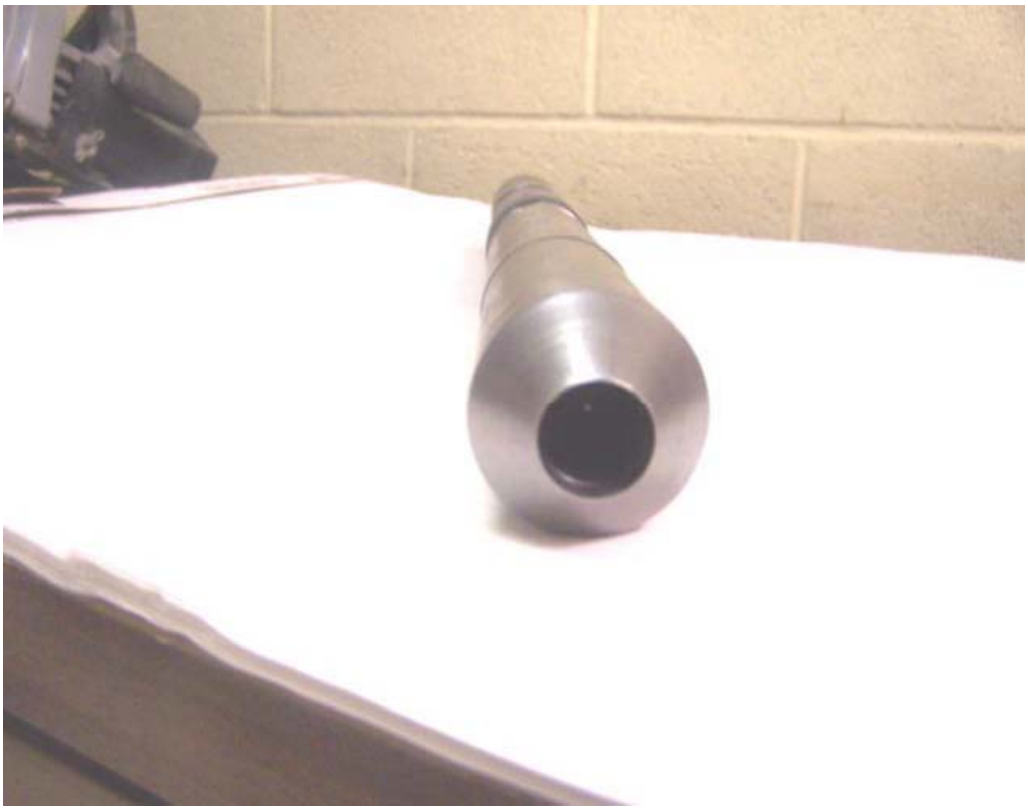

Figure 3-9. Probe tip opened for vertical flow

Figure 3-10. Probe tip closed for horizontal flow

3.6 Modifications to VAHIP

In October 2010, it was determined the probe could not function properly with the 2006 design. Debris intrusion was still an issue, although as of 2010, the issue had become concentrated along the side screens. In response, researchers began to develop a “smear-proof” design. Several design alternatives were considered. These alternatives fell into two categories: (1) internal rotational solutions; and (2) internal expandable solutions. External protection for the VAHIP horizontal slits was unacceptable because external protection would disturb the surrounding soil thereby defeating the purpose of the “in situ” nature of the test.

Investigators initially concluded that the latter category of solutions – internal expandable devices (bellows, balloons, cone attachments, etc.) were unacceptable. This category of solution requires several moving parts with potential for breakage. Because the final version of the VAHIP must be robust enough to withstand harsh field conditions, the goal became to minimize sensitive moving pieces. This preliminary conclusion led to a series of internal rotational designs.

3.6.1 Wire/Heavy Nylon Brush – Design A

The first proposed revision to the probe (Figure 3-11) included an internal wire or nylon brush attachment (A1) which would be used to dislodge fine sand or clay particles stuck in the probe. This brush would be replaceable; would attach to the inner shaft (A3) in two pieces with screws, much like a shaft collar; and would rotate in tandem with the shaft. This design included horizontal slits (A2) which would allow water to flow outward from the probe into the surrounding soil. By measuring the flow rate out of the probe, the permeability of the soil could be determined. To operate the brush, the probe’s

internal shaft was to be rotated back-and-forth. This design precluded independent horizontal and vertical tests.

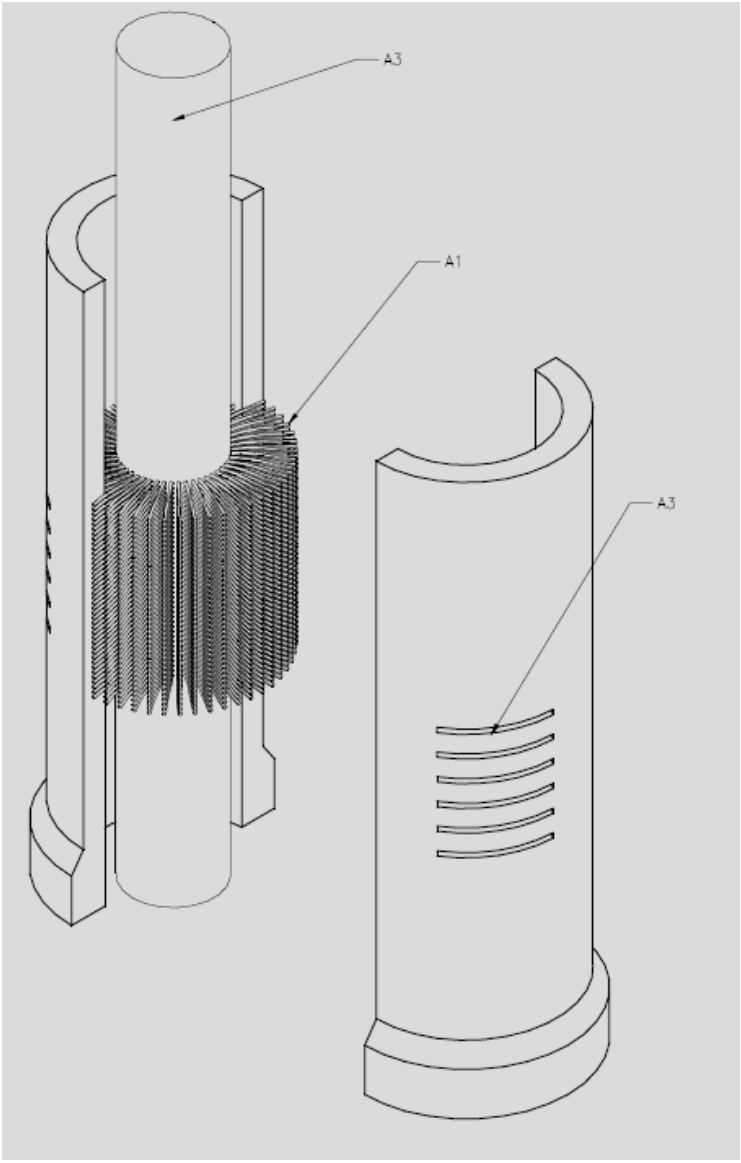

Figure 3-11. Wire/Heavy nylon brush schematic

3.6.2 Independent Vertical/Horizontal Probe – Design B

This design (Figure 3-12) looked to separate the vertical and horizontal flows. The idea called for a series of internal O-rings which would seal the inner shaft completely when “closed.” The probe would be lowered in the closed position until the desired depth was reached, and then opened. By slowly raising the inner shaft, water

would be released from the bottom of the probe allowing vertical permeability to be measured. By raising the shaft further, the O-rings would no longer seal the upper part, allowing water to flow laterally, while stopping the vertical flow. This would allow only the horizontal measurement to be taken. The probe can then be flushed with water, clearing any debris which may have entered during the tests. Any “smearing” was to be eliminated using the flushing technique.

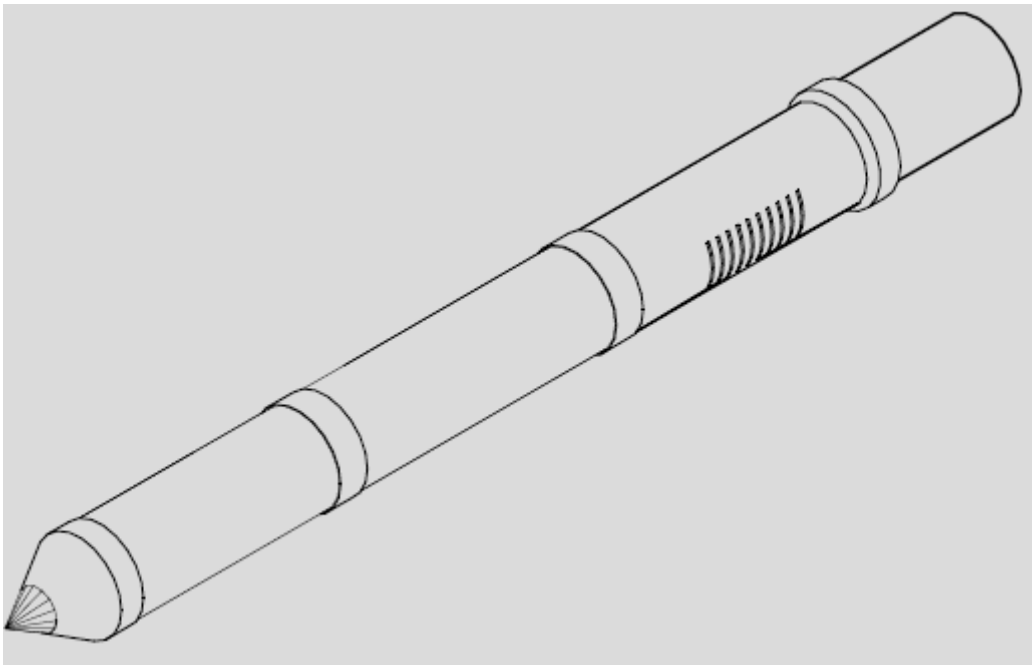

Figure 3-12. Wire/Heavy nylon brush full probe schematic

3.6.3 Swiveling Machined Metal Teeth – Design C

Another design (Figure 3-13), involved a set of machined “teeth” (C2) which would be part of the inner central shaft (C1). The piece would be machined out of a single piece and the teeth would not be removable. The outer, slotted sleeve of the probe would be made up of two halves (C3 & C4) joined together by 4 screws. This solution however, made no improvement on the issue of separating flow, and would not allow the inner shaft to be raised and lowered. It was therefore rejected.

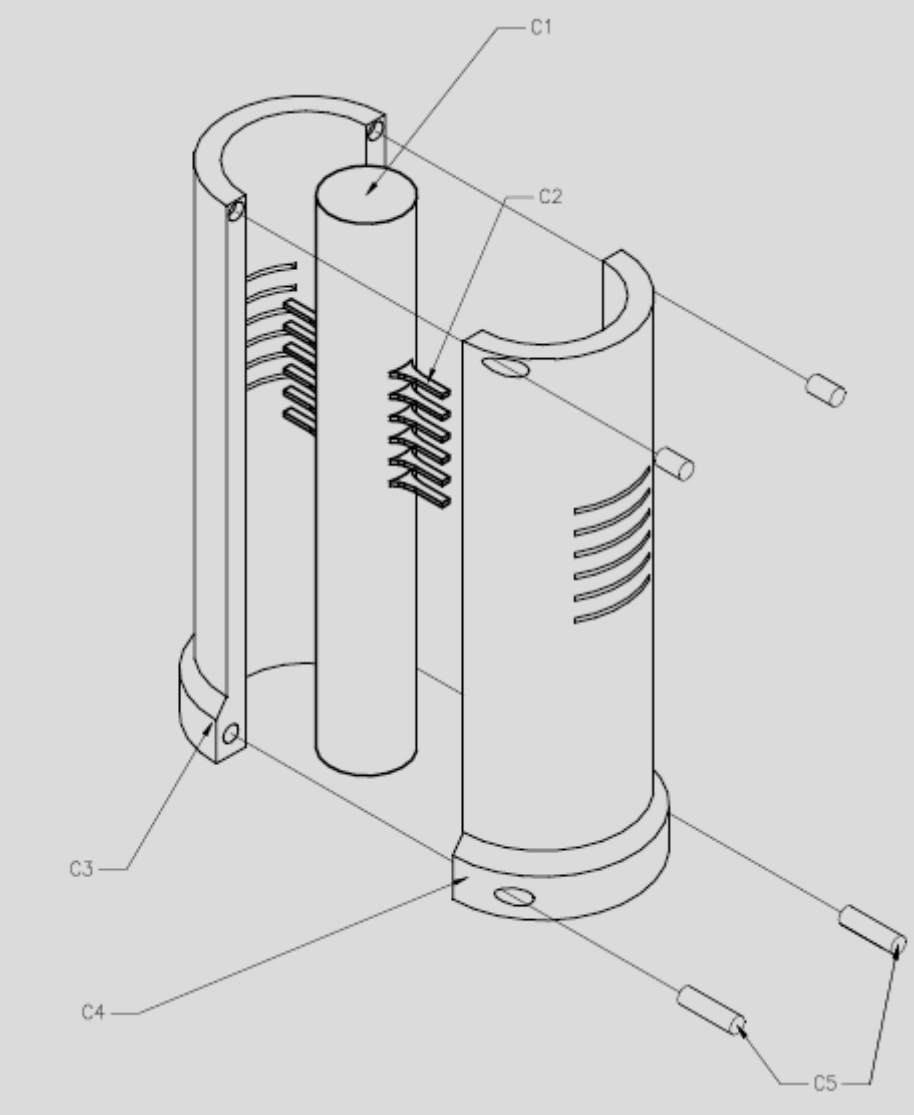

Figure 3-13. Swiveling machined metal teeth schematic

3.6.4 Swiveling Machined Metal Teeth Revision – Design D

To separate the vertical and horizontal flow of water, design C was modified (Figure 3-14) to allow the inner shaft (D1) to be raised and lowered without affecting the metal spikes used to clear the slots. The spikes would no longer be machined into the inner shaft; instead they would be integrated into a sliding collar (D2) which would slide down onto the shaft. This design would allow the center rod to be raised and lowered independently from the collar, but would turn with the collar when test depth was

reached. Both the collar and the shaft would be keyed (D3) to help turn the spikes when necessary. The outer sleeve of the probe would be made up of two halves as in part C (D4 &D5) and joined together by four screws (D6). Debris would be cleared by rotating the teeth back-and-forth. Flow separated could be achieved using the same procedure discussed in Design B.

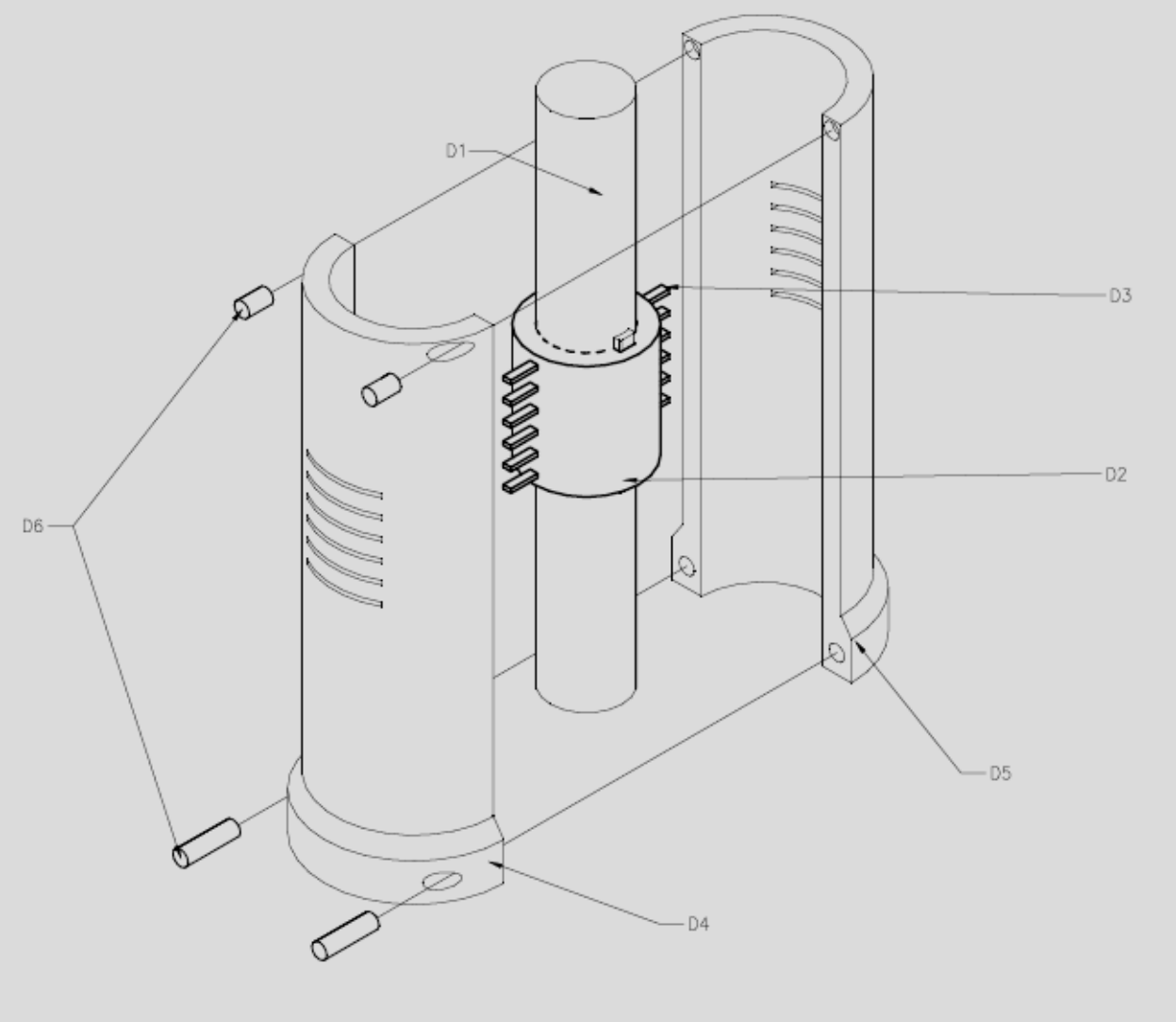

Figure 3-14. Revised swiveling machined metal teeth schematic

3.6.5 Recessing the Slots Relative to the Rest of the Probe – Design E

Using simple changes to the original design of the probe, recessed slots were designed to keep debris from jamming the probe (Figure 3-15). This design was

ultimately rejected because the soil next to the slots would not have been in contact with the outside walls of the probe. Because of this, the water would have not exited the probe in a horizontal direction.

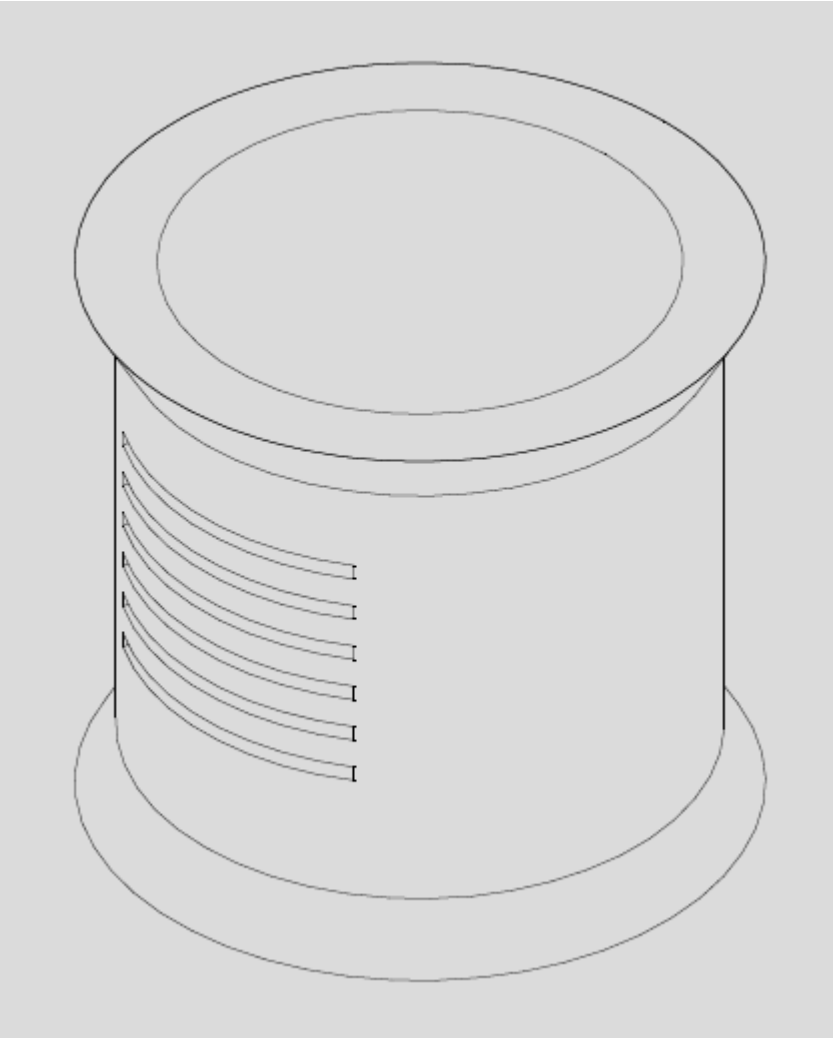

Figure 3-15. Recessed slot schematic of horizontal flow slots

3.6.6 Rotating Shield – Design F

This solution (Figure 3-16) took the recessed slots proposed in Design E, and added a shielding mechanism to the existing slots (F1). The probe would be lowered to the desired depth with the shield covering the slots. Once there, the shield would be rotated exposing the slots and allowing water to flow outward. The shield would be attached to the inner shaft through two slots by one or two “arms” (F3), and actuated by

rotating (F2). The outer sleeve of the probe (F4) would have a recessed channel in which the shield(s) could rotate. A significant hurdle to this design is the difficulty associated with sealing F1 to F2 to prevent loss of volume before measurements are taken. Secondly, the shield arms (F3) would need to be strong enough as to prevent failure when rotating the shield open/closed. Finally, the soil would most likely be disturbed by the shields, and cause the results to be inaccurate.

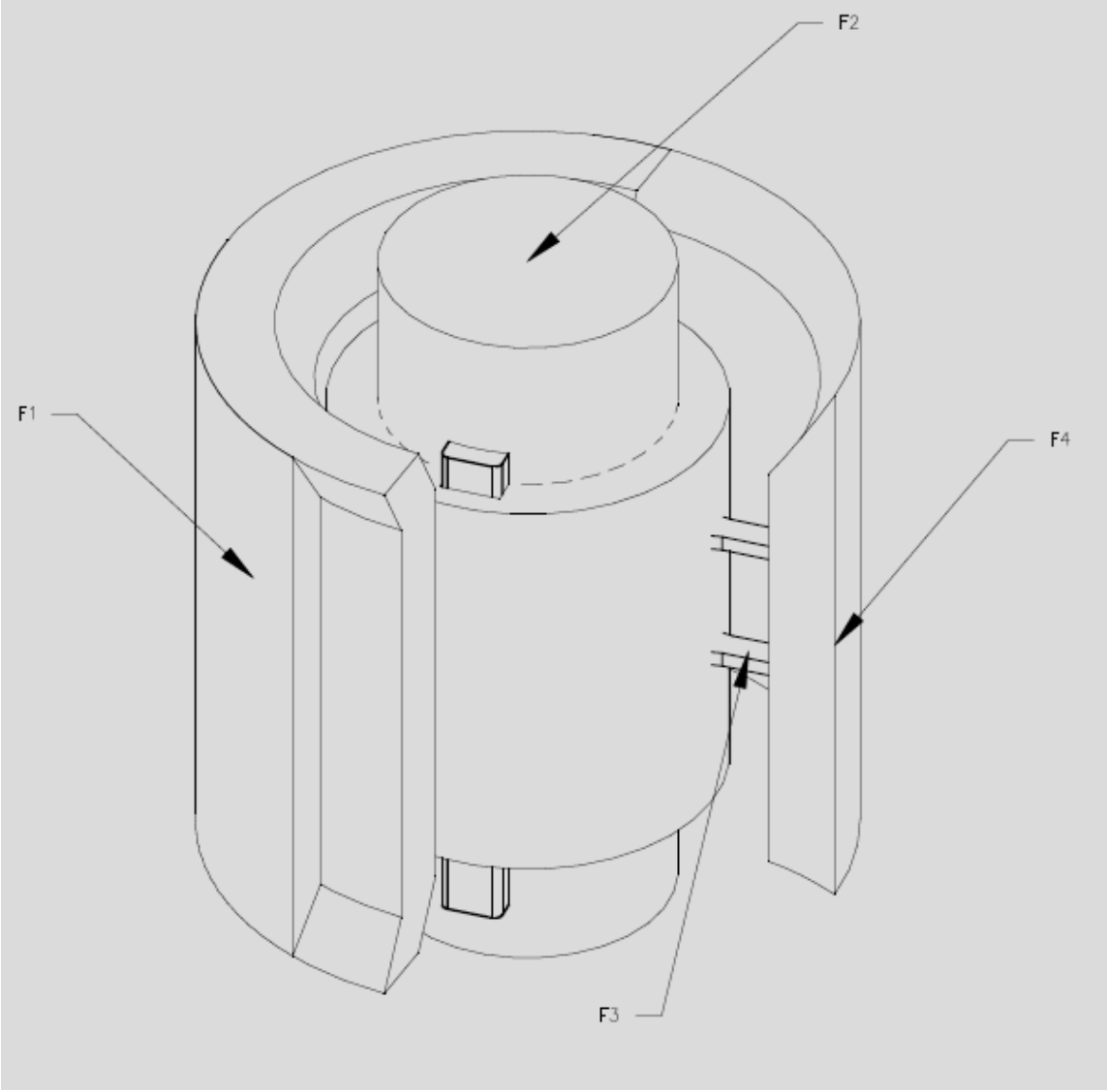

Figure 3-16. Rotating shield schematic

3.6.7 Sealing Rubber Attachment – Design G

This design (Figure 3-17) involved having an inner lobed shaft (G1) which could be rotated about its axis so that it put pressure on an internal flexible rubber insert (G2). The insert/membrane would be located in the probe section containing the horizontal slots (G3) and would be loosely attached to the inner wall of (G3). The membrane would be pressed onto the inner walls of the probe by a camshaft, sealing the slots until the probe reached the desired depth.

Vertical data would be obtained first by pulling up on the probe's inner rod. To obtain the horizontal measurements, the inner shaft would be rotated 90 degrees allowing the rubber to contract and water to flow out. However, initial testing indicated problems with the durability of the rubber membranes. The horizontal slots would shear off pieces of the rubber membrane when rotated out of the closed-off stage. Over time the sealing properties of the membrane became compromised as more of the membrane was lost in rotation. This design was determined to be ineffective.

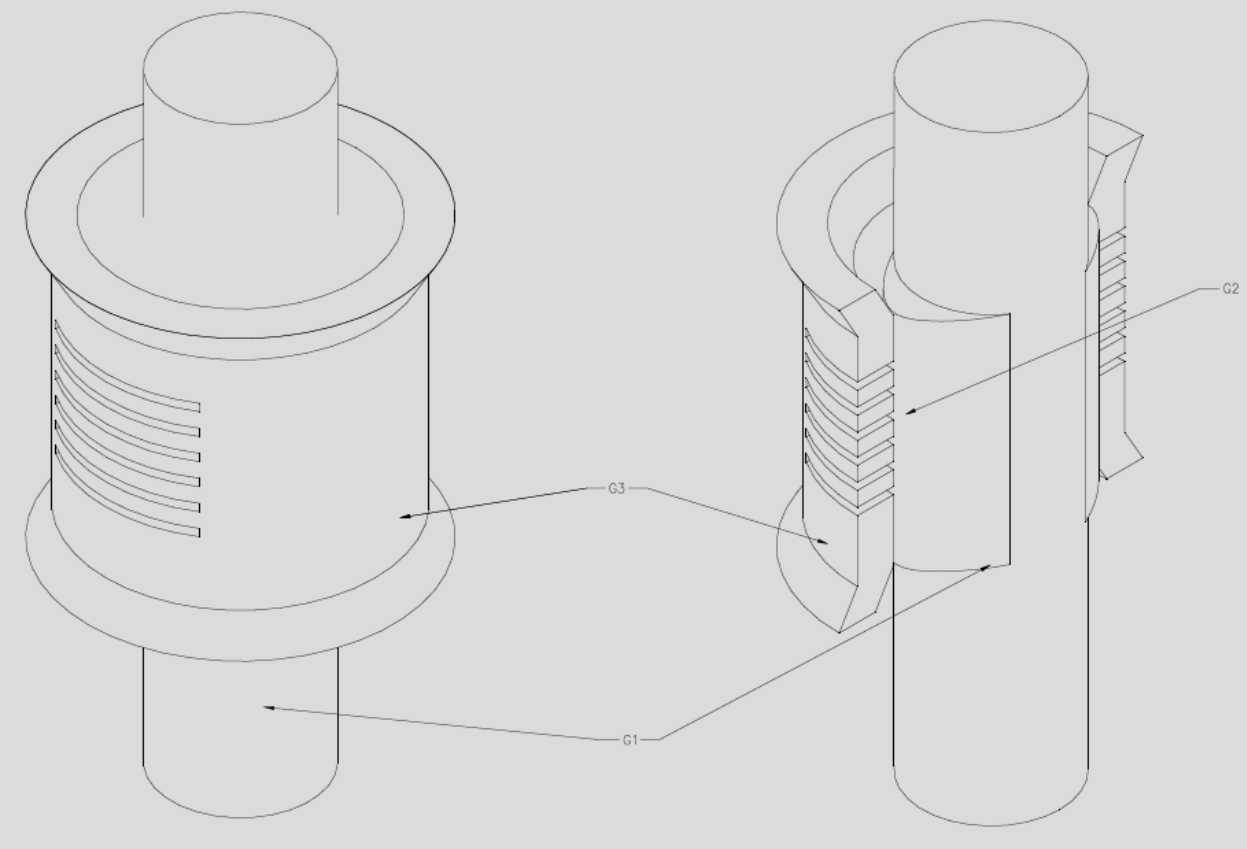

Figure 3-17. Sealing rubber attachment schematic

3.7 Development of New Prototypes

After much investigation and initial testing, researchers decided on two possible prototypes – a rotating wire brush and rotating metal teeth.

3.7.1 Wire Brush Prototype

Figure 3-11 from Section 3.6.1 is reproduced here to illustrate the wire brush design.

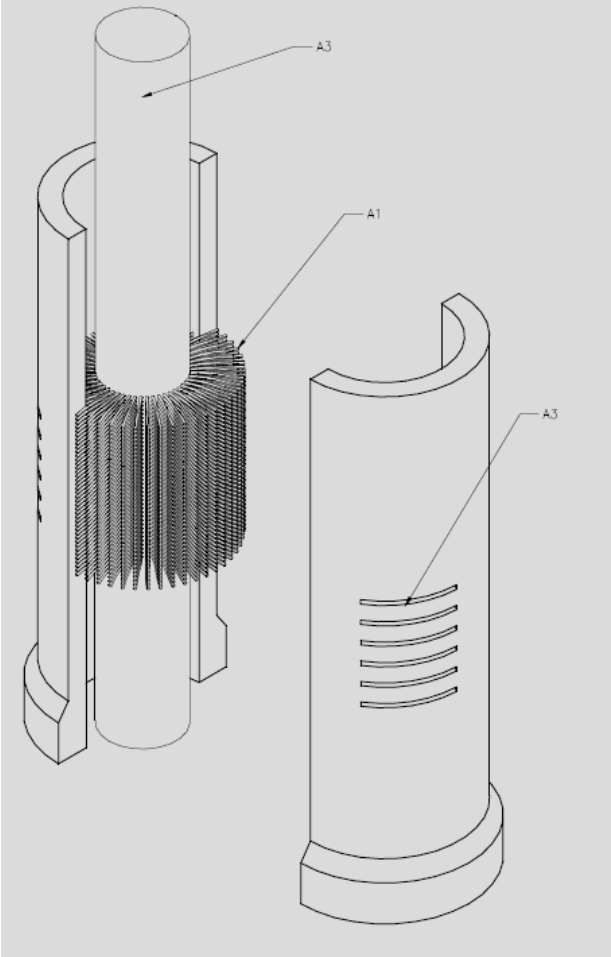

Figure 3-18. Wire brush schematic for VAHIP design

Rather than attach brushes to the entire VAHIP inner-rod circumference investigators realized that two more elegant solutions existed:

1. Two series of linear brush strips could be attached at ninety degree intervals. Thus, from the top-down, brushes would be present from zero to 90 degrees, and 180 to 270 degrees. Before a test, the brushes would be positioned such that they penetrated the horizontal slits (the “protection position”). When it was time to run a test, the brushes would be rotated ninety degrees such that the brushes no longer obstructed the slits. After the test, brushes would be returned to the “protection” position as the probe was pushed to a new depth.

2. Instead of dividing the VAHIP along its diameter (such that there were two series of slits), the slits could be made in three distinct intervals. Thus, holes could be machines along ninety degrees of the probe while thirty-degree gaps would separate the slit-groups. Then, wire brushes could be attached to the inner rod at 120 degree intervals. Before a test, the inner rod would be rotated while brushes would poke through the slits. Several rotations were thought to be enough to remove smeared debris that could disrupt a test.

While the probe's initial design showed a series of probes with "split" outer cylinders, investigators realized that splitting the probe in half and re-attaching with a series of screws may be problematic. Outer casing wall thickness is relatively thin (0.25 inch). Because of this, a series of tiny screws would be required to reattach the two split halves of the probes together. A screw series may prevent field engineers from having the ability to take the instrument apart and clean it between tests.

A thicker wall was considered, but eventually this was ruled out in favor of using as much of the existing probes as possible. It was thought that if the wire brushes were elastic enough and short enough, the inner rod could be inserted into the VAHIP with the brushes, and some of them should penetrate the horizontal slits on their own.

When the brushes were trimmed to be short enough to fit within the inner rod-outer casing clearance cavity, investigators noticed a "matting effect" where the brushes failed to penetrate the horizontal slits. While expanding the clearance between the inner rod and outer casing was considered, investigators did not think this would be a viable solution. Instead, it appeared that "matting" would continue – albeit further along the brush length. Ultimately, the wire-brush solution was deemed to be ineffective and it was abandoned.

3.7.2 Metal Teeth Prototype

Once the wire brushes had been abandoned the focus was on the metal teeth alternative as discussed in Sections 3.6.3 and 3.6.4.

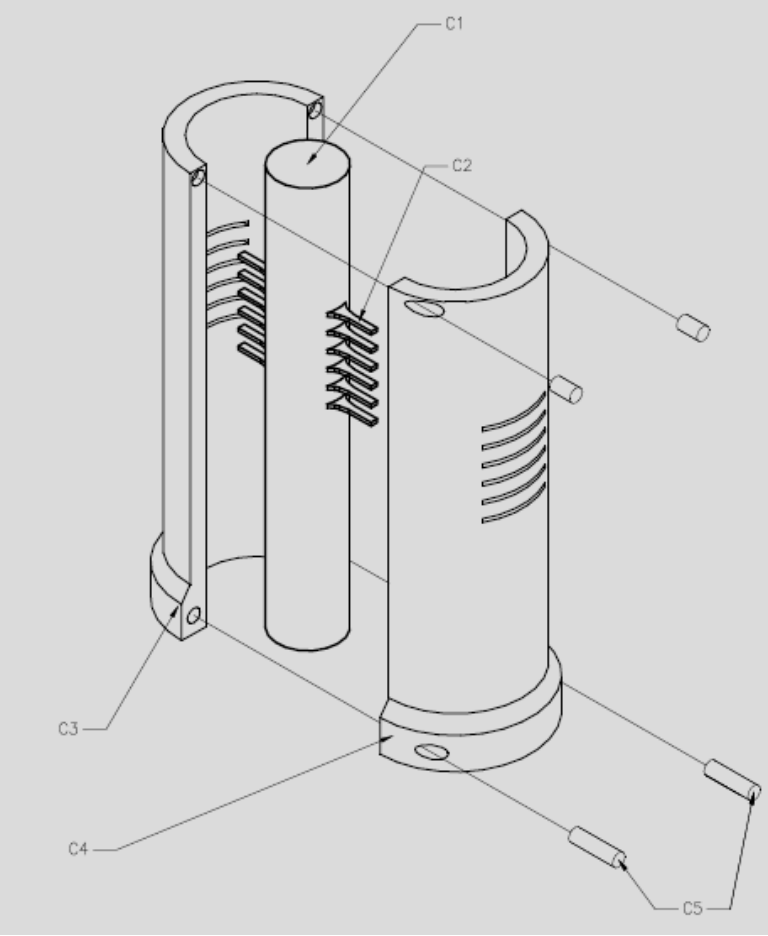

Figure 3-19. Metal teeth prototype schematic

Again, investigators did not wish to “split” the probes outer-casing due to concerns addressed in Section 3.7.1. Rather, two metal “teeth” were constructed and two corresponding grooves were machined along the device’s inner rod such that the device could still move up-and-down to initiate a vertical permeability test (Figure 3-20 and Figure 3-21). Because the grooves extend to the bottom of the inner rod, the rod could still be inserted into the probe (Figure 3-22).

Figure 3-20. Photograph of VAHIP metal teeth

Figure 3-21. Photograph of teeth and grooves

Note – grooves adjacent to “teeth groove” are leftover from wire brush prototypes. Rather than machine a new rod, existing material from the abandoned design to save material/time were used.

Figure 3-22. Rod insertion into VAHIP

The metal teeth function as designed. The metal teeth effectively moved back-and-forth when the inner rod is twisted and they allowed the inner rod to be lifted such that a vertical permeability test could be initiated.

Figure 3-23. Completed smear-resistant VAHIP prototype

However, preliminary testing appeared to indicate that this design method would be ineffective. Even though the metal teeth could remove debris from the horizontal

slits, this design did not prevent debris from entering the slits prior to the rotational cleaning. The effect of this was that the instrument had a tendency to “bind up” when driven to test depth such that a vertical test could not be conducted. To make matters worse, initiation of a vertical test caused sediment to enter the bottom of the probe when the probe’s inner rod was pulled vertically – thereby preventing further inner-rod movement. Another issue with the design is that there was no control of the initial horizontal flow.

At a March 10, 2011 demonstration meeting, FDOT indicated that they would prefer a method where the rods and possibly the probe can be filled with water, and a valve mechanism could be installed to signify the “beginning” of a test. Based on several emails between UF and FDOT and discussion on June 2, 2011, researchers ultimately determined that a probe was required that could be “closed” until the probe reached test depth and “opened” when a test began.

3.8 New Design Prototype

In previous design attempts researchers abandoned the idea of an internal expandable solution. As discussed, it was thought that this method would be too complex for quick assembly and disassembly in the field, and that this complexity may lead to breakage. Since the new design goal was to develop an “open” and “closed” system, researchers were forced to re-explore the internal expandable solution. Following the new design criteria, a new probe was designed.

The new probe has many of the old design features and from an external standpoint, looks similar to the old probes. The primary difference between the old probes and the new probe is that the horizontal slits were replaced with vertical slits.

Vertical slit alignment allowed a system of tracked “keys” to be developed such that the keys can fill the vertical slits when the probe is pushed to test depth and can be opened when a test is initiated. The vertical “keys” were inserted into grooves along the inner circumference of probe’s outer-rod-casing such that once in place, rotational motion will not cause them to be dislodged from their tracks. In total, the probe was designed with 12 of these track-key slits such that horizontal flow is achieved in 30-degree increments around the probe’s circumference.

The new design also made use of four O-rings: two in the tip; one midway through the probe; and a final O-ring in the top portion. The tip and top portion O-rings were strategically placed within the probe to ensure that only flow in the desired direction occurs during stage lifting (adding the best elements from Design B above). The mid-probe O-ring was introduced to prevent water from entering the top portion of the probe and spilling out of the horizontal permeability slits during vertical testing. The top O-ring prevented water from exiting the top of the probe.

The new probe design also included a friction reducer. As the probe is inserted into the ground, a newly designed wider top-section creates a void in the ground that is larger than the AWJ rods’ outer diameter (2.0 inch vs. 1.625 inch). By creating a larger void than the AWJ rods’ outer diameter, movement of the rods becomes easier when the probe is pushed into the ground because side friction of the rods extending to the surface is eliminated.

Rather than machining the new prototype out of stainless steel, a PVC model was built to test the probe’s relatively complex mechanical components. Results from preliminary PVC tests gave researchers the information needed to make improvements

to the device. A three-dimensional design model of the new prototype is presented from Figure 3-24 through Figure 3-27.

Figure 3-24. Three-dimensional isometric view of new probe design in “closed” position.

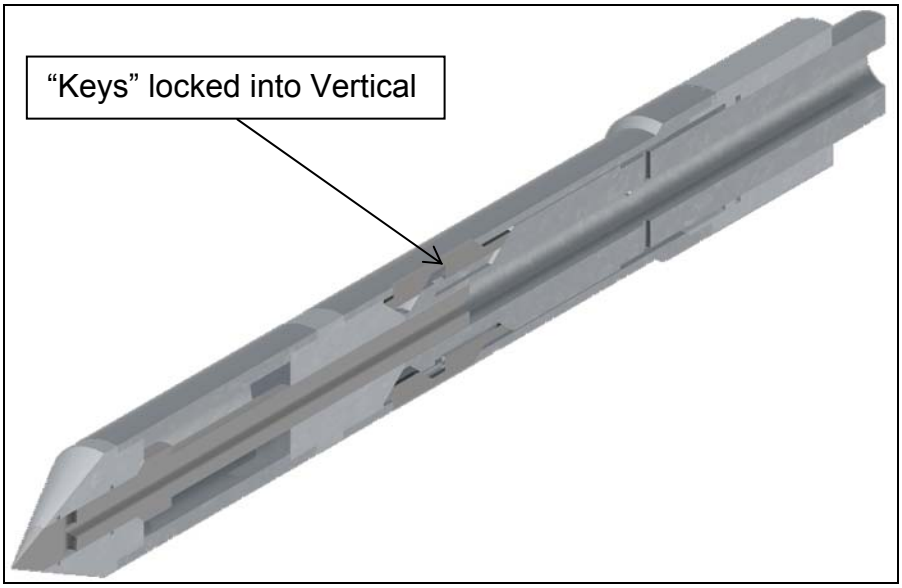

Figure 3-25. Three-dimensional isometric cutout of new probe in “closed” position.

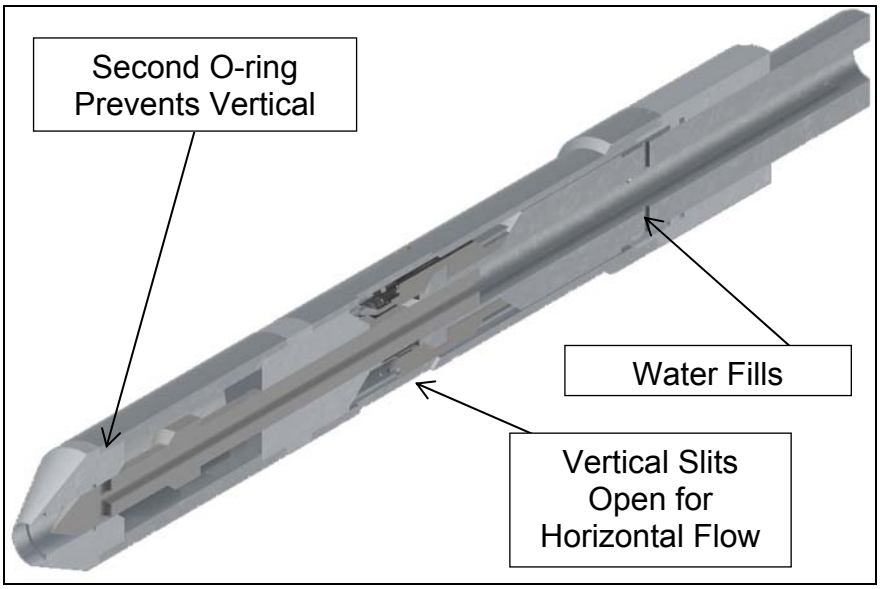

Figure 3-26. Three-dimensional schematic of first-stage of test where water flow paths are indicated.

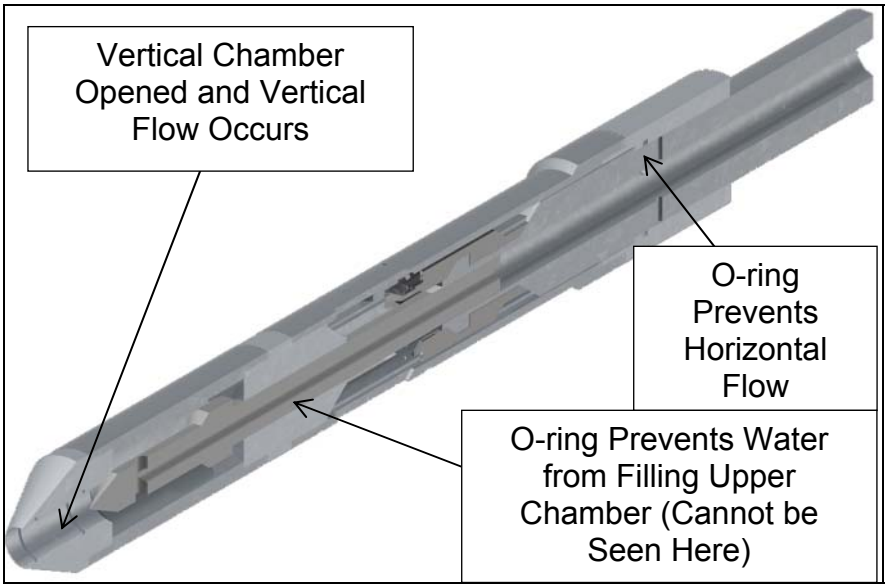

Figure 3-27 Three-dimensional schematic of second stage of test where water flow paths are indicated.

As indicated, the probe's inner rod was to be lifted one inch to open the vertical slits. Water would fill the chamber and horizontal flow would be initiated. Then, the probe's inner rod would be lifted another one inch to allow water flow out of the probe's bottom openings while preventing flow from moving horizontally. As such, horizontal and vertical tests were now independent from one another.

The new probe design is only one of two elements that researchers recommend to alleviate some of the issues discovered during preliminary testing. In addition to providing a "closed" probe design, researchers also believe that a new testing procedure will be required to prevent sediment from entering the probe during vertical and/or horizontal testing. Specifically, after testing, the probe must be "flushed" using high-pressure water (from the device's reservoir tank) to prevent sediment intrusion between tests.

3.8.1 Initial Sand-Barrel Testing

The prototype probe was fabricated in the middle of July 2011, and preliminary sand-barrel testing was conducted to identify the probe's weaknesses. The procedure for sand-barrel tests was as follows:

1. A 55 gallon barrel was filled approximately 1.0 foot with an A-2-4 soil.
2. The probe was inserted into the barrel at a fixed location.
3. Approximately 6 inch soil lifts were added to the barrel.
4. Each lift was compacted using a tamping rod.
5. Steps 3 and 4 were repeated until the probe was buried.
6. The water vessel was attached atop the probe and filled.
7. The water vessel's valve was opened until the probe was filled. Once the water level in the tank had stabilized the probe was defined as "ready-for-testing."

8. The inner rod of the probe was retracted one inch by pulling upward on the AWJ connection piece. This “first-lift” allows water to flow out of the probe’s horizontal slits, and it marks the beginning of the “horizontal test.”

9. Water was allowed to flow until the approximately four inches of water had been drained from the water vessel. This point marks completion of the “horizontal test.”

10. The inner rod was retracted an additional one inch to stop horizontal flow and allow vertical flow to begin. This marks the beginning of the “vertical test.”

11. Again, water was allowed to flow until approximately four inches of water had been drained from the water vessel. This point marks completion of the “vertical test.”

12. While water was still flowing, the inner rod of the probe was pushed down two inches. Thus, the probe was flushed as it was closed.

13. The probe was pulled out of the sand barrel and brought to a sink where excess debris was cleaned from the outside of the probe using an irrigation bottle filled with water.

14. The probe was disassembled over a water-filled pan so that debris that entered the probe during testing was collected.

15. The pan was carefully drained and inspected for remaining debris.

Assembly and disassembly of the probe were also conducted to ensure both could be accomplished quickly and efficiently. The individual components of the probe can be seen in Figure 3-28.

Figure 3-28. Disassembled probe showing individual components

At the July 28, 2011 FDOT Geotechnical Research in Progress (GRIP) meeting, a video was presented to demonstrate quick probe assembly. As shown in the video, assembly time is approximately one minute and no external tools or equipment are required. Figure 3-29Figure through Figure 3-31 are presented to illustrate the probe's testing stages:

Figure 3-29. Closed stage

Vertical slits in the outer shell and a series of internal tracked keys that lock into the vertical slits when the probe is closed appear to prevent smearing and debris intrusion. This stage is used to push the probe into the ground.

Figure 3-30. First lift stage – horizontal flow

The new probe uses a two-stage lifting system. The first stage is used for horizontal flow. The inner core of the probe is lifted approximately one inch, and the tracked keys retract so that water may flow freely from the probe's outer shell. O-rings prevent vertical flow.

Figure 3-31. Second lift stage – vertical flow

In the second stage, the probe's inner rod is pulled up an additional inch. Water is now free to flow through the vertical flow port located in the tip of the probe. O-rings are placed in the top and mid-section of the probe to prevent horizontal flow during this stage.

3.9 Redesigned Prototype

At the 2011 GRIP meeting, FDOT indicated that they needed a way to "know" the inner rod's relative position with respect to probe's outer shell. Investigators determined that the best solution was to provide a series of locking mechanisms during each lift-stage such that when the specified lift-stage ended (i.e., the inner rod had moved up a specified distance relative to the other shell), the probe could be locked into place – thereby assuring "open" and "closed" positions.

To create this locking mechanism, a rotational component was designed. A small "knob" was added to the inner rod (Figure 3-32 and Figure 3-33), and a track was added to the probe's lower chamber (Figure 3-34). Because there was some concern about the possibility of the probe's outer shell "slipping" (i.e., rotating within the soil), wings were added to it (Figure 3-35).

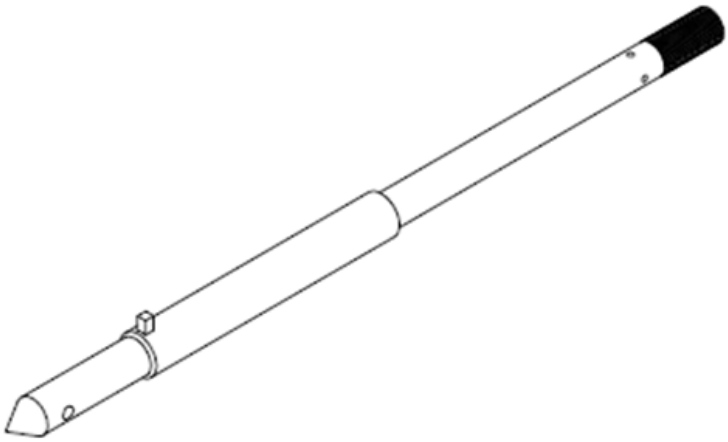

Figure 3-32. New inner rod with “knob”

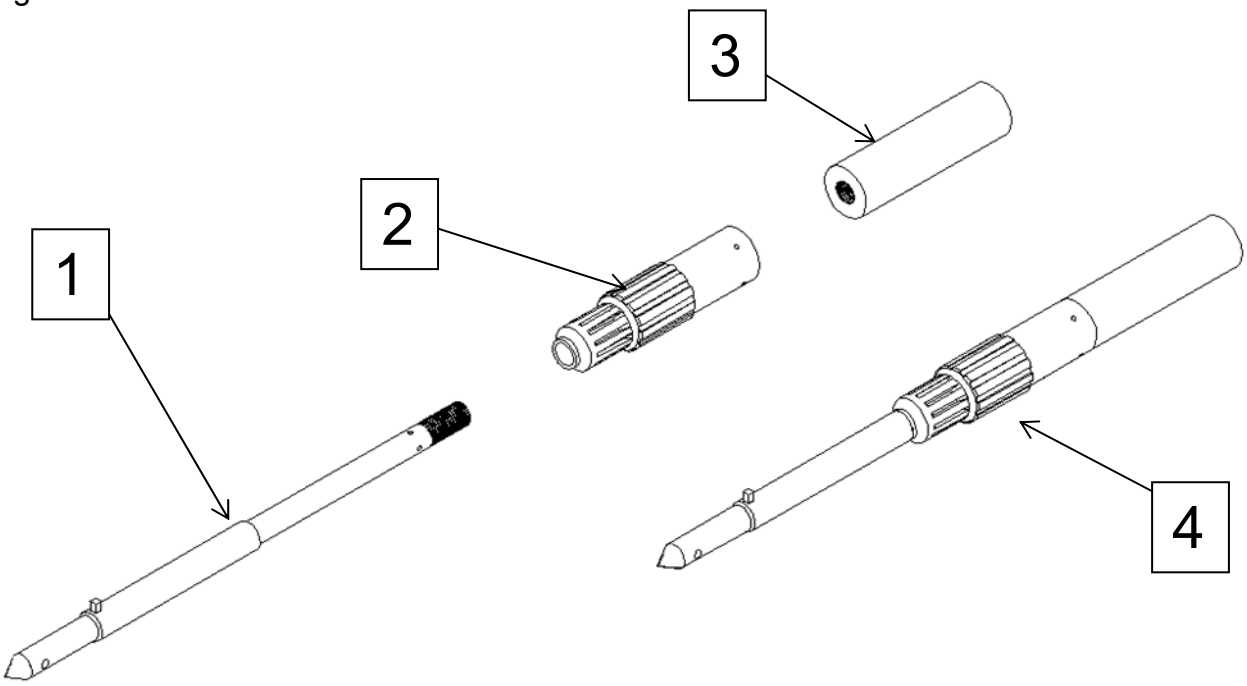

Figure 3-33. New inner rod attached to freely rotating piece through tracked inner-core

1. New inner rod
2. Tracked inner-core male piece
3. Freely rotating piece that meets with the AWJ connection
4. Inner rod inserted through the tracked inner-core male piece and attached to AWJ connection

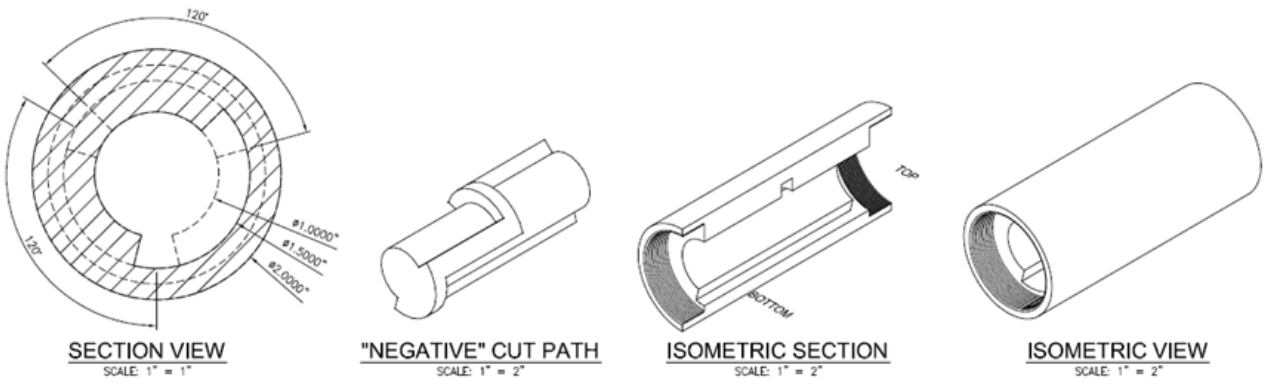

Figure 3-34. New lower chamber with tracking system

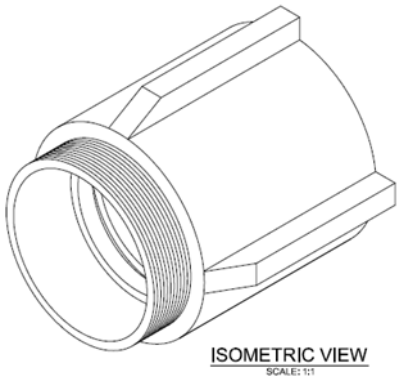

Figure 3-35. Friction reducer with “wings” added

A testing procedure for the “locking” probe was developed:

1. The closed probe is connected to the SPT/CPT rig drill rods via an AWJ connection and pushed to the required depth below ground.

2. The water vessel is attached atop the drill rods via an AWJ connection piece.

3. Water is introduced to the system and the probe is allowed to fill completely (as determined by water-level stabilizing in the water vessel). The probe is now ready to begin testing.

4. The closed probe’s inner rod is rotated clockwise approximately 120 degrees by rotating the connected drill rods at the surface. After 120 degrees, the tracks will prevent any further rotation. The inner rod is then lifted 1.75 inches and rotated an additional 60 degrees in the clockwise direction (the track will prevent any more than 1.75 inches of vertical movement). The probe is now locked into the open horizontal flow position, the tracked keys are retracted, and the vertical slits are open. Water will begin exiting the probe and data can be recorded for horizontal flow.

5. After horizontal testing, additional water can be introduced to the water vessel if necessary.

6. The inner rod is rotated 60 degrees clockwise, lifted 1.75 inches, and rotated an additional 60 degrees. The probe is now locked into the open vertical flow position and horizontal flow is restricted by O-rings. Water is now free to flow through the vertical flow port in the probe's tip. Data can now be recorded for vertical flow.

7. After vertical testing is complete, the water vessel is refilled and the pressure tank is attached to the water vessel. Pressure is then added to the water vessel (exact pressure needed is to be determined).

8. The inner rod of the probe is now rotated the final 60 degrees and then slowly pushed downward 3.5 inches. This final stage flushes debris from the system.

9. When the probe can no longer be pushed downward, the 3.5 inches. drop has been reached. The probe is rotated another 60 degrees and it can be pushed to a new depth.

The degrees of rotation discussed in this section are general "rules of thumb" and do not need to be exact. The operator will know when the probe has been rotated enough for each stage because the track ensures the knob will reach a "dead end" before the inner rod can be lifted.

In the closing stage the knob is returned to its original position. The 60 degree rotation at the end of the closing stage is to ensure the probe is fully closed. If the probe is unable to be closed the likely cause is debris intrusion. To fix this issue, the inner rod can be retracted upwards again and a greater flushing pressure can be applied to the probe. Note, clockwise rotation was chosen so that the probe and drill rod threading are not loosened.

3.9.1 New Steel Probe

On March 26, 2012, a finalized steel probes was manufactured based upon the PVC prototype. The mechanics of the probe functioned as designed. The new probe tracking system now provides a way for field workers to ensure the probe is in the appropriate stage of testing. The new steel probe is shown in Figure 3-36.

Figure 3-36. New steel probe with AWJ rod attachment

3.9.2 Development of the New Water Vessel

To accompany the new probe, researchers also developed a new monitoring station. The previous Plexiglas standpipe was consisted of a 1.5 inch outer diameter (1.13 inch I.D.) Plexiglas tube mounted on top of a 4.0 inch diameter (3.55 inch I.D.) Plexiglas tube. Water was introduced through an open male quick connect which was threaded to the top of the four inch tube. Water level or head readings are obtained using either the bigger or smaller tube as appropriate during testing. It was expected that during testing of soils with low permeability, the smaller standpipe would be utilized in monitoring water level drops and vice versa. A smaller, open, male quick connect was threaded into the top of the 1.5 inch (smaller) tube and was used to apply an additional pressure head when testing if necessary. An AWJ male thread welded to a four inch diameter steel plate formed the base of the Plexiglas standpipe thus making the assembly easily compatible to an SPT rod. This device (Figure 3-37) had a number of advantages:

- Changes in water levels were easy to read.
- It could be easily attached to an SPT rod.
- It was easily filled with water.
- It was capable of being pressurized to increase head.

Figure 3-37. Picture of flow measurement device (FMD)

A control panel (Figure 3-38) was designed to allow the operator to easily control the test from one location. It regulated flow into the Plexiglas Flow Measuring Device (FMD), introduced pressure to the FMD, and maintained nearly constant flow rate during constant head tests via an internal pressure tank and a series of valves. Flow rates were measured with a micro-flow sensor that was connected to two connector ports installed on the panel.

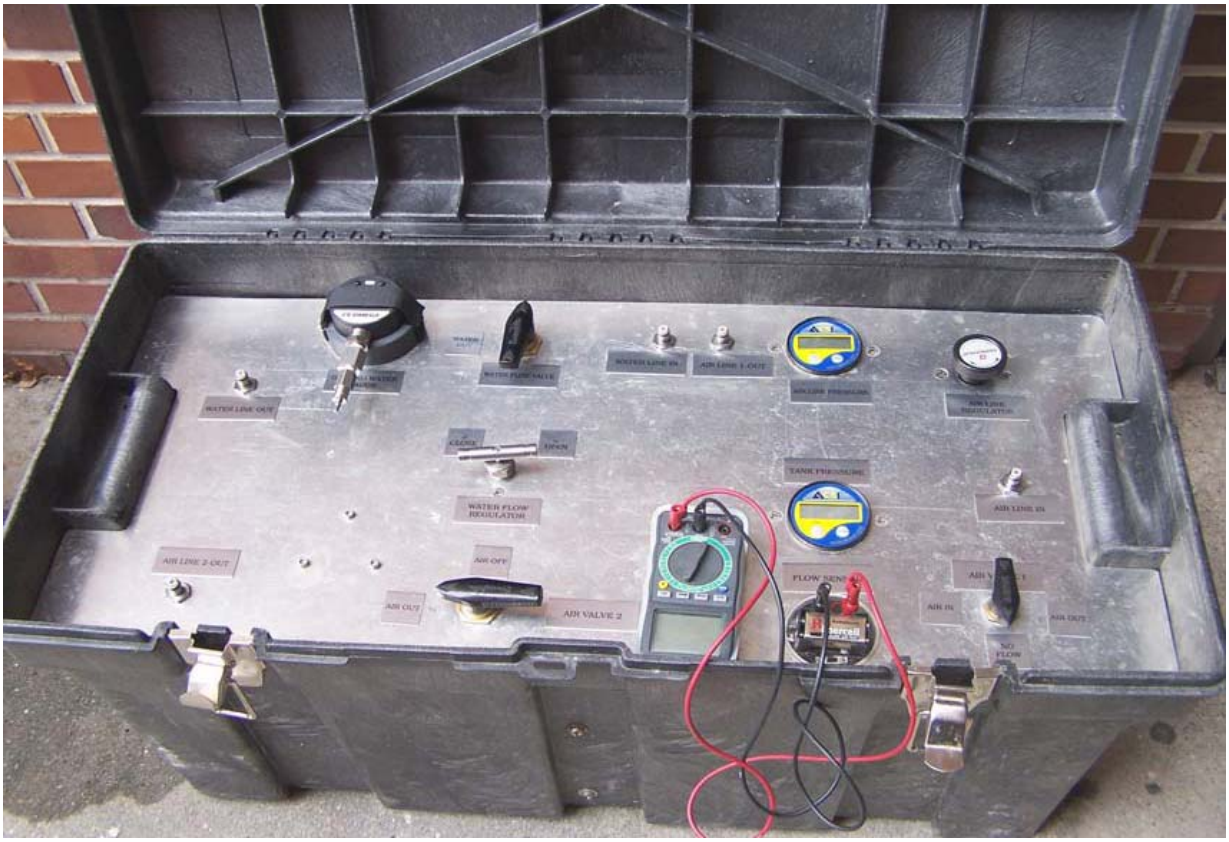

Figure 3-38. Picture of control panel

3.9.2.1 Water Vessel

The control panel was equipped with a 7 gallon air tank and a Buell 12 volt air compressor, which was used to pressurize a 13 gallon Nalgene water container. This system was capable of running one series of tests (falling head vertical and horizontal, constant head vertical and horizontal). After the series of tests, both the water container and the air tank needed to be refilled with water (depending on the initial saturation state of soil) or compressed air. Since most SPT/CPT rigs are equipped with air and water tanks, this should not be inconvenient.

3.9.2.2 Methods of Monitoring

While this system had a number of advantages, investigators ultimately determined that he system was too complicated and bulky to be used in the field. To

simplify testing, researchers sought to develop a better method for monitoring the amount of water added to the ground during a permeability test. Researchers identified three improved alternatives for tracking the water's flow rate through the soil during a test:

- Method 1. Build a small falling head water vessel, and attach a scale to its side to track the amount of water used during a test. Star a stopwatch at the beginning of each test, and record the water level in the vessel as a function of time. Thus, average flow rate is computed directly as change in water volume divided by change in time.

- Method 2. Attach an ultrasonic sensor to the top of the falling-head vessel, and connect an LCD screen to the sensor to read its output signal. A small battery (12 to 15 volts) attached to the ultrasonic sensor powers the instrument. At the beginning of the test, record the water level from the LCD readout and a timestamp. At the end of the test, record the new water level from the LCD readout and a new timestamp. Calculate average flow rate directly, similarly to method 1.

- Method 3. Attached an ultrasonic depth sensor to the top of the falling-head vessel, and attach a National Instruments USB analog capture (DAQ device) unit to a laptop computer's USB port. The computer records depth data, and it provides electricity to the sensor. Because ultrasonic sensors require 12 to 15 volts of electricity, a DC step-up voltage regulator, a device capable of converting 5 volts of electricity to up to 24 volts, is required. A LabVIEW computer program is needed to read water depth signals from the sensor and to record a timestamp such that water level and time would be recorded in real-time. This setup allows for real-time flow rate data during a test, and it does not require an external battery. However, it does preclude investigators from running a test without a laptop.

UF contacted FDOT regarding these options on March 21, 2011. FDOT responded on March 22, 2011, and indicated that they would prefer to keep the method for measuring flow rate as simple as possible. Hence, Method 1 was pursued from this point forward.

3.9.2.3 New Water Vessel

UF researchers developed a small falling head vessel with US and SI unit scales attached to its sides to track the quantity of water used during a test. A stopwatch was

started at the beginning of each test, and the water level in the falling head vessel was recorded. At the end of the test, the new water level and final time were recorded. From here the inputs were entered into an analysis program and an average flow rate was calculated. Photographs of the new system are presented in Figure 3-39 and Figure 3-40. Initial trials appeared to indicate that the new design was functioning as designed. However, when the vessel was tested under pressure the bottom of it fractured. Therefore, a more robust design was required.

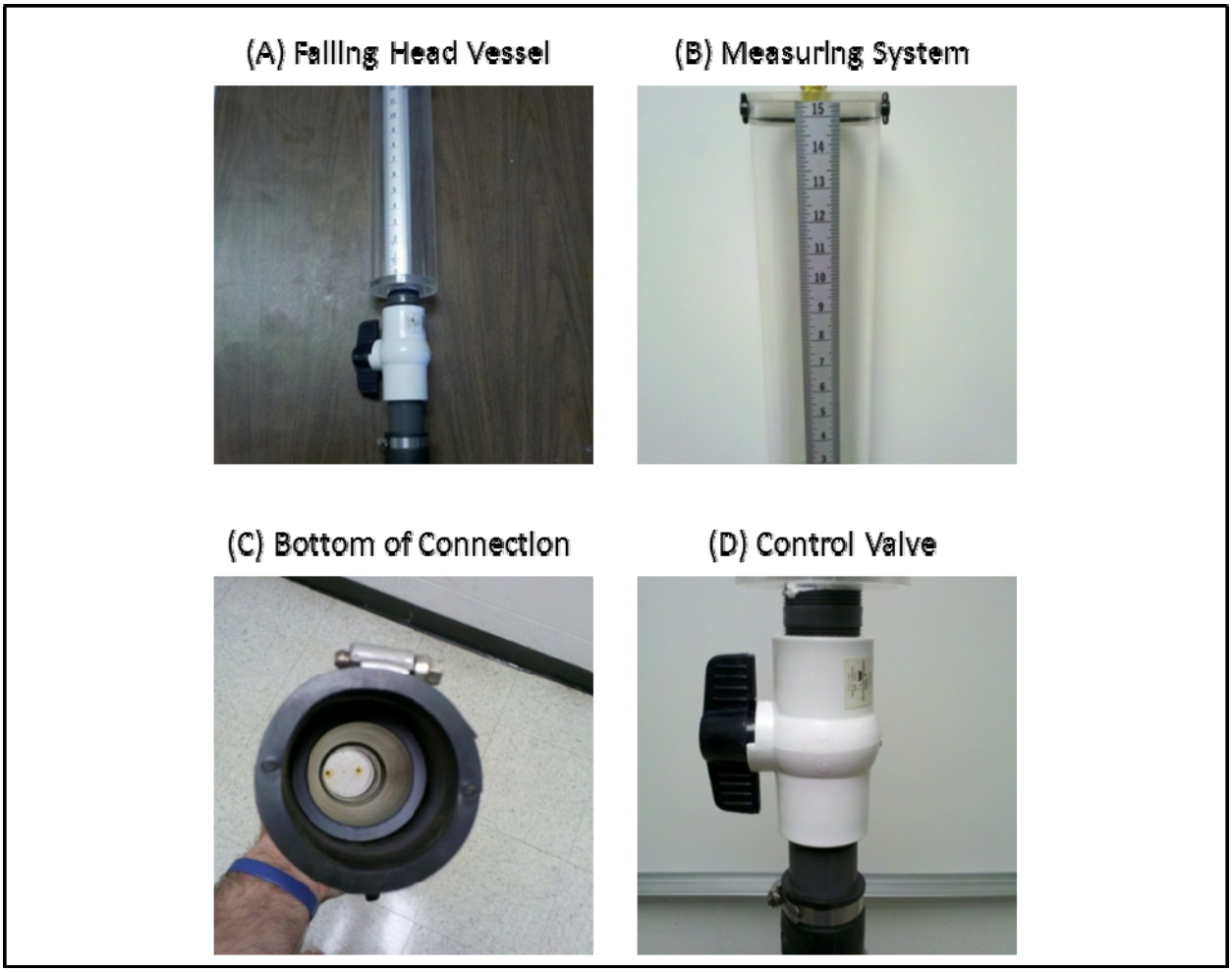

Figure 3-39. Photographs of the water-control vessel

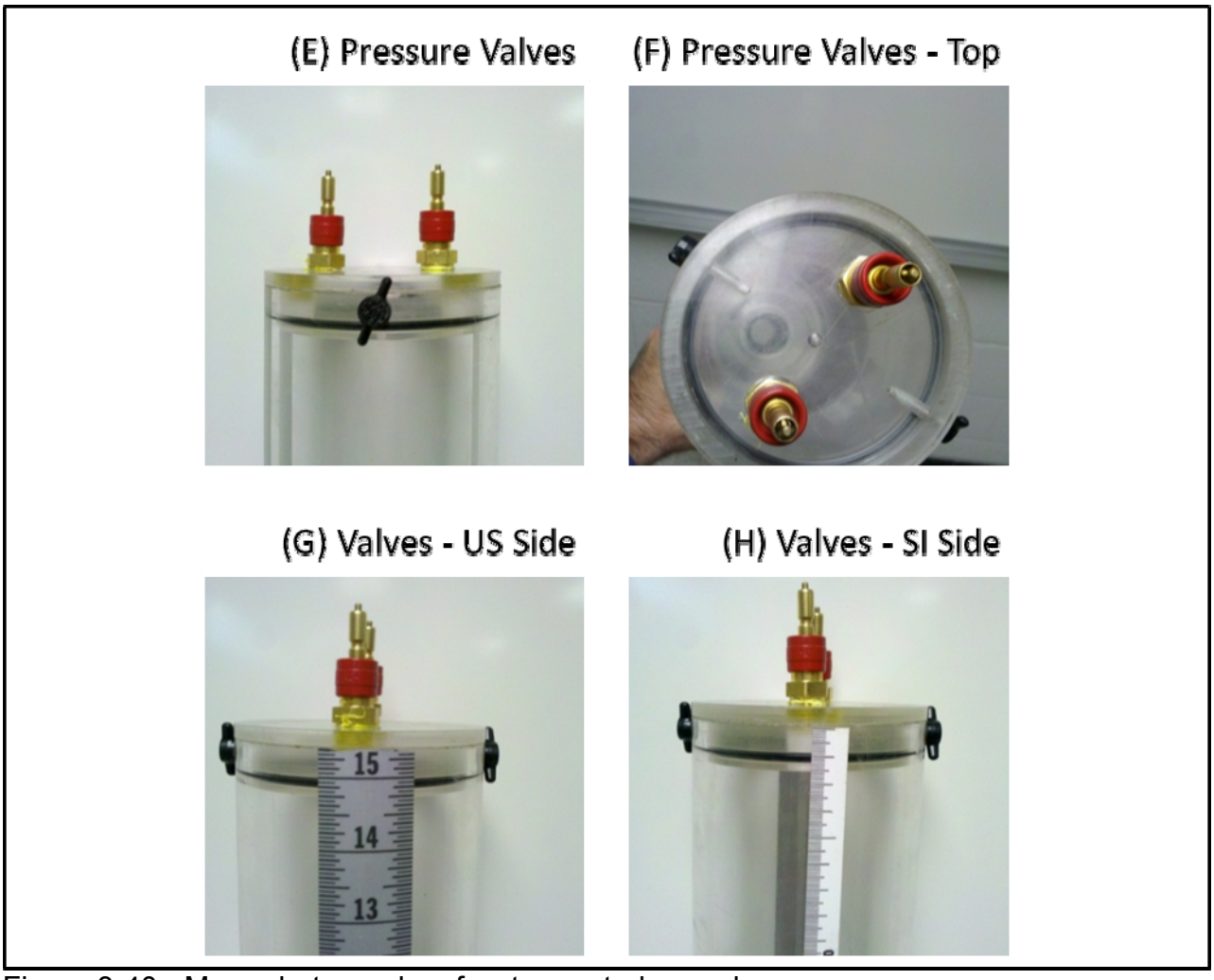

Figure 3-40. More photographs of water control vessel

3.9.2.3 Development of Robust Monitoring Devices

Two designs were developed for further testing. The first design was a pressurized monometer. A steel pressure vessel was fit with a tube so that water levels could be monitored (Figure 3-41).

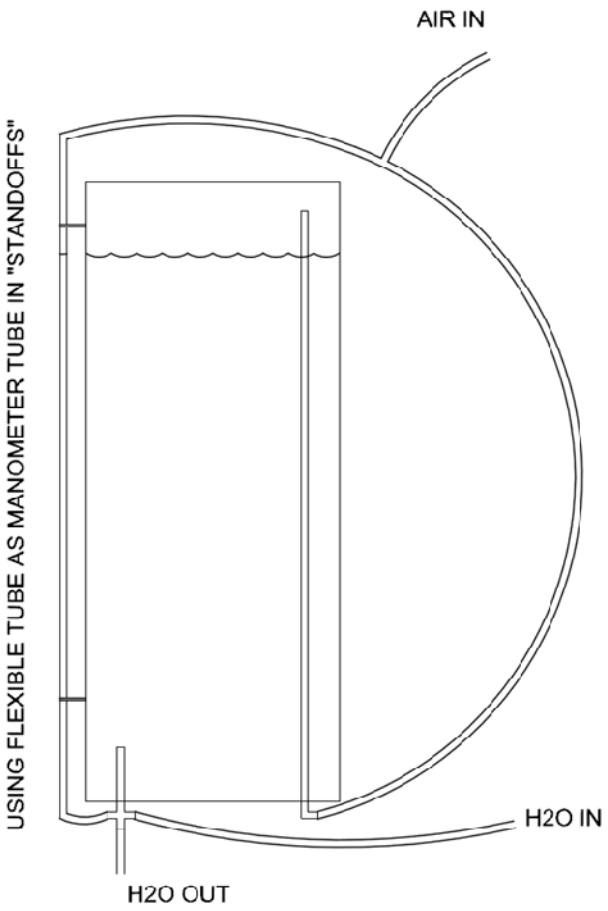

Figure 3-41. Pressurized monometer

The air intake pressurized the inside of the tank and its side tubing. This created an equilibrium pressure in both components, and it showed the water-level inside the tank. A prototype was developed using a beverage keg (a cost-effective pre-existing pressure vessel) turned upside down with tubing, flow ports, and a pressure regulator (Figure 3-42).

The prototype was tested and the results revealed several issues. First, the tank took nearly 30 minutes to fill, which is far too long for a VAHIP field test. Secondly, water was often forced from the monometer to the pressure intake, thus ruining the test. Third, the monometer water-level rarely stabilized, making it difficult to obtain an accurate reading.

Researchers hypothesized that increasing the keg's connection port openings might improve the results. A machinist was contacted to determine the feasibility of installing larger connections, but the machinist indicated that the wall thickness of the keg was too thin. While larger ports could be installed, the keg's structural integrity under pressure would be compromised. Because of these complications, researchers concluded that the pressurized monometer design was becoming too complicated. This solution was abandoned and the second new design was explored.

Figure 3-42. Pressurized monometer prototype

3.9.2.4 Pressurized Water Vessel

The second design was a new pressurized tank similar to the original water vessel. The new water vessel consisted of a transparent cylindrical tank with a unit scale attached to its sides. However, the new vessel was fabricated from a 2 feet by 6 inches diameter, schedule 40 PVC transparent pipe rated at 90 psi instead of the original clear acrylic. Two 0.5 inch steel plates with O-ringed grooves closed the vessel on its ends. The plates were connected using four threaded compression rods. The top plate included a quick-connect so that the vessel could be refilled and pressure testing could be initiated. The bottom plate included a male AWJ connection. A schematic is shown in Figure 3-43.

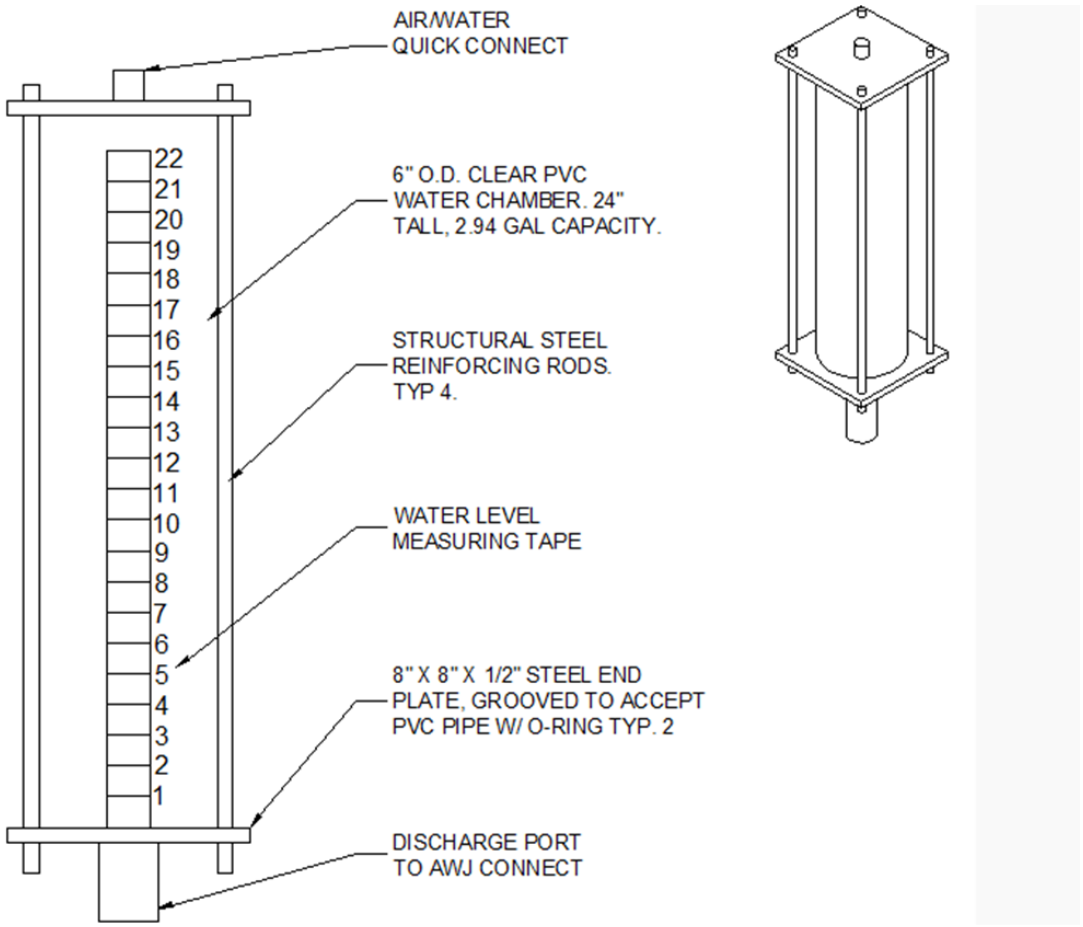

Figure 3-43. New water vessel schematic

Fabrication of the water vessel was completed on October 24, 2011. However, during initial sand-barrel tests researchers found that the new design made the container-drill rod-probe setup top-heavy when connected. It was believed the lack of stability in the design may cause the PVC to crack during pressurized flushing; and may lead to inaccurate results.

3.9.2.5 Modified Water Vessel with Support Stand

The new water container was slightly modified to address the deficiencies discussed above. First, a new flow port with a removable cap was added atop the water tank. This allows the user to fill and refill the tank quickly with a standard hose. Once the tank has been refilled, the cap is securely tightened and testing or pressurized flushing can resume.

Secondly, a system was developed where the falling head vessel would not move with the probe and AWJ rods during stage lifting. A new exit port for the water tank was designed. The container attaches to the AWJ rods via a flexible tube and a quick connect. Finally, a support stand was added, both to stabilize the unit and so that an operator could take readings from the same position during testing. Photographs of the new water vessel are presented in Figure 3-44 through Figure 3-46.

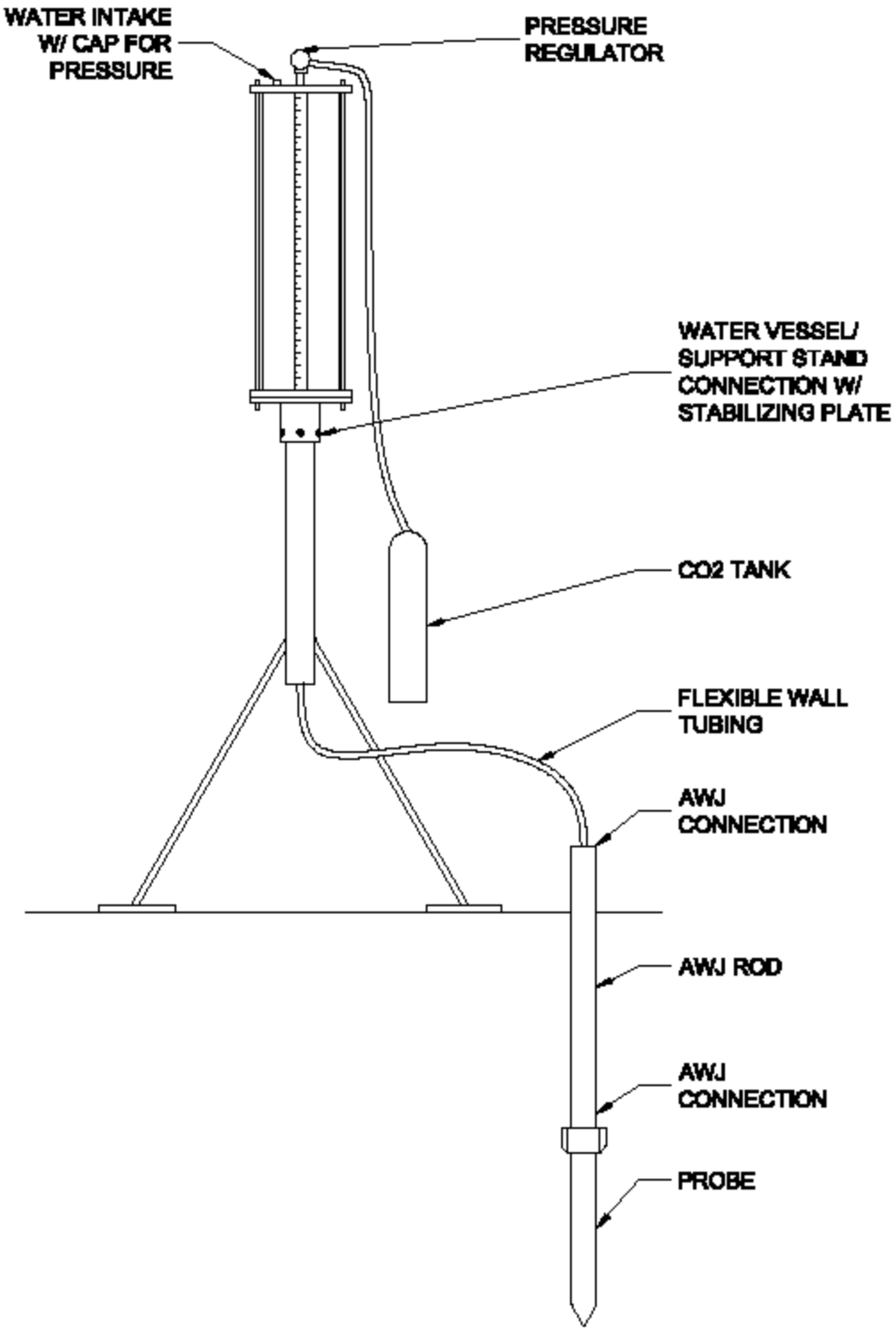

Figure 3-44. Schematic of the modified water vessel

Figure 3-45. New water vessel and support stand

Figure 3-46. Top of new water vessel with standard hose connection and quick connect

Initially, researchers had planned to pressurize the water vessels with CO_2. However, due to cost it was later determined that a pressurized air tank, which can be refilled in the field using a portable air compressor, should be used instead.

3.9.3 Initial Testing – SMO Test Pit

Once the water vessel had been finalized, sand-barrel testing began. Tests appeared to indicate that the probe and water vessel functioned as designed. All test stages were able to be initiated, and pressurized flushing appeared to eliminate sand

intrusion. Because of these results, investigators presented the device to FDOT in the beginning of April 2012.

Upon receiving the probe, FDOT conducted a preliminary test. Using the test pit at SMO, a hole approximately 4 feet deep was excavated, the probe was placed inside, attached to an AWJ rod and the hole was then back-filled. The water vessel was attached and water was introduced to the system. During the test, FDOT workers and UF researchers discovered that at greater depths the elevation head caused water to prematurely exit through the horizontal vents of the probe prior to testing. A stable head could not be obtained in the water vessel and proper testing could not take place. Both parties agreed this issue would need to be addressed before field testing could continue. UF researchers then developed two methods to prevent the premature leakage.

3.9.4 Probe Modification – Preventing Premature Leakage

A discussion of the solutions to prevent the premature leakage issue is presented in the following sections.

3.9.4.1 Testing Environment

At the SMO demonstration on April 4, 2012, FDOT workers indicated that real-world testing would only be implemented at depths of approximately 25 feet. To simulate a similar environment, researchers used a 45 foot hose hung from the fourth floor of Weil Hall at the University of Florida attached to the water vessel and probe. Water was added to the water vessel and subsequently to the probe. This allowed researchers to investigate any leakage from the probe at a depth of nearly 50 feet (providing a factor of safety of 2).

3.9.4.2 First Method of Probe Modification

The first of the two methods called for new exit flow ports to be added to the probe's inner rod (Figure 3-47). Likewise, the existing exit ports were sealed. This allowed for new O-ring placement. By adding the new flow ports to the inner rod, the testing order (horizontal versus vertical) was reversed. Because this order was arbitrary and had been reversed in the past, this solution was acceptable. Modifications can be seen in Figure 3-47.

Figure 3-47. First probe modification – repositioned inner rod flow ports

The newly modified probe was then tested as discussed earlier in this section. Results appeared to indicate that the probe no longer leaked. However, due to the new placement of the exiting flow ports within the inner rod, horizontal flow did not exit the probe as researchers desired. In the original design, inner rod flow ports exited into the upper chamber of the probe's outer shell. This allowed water to fill the probe's annulus and exit evenly through the device's horizontal slits. Now, water only exited in four directions. Therefore, this method was determined to be ineffective.

3.9.4.3 Second Method of Probe Modification

The second method to prevent premature leakage required a new inner rod and cone tip to be manufactured. By using a shorter inner rod and cone tip researchers were able to use the existing tracking system. Plus, this design prevented the need to manufacture an entirely new probe. The new inner rod is similar to the old rod, except the length of its lower portion is reduced.

By reducing the length of this section the tracked inner-core male piece remains stationary during the first stage of the testing. The inner rod tip is retracted during this stage and vertical flow is provided. However, the “keys” remain in place and the outer shell remains closed, thus preventing debris from intruding into the horizontal slits. During the next stage of the test, the thicker inner rod section comes in contact with the tracked inner-core male piece and the “keys” are retracted. This provides horizontal flow. The O-rings that were previously placed in the outer shell of the upper chamber, that restrict unwanted flow, were removed and placed on the inner rod surrounding the inner rod exit ports. Modifications are shown in Figure 3-48.

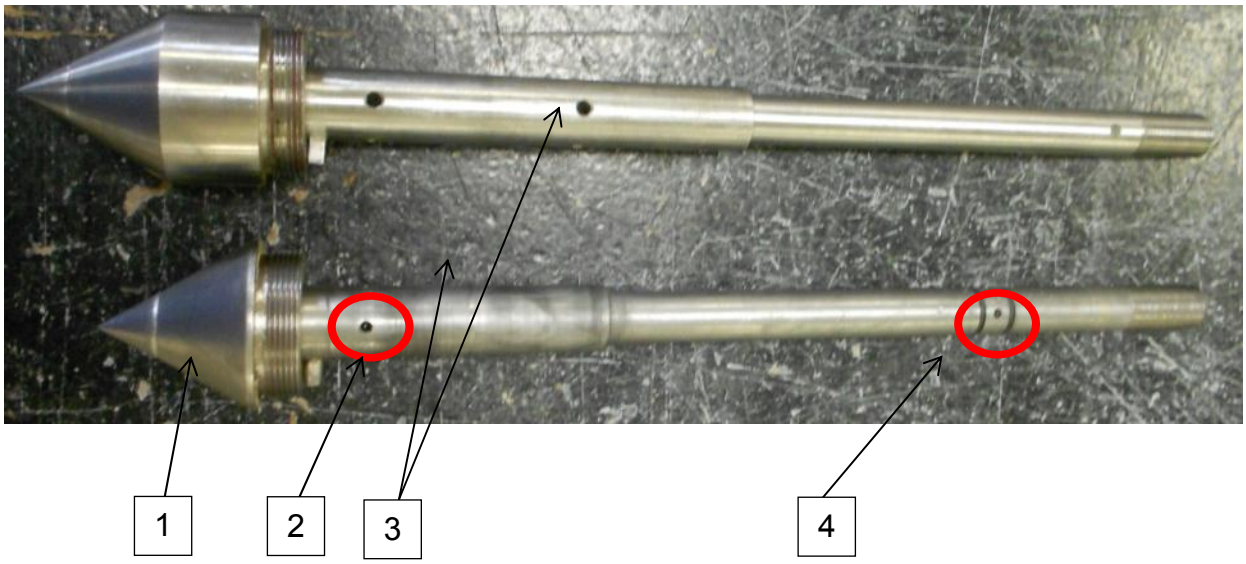

Figure 3-48. Second probe modification: (1) the shorter cone tip; (2) new inner rod vertical flow port; (3) reduced length of the thicker inner rod section; (4) new inner rod horizontal flow port with O-rings

Testing was conducted as stated previously in this section. The probe was able to prevent premature leakage at a simulated test depth of nearly 50 feet. The probe was also tested at both lift stages to ensure water was properly routed in the desired direction at the proper time. In all trials the probe appeared to perform as designed. Photographs of this testing phase are shown in Figure 3-49 through Figure 3-53.

Figure 3-49. Water vessel with 45 foot hose attached on the fourth floor of Weil Hall

Figure 3-50. Hose attached to falling head vessel hanging from fourth floor of Weil Hall

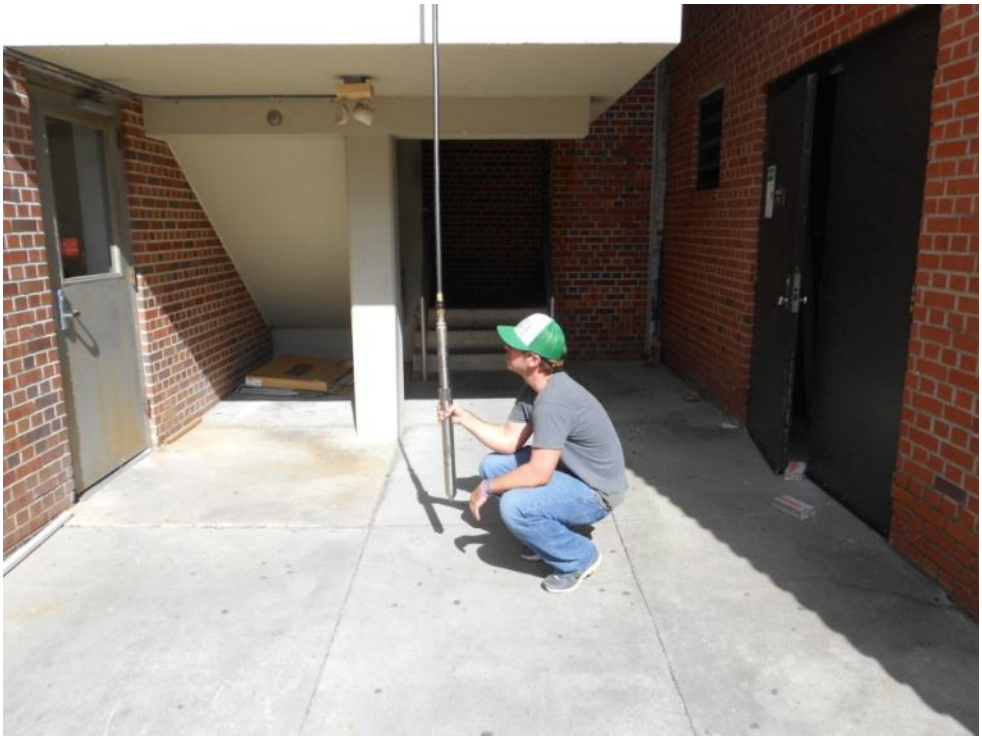

Figure 3-51. Probe attached to hose and monitored for leakage

Figure 3-52. AWJ rod connections failing before the probe

Figure 3-53. Probe going through all stages of testing

3.9.5 Field Test – Second SMO Visit

After researchers determined the new modifications were successful, UF researchers returned to the SMO on May 24, 2012 to conduct field tests on the newly modified probe. The first test was conducted at a depth of 5 feet and the second at 10 feet. The probe was connected to AWJ rods and pushed into the ground using a standard SPT drill rig.

At a test depth of 5 feet, the probe was connected to the water vessel and moved into the vertical flow position and allowed to run for several minutes. The probe was then moved into horizontal position and also allowed to run for several more minutes. All rotation and stages of lift were able to be conducted by researchers using only their hands to control the probe's movement at the bottom of the hole via AWJ rods.

Once vertical and horizontal flow tests were complete, the probe was then rotated into the closing stage, successfully closed, and rotated into a locking position. The probe was pushed down to the next test depth of 10 feet.

At 10 feet, rotation became more difficult as the increasing length of the AWJ rods provided additional skin friction that resisted rotation. However, researchers were able to use a large wrench to rotate and lift the probe and AWJ rods. Both horizontal and vertical flow directions were successfully tested and the probe was able to be closed and retracted to the surface.

During the field test, the flow was monitored but not recorded. The goal of the field test was to determine if the probe functioned correctly under field conditions and not to determine permeability values. Although, investigators noticed that the vertical flow rate appeared to be approximately the same at both test depths. However, at 5 feet, the horizontal flow rate was much lower than the vertical flow rate. At 10 feet, the horizontal flow rate was greater than the vertical flow rate. Pictures of the field tests can be seen in Figure 3-54 through Figure 3-57.

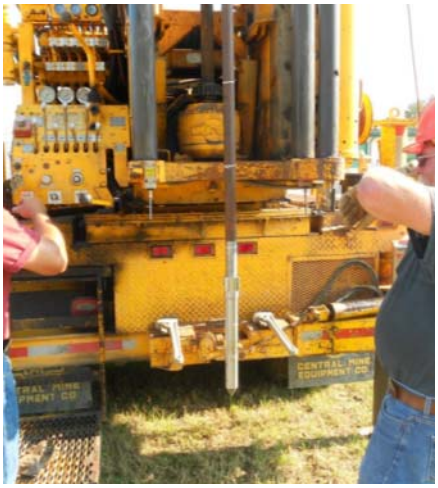
Figure 3-54. Probe attached to the SPT drill rig

Figure 3-55. Probe being inserted into the ground

Figure 3-56. Probe being rotated and lifted to the respective test position

Figure 3-57. Water vessel being monitored for flow

3.9.6 FDOT Recommendations

Throughout the testing, FDOT workers and UF researchers made note of any issues found with the probe and the water vessel. One issue with the probe was that large amounts of torque caused some of the probes pieces to begin unthreading. This was an issue caused by an oversight in the design process. As researchers initially believed that all-clockwise rotation would provide a tightening of the threads, it was overlooked that the inner rod rotation in this direction would cause a loosening to the outer shell. This was due to the knob on the inner rod pressing against the outer shell's tracks.

Thread locker was used to try to remedy the problem but with a large enough torque the bonds were broken. FDOT workers also indicated that they would like UF researchers to develop a tracking system at the top of the hole to monitor the probes inner rod rotation and stages of lift. The final request was for UF researchers to design a smaller final version of the probe.

3.9.6.1 Addressing FDOT's First Recommendation

The first request to be addressed was to eliminate the unthreading of the probe under higher torques. Researchers tried to develop a solution to remedy this problem and also presented the issue to local machinists. The final conclusion was that set screws must be added to three separate locations on the outer shell to secure all threading. Researchers had tried to avoid using any of these in earlier designs to allow for easier assemble and disassemble. However, to salvage the first of the steel probes, the set screws were unavoidable. The set screw modification can be seen in Figure 3-58.

Figure 3-58. Probe with set screws added to prevent unthreading

3.9.6.2 Addressing FDOT's Second Recommendation

At the May 24, 2012 field test, FDOT workers indicated that they wanted a way of tracking the probe's rotation and stages of lift at the top of the hole. In response, researchers developed a coordinate dial that allows workers to know the positioning of the probe from the top of the hole (Figures 3-59 through 3-63).

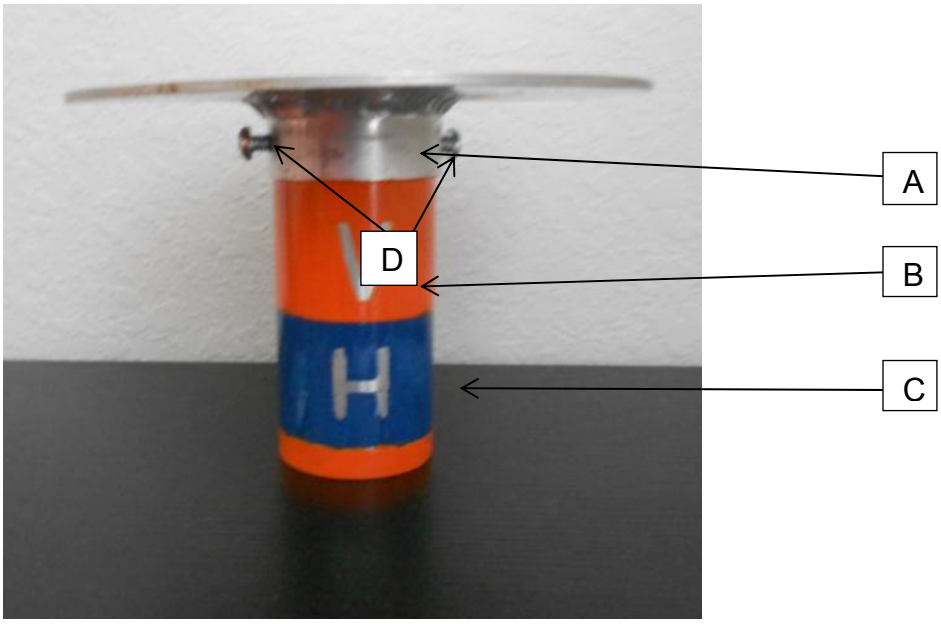

Figure 3-59. Profile view of coordinate dial prototype: (A) ground level position; (B) vertical flow stage tracking section; (C) horizontal flow stage tracking section; (D) set screws

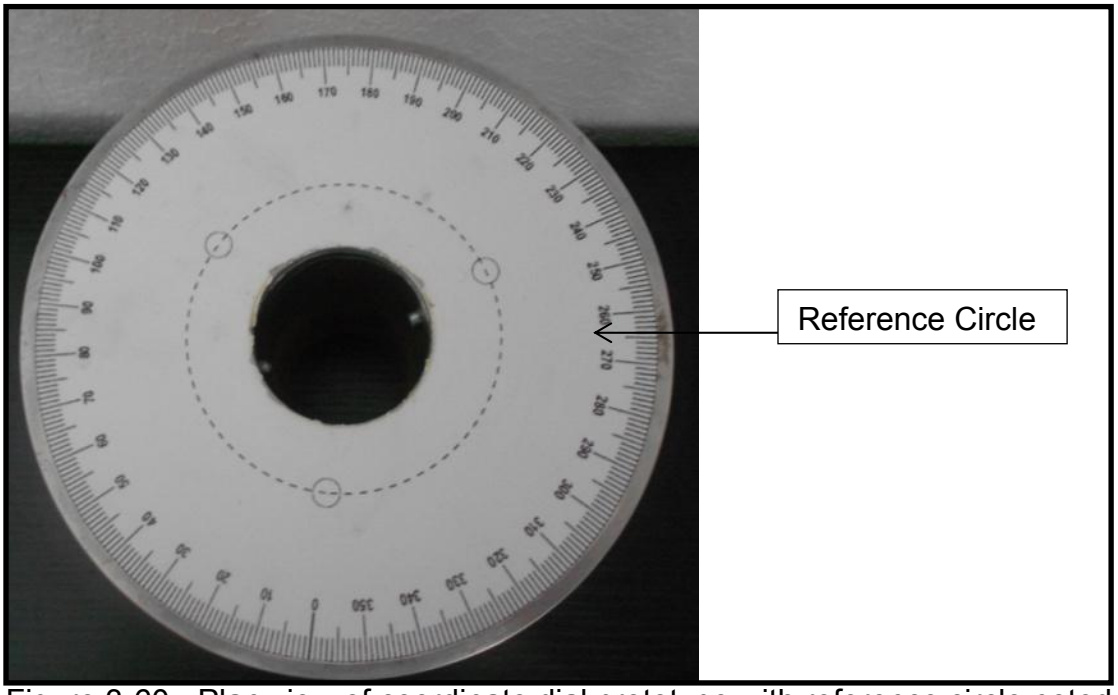

Figure 3-60. Plan view of coordinate dial prototype with reference circle noted.

Once the probe has been pushed to the desired test-depth, the dial is slipped onto the probe's AWJ rods such that "Position A" in Figure 3-59 is level with the ground surface. The sets screws seen in Figure 3-59 are tightened using a Phillips head screw driver so that the dial is secured into position.

A reference stake is placed at coordinates 60, 180, or 300 degrees (depending on which stage is being conducted) because a 60-degree turn is required to transition among the probe's stages. When rotating the probe, the operator will know that he or she has achieved a full 60-degree turn when the reference stake is aligned with the dial's appropriate reference circle.

The 1.75 inch vertical lift is tracked by the orange section labeled B in Figure 3-59. The operator will know if the probe has been pulled too far upward if the blue section (C in Figure 3-59) of the dial comes out of the ground. Similarly, during the final

stage of lift, if the bottom orange section of the devices becomes exposed, the operator will know if the probe has been lifted too far. Figure 3-61 through Figure 3-63 present the coordinate dial during field testing.

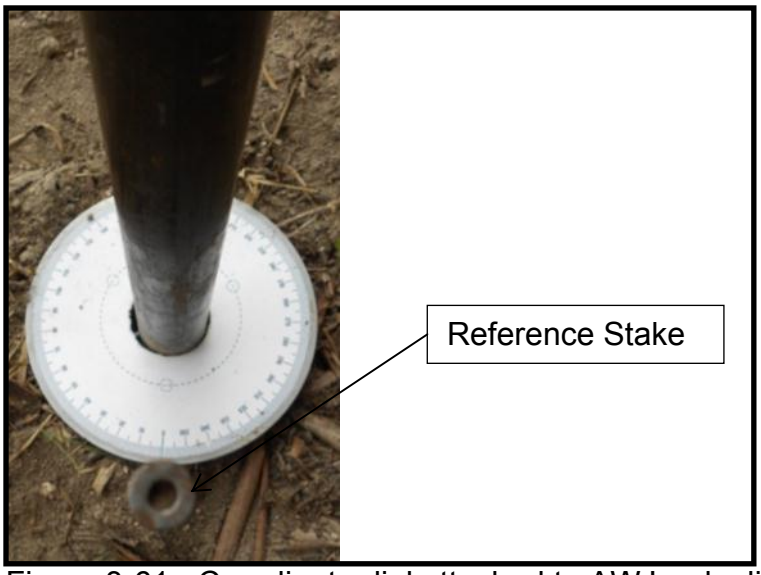

Figure 3-61. Coordinate dial attached to AWJ rod, aligned with reference stake


Figure 3-62. Coordinate dial displaying orange section indicating vertical flow


Figure 3-63. Coordinate dial displaying blue section indicating horizontal flow

3.9.6.2 Addressing FDOT's Third Recommendation

After field tests indicated that the new tracked probe design can be used successfully in the field, FDOT indicated they would like to see a scaled down version of the probe for the final design. Researchers redesigned the device, and the new probe's mechanics are almost identical to the previous design except that the threading issue has been addressed. The new probe design is presented side-by-side with the larger probe in Figure 3-64 and Figure 3-65.

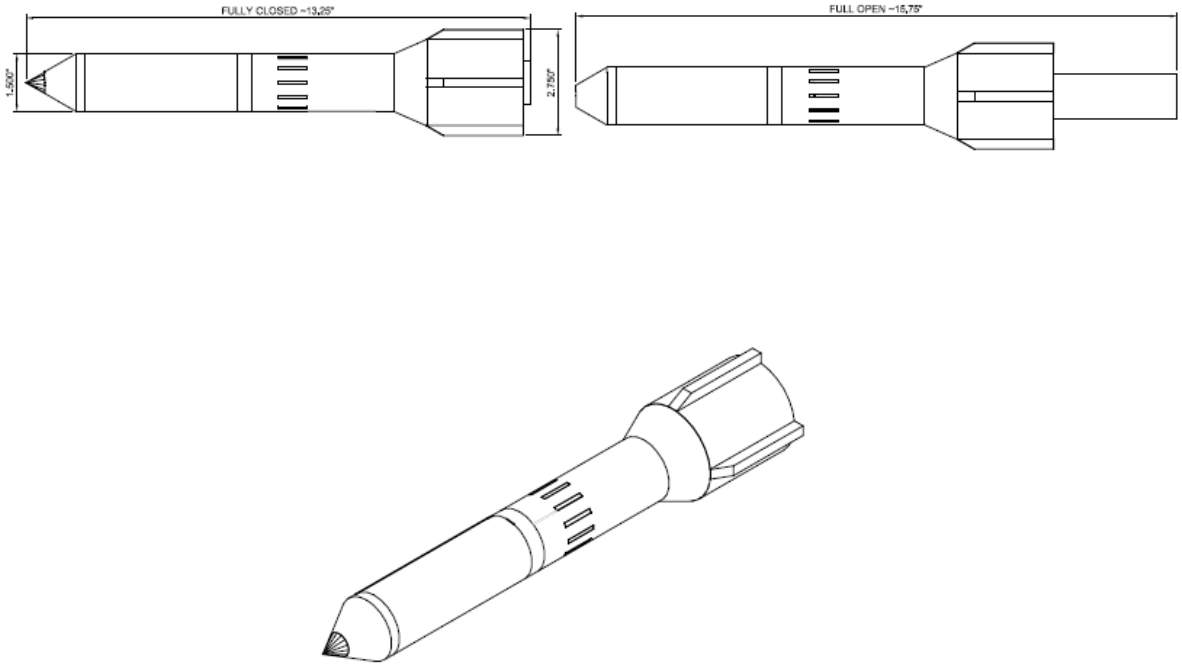

Figure 3-64. New probe design

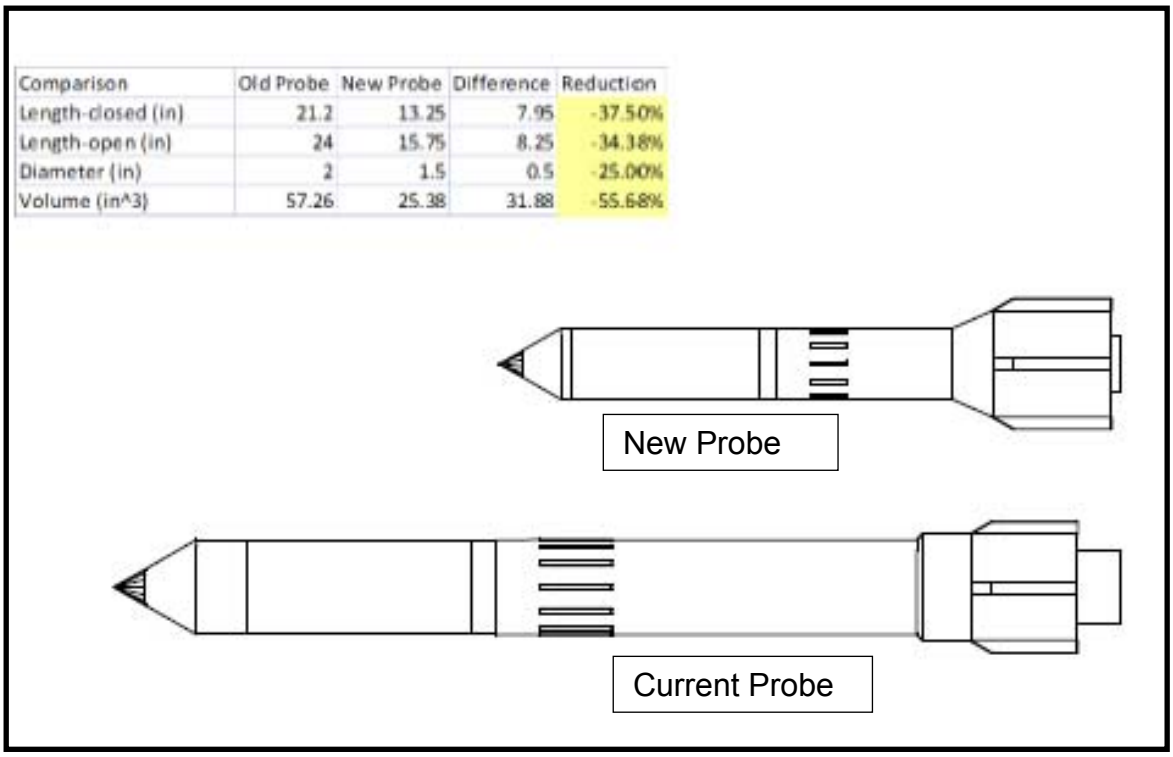

Figure 3-65. Comparison of the new probe (top) design and the old probe (bottom) design.

3.9.7 Development of "VIP" Probe

At the 2011 Geotechnical Research in Progress Meeting (GRIP), W. R. Wood of Loadtest pointed out that typically, permeability is a scalar quantity, and that water should flow along the path of least resistance. While conclusive data has yet to be obtained to test this hypothesis, FDOT indicated at the 2012 GRIP meeting that an in situ vertical-only version of the probe was still an improvement over existing testing techniques. Therefore, a vertical in situ probe was developed (VIP, Figure 3-66). As implied, the VIP is simply the bottom half of the VAHIP. Because it only tests vertical permeability, it is a much simpler device. And it is much less costly than the VAHIP. This device was tested on November 28, 2012. While the test did not as effective as

anticipated, investigators believe that the device could be made effective with some modifications. Discussion of tests with the device is included in Section 5.1.4.

Figure 3-66. Vertical in situ permeability probe (VIP)

CHAPTER 4
PROCEDURE FOR FIELD USE AND DATA REDUCTION

4.1 Outlined Field Test Procedure

The following field permeability standard test procedure is recommended when using the 2012 VAHIP probe.

4.1.1 Pre-field Preparation

1. The VAHIP must be cleaned and rid of any foreign material that would hinder water flow. Refrain from adding lubricants to the probe as they may cause unwanted debris to adhere to the inner components of the probe and cause the unit to malfunction.

2. Prepare all materials and tools listed in the equipment check list in Appendix A.

4.1.2 Probe Assembly

The following procedure is provided to instruct new VAHIP users in proper assembly of the device. Images of assembly have been included to better illustrate the process. An Allen key will be needed to tighten set screws into the probe. The total process should take 3 to 5 minutes depending on the experience of the user.

Assembly steps:

1. Attach piece A to B by threading the ramped end of piece B into the smaller diameter end of piece A.

Figure 4-1. Probe assembly step 1 showing Part A and Part B

2. Grip piece C with one hand and place the keys (the 12 pieces labeled D), into the designated slots. Remember to keep a good grip on piece C and the keys when proceeding to step 3.

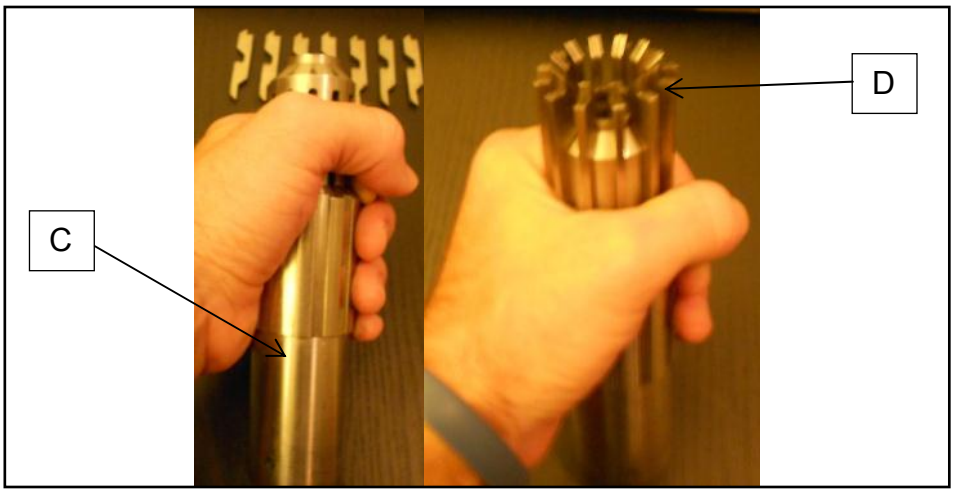

Figure 4-2. Probe assembly step 2 showing Part C and Part D

3. Place piece C with the keys lodged in their designated positions into the larger diameter opening of piece A. Push piece C into piece A until the keys engage and can be seen in the openings of piece A.

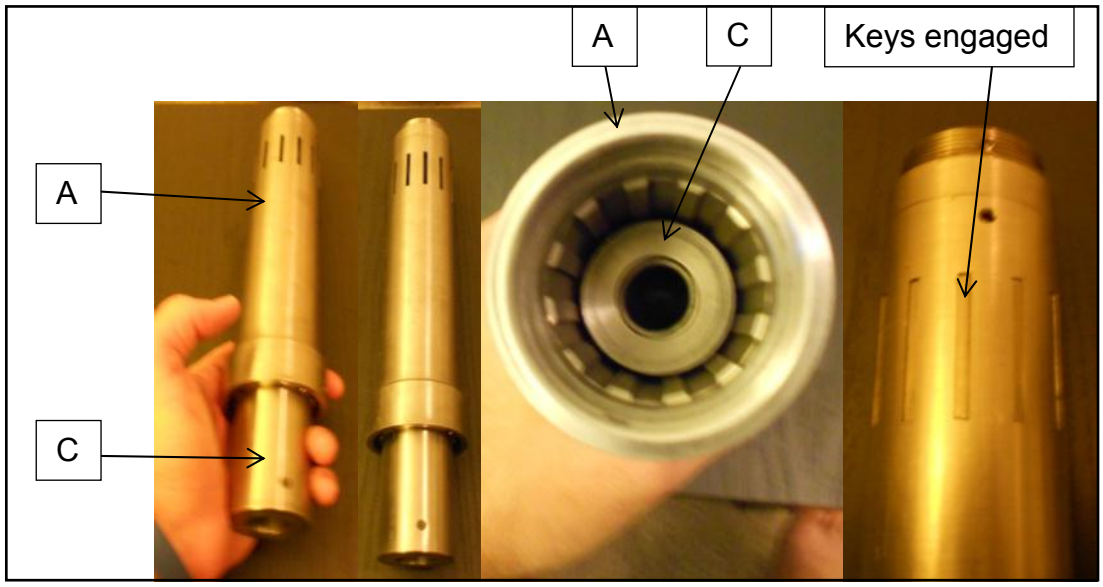

Figure 4-3. Probe assembly step 3 showing Part A, Part C, and the keys

4. Thread piece E into the larger diameter opening of piece A.

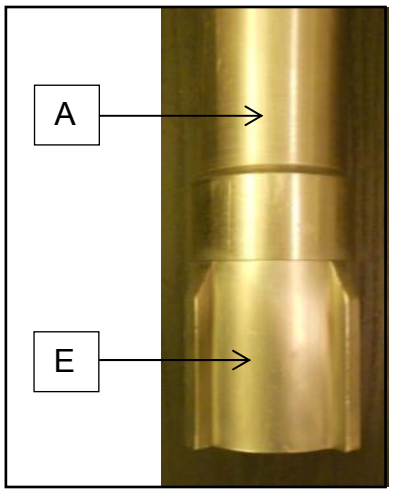

Figure 4-4. Probe assembly step 4 showing Part A attached to Part E

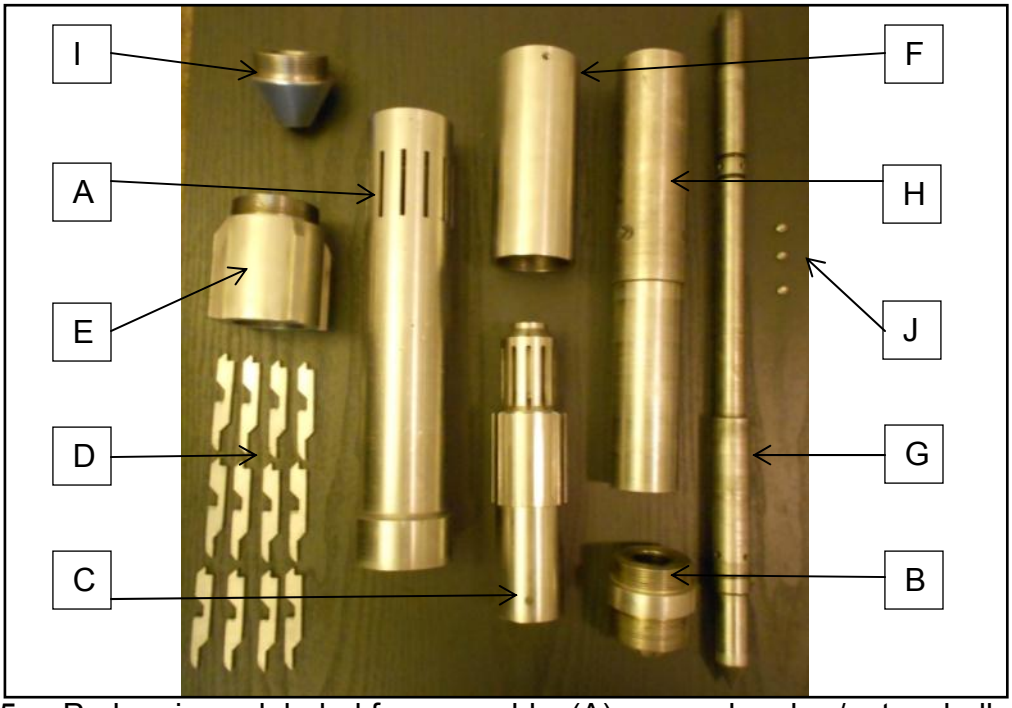

Figure 4-5. Probe pieces labeled for assembly: (A) upper chamber/outer shell; (B) ramped connection; (C) tracked male inner core; (D)12 keys; (E) friction reducer with wings; (F) tracked lower chamber; (G) inner rod with knob; (H) AWJ connection; (I) cone shaped tip; (J) 3 set screws

5. Thread piece F onto piece B.

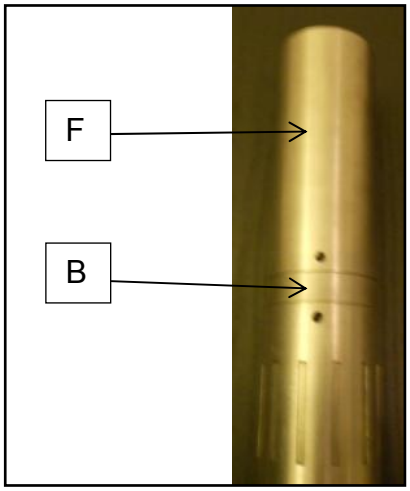

Figure 4-6. Probe assembly step 5 showing Part F attached to Part B

6. Place the threaded end of piece G through pieces F, B and C contained within piece A. Make sure the knob of piece G is placed into the larger drop down-slot of piece F.

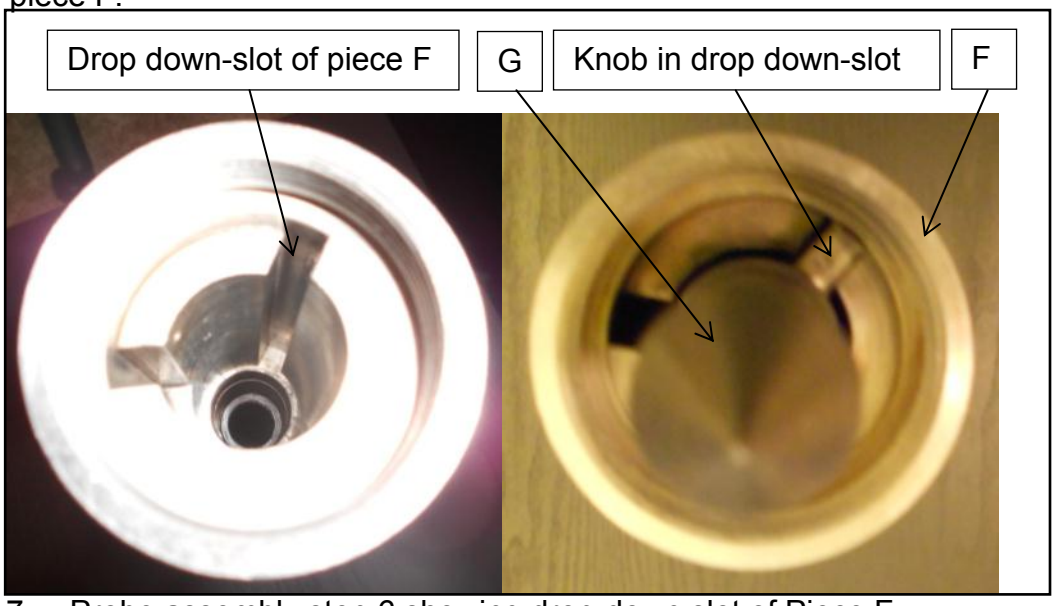

Figure 4-7. Probe assembly step 6 showing drop-down slot of Piece F

7. Insert and push the smaller diameter end of piece H into piece E until piece E comes in contact with the threading of piece G. Once the two pieces are in contact, turn piece H in a clockwise direction. This threads piece E into piece H. Once threading is complete push piece H until the knob of piece G is exposed in piece F. Rotate piece H slightly so the knob is no longer in the drop-down slot of piece F and proceed to step 8. Make sure not to over tighten the threading performed in step 7.

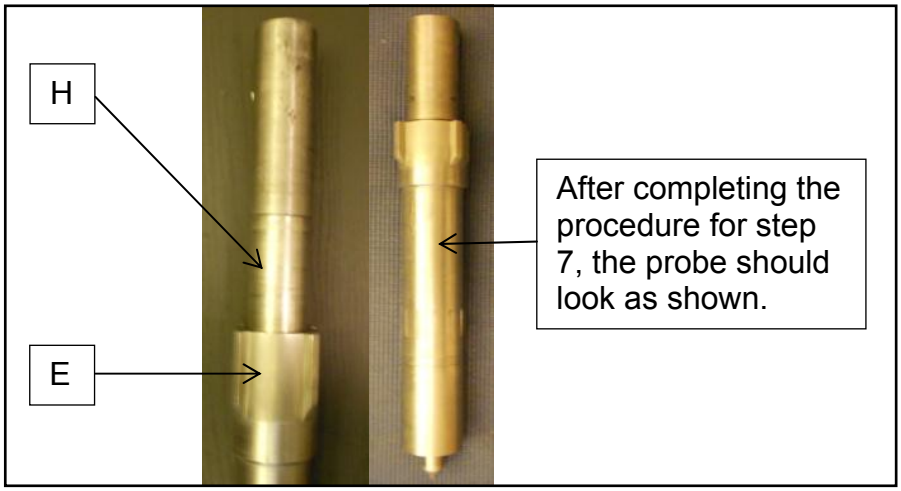

Figure 4-8. Probe assembly step 7 showing Part H connected to Part E

8. Thread piece I into piece F.

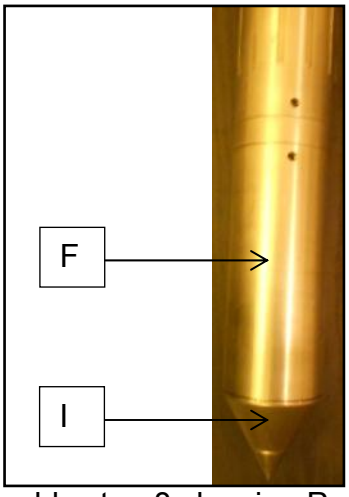

Figure 4-9. Probe assembly step 8 showing Part F connected to Part I

9. Thread the three J pieces into the threaded openings of pieces A and F. The probe is now fully assembled.

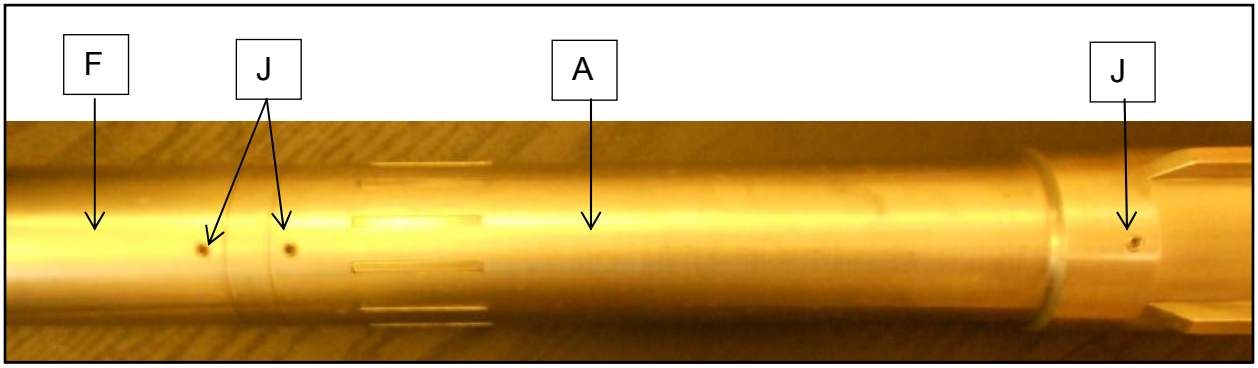

Figure 4-10. Probe assembly step 9 showing set screws

10. Inspect the probe to ensure everything is installed and functioning correctly.

Figure 4-11. Probe assembly step 10

4.1.3 Water Vessel and Support Stand Assembly

1. Place the support stand in the upright position with the legs locked in place.

2. Run the quick connect end of the flexible tubing through the support plate opening on the support stand.

3. Attach the quick connect end of the flexible wall tubing to the bottom plate quick connect of the water vessel.

4. Carefully place the water vessel onto the support plate of the support stand. Pull the excess flexible wall tubing through the opening of the support plate. Ensure that all four steel rod ends of the water vessel fit securely into the four respective holes of the support plate. The water vessel and support stand assembly is now complete.

4.1.4 Field Test Procedure

1. Fully assemble the probe and ensure that it is in the closed stage discussed in Section 4.1.2.

2. Fully assemble the water vessel and support stand; and place it in an area that will not hinder the SPT rig pushing the probe into the ground. Try to find a location with level ground.

3. Place an O-ring between the probe's AWJ female connection and the male end of the SPT rig's AWJ rod. Tighten the probe onto the AWJ rod ready for insertion on the SPT rig.

4. Advance the probe to the desired test depth using the SPT rig's push technique.

5. Disconnect the drive head of the SPT rig and slide the coordinate dial over the AWJ rod extending out of the ground. Ensure the dial is placed at ground-level, tighten the set screws and place the reference stake in its respective position.

6. Attach the water vessel's AWJ connection to the AWJ rod extending out of the ground, and place an O-ring between the connections.

7. Remove the cap of the water vessel, attach the SPT water hose, and add water until the water vessel is filled and the water level indicator stabilizes.

8. Rotate the AWJ rod extending out of the ground approximately 60 degrees clockwise, lift 1.75 inches, and rotate an additional 60 degrees clockwise Track the probe's rotation and lift using the coordinate dial.

9. When the probe is lifted 1.75 inches, water is released in the vertical direction. The final 60 degree rotation locks the probe into the vertical position. At this point, start the vertical test; begin recording time and flow measurements. Data should be recorded until flow rate stabilizes.

10. After vertical testing has been completed, quickly rotate the AWJ rods 60 degrees clockwise, lift 1.75 inches, and rotate an additional 60 degrees clockwise to lock the probe into the horizontal flow position. Track the probe's rotation and lift with the coordinate dial.

11. Attach the SPT rig water hose to the water vessel cap again and refill the water vessel. There will be no restriction of flow as soon as the water vessel is filled completely. At this point, start the horizontal test; begin recording time and flow measurements.

12. When horizontal testing is complete, refill the water vessel, attach the water vessel cap and pressure tank quick-connect. Allow the water vessel to drain until it is approximately three-quarter full and slowly bleed compressed air from the air tank into the system to flush.

13. While the system is flushing, rotate the AWJ rod 60 degrees clockwise, push downward 3.5 inches, and rotate a final 60 degrees clockwise. Track the probe's rotation and lift with the coordinate dial. If the probe is unable to be closed, lift the AWJ rods upward 3.5 inches, and allow flushing to resume until the probe can be closed. More water may need to be added to the water vessel, and the air tank may need to be refilled to increase the pressure.

14. After the probe has been flushed and rotated the final 60 degrees, lock it into the closed stage. It is ready to be pushed to the next test depth. The coordinate dial should now be back at the original position and needs to be removed before adding more AWJ rods to proceed to the next test depth.

4.1.5 Test Types

The previous probes incorporated both falling head and constant head testing. However, FDOT indicated they would prefer to keep the testing methods as simplified as possible, and therefore only the falling head technique is discussed.

4.1.5.1 Falling Head

1. Use a stop watch, the unit scale attached to the water vessel and data sheet for recording the data.
2. Take an initial reading of the water level in the water vessel and start the stop watch at the same time.
3. Take a reading every 30 seconds and record each reading on the data sheet.
4. Repeat steps 2 and 3 as many times as needed. Use average readings in the data analysis and disregard any outlying values.
5. Enter recorded data into the respective test type, vertical or horizontal, using the computer analysis program to determine permeability.

4.2 Alternative Testing Procedure

An alternative procedure may be desired to minimize uncontrollable effects during driving such as clogging of slots, friction and stress on the probe. Pre-boring or pre-drilling a hole prior to insertion of the probe was considered in the 2007 VAHIP Final Report. The following procedure should suffice however it has not been implemented in the field either on the 2005, 2006, or current 2012 probes.

Pre-drilling is a method which may be used for testing in stiff material to reduce stress or in materials with a higher potential of clogging the probe horizontal slots. The main premise is to drill a borehole to a depth that is a minimum of 2 feet less than the desired test depth. A borehole of lesser diameter than the probe can be drilled at the last 2 feet if material is very stiff. The VAHIP probe can then be advanced in the pre-drilled hole and testing performed as previously described (Bloomquist, 2007).

4.3 VAHIP Maintenance

- **Cleanup.** Disassemble the probe and wash with clean water and wire brush removing all soil particles from flow ports and connecting parts.
- **Routine Inspections.** The probe should be inspected after each cleanup for deformed and/or worn parts. Note deformities and replace parts as needed.

- **Storage.** The VAHIP and water vessel components should be stored in a cool dry place to prevent oxidation to steel components.

4.4 Data Reduction

Data should be collected in the field using data sheets. The spreadsheet developed for the 2012 VAHIP (Appendix B) should then be used to calculate permeability from test results. Probe and tank dimensions have been preloaded in to the spreadsheet. However, these dimensions can be quickly changed if future designs are different from the current model. The data is reduced using borehole permeability (Hvorslev's) theory for falling head in a borehole. The following is brief description of previous data analysis techniques and updated recommendations.

4.4.1 Previous Falling Head Test Data Recommendations

The falling head test is outlined in Section 4.1.5.1. The time required for the level of water in the pipette to drop from an initial level of H_1 to a final level of H_2 within a time step, Δt, was recorded for each test performed. During Project BD-545, RPWO #15 (the 2007 report), the following equations were derived for horizontal and vertical permeability respectively:

For horizontal flow, permeability was determined using the equation:

$$k = \frac{\pi d^2}{4F\Delta t} \ln\left(\frac{H_1}{H_2}\right) \quad (4\text{-}1)$$

where:

- d = pipette diameter
- Δt = the change in time
- H_1 = the initial water-level
- H_2 = the final water-level after Δt
- F = the shape factor which for the device used is given by:

$$F = \frac{2\pi L}{\ln\left(\frac{L}{D_h} + \left(\sqrt{1 + \left(\frac{L}{D_h}\right)^2}\right)\right)} - 2.75D_v \quad (4\text{-}2)$$

where

- d = the pipette diameter
- L = effective screen length of the probe's horizontal vents
- D_h = Inner diameter of the probes uppermost chamber/outer shell.
- D_v = diameter of the probe's vertical flow port,

The vertical flow during the falling head test was calculated using the equation:

$$k = \frac{\pi d^2}{11 D_v \Delta t} \ln\left(\frac{H_1}{H_2}\right) \quad (4\text{-}3)$$

where:

- d = pipette diameter
- D_v = diameter of the probe's vertical flow port,
- Δt = change in time,
- H_1, H_2 = initial and final levels of water in time Δt.

4.4.2 Hvorslev Reanalysis

Investigators reanalyzed Hvorslev's original paper to verify the data analysis equations. This reanalysis appears to indicate that previous researchers may have inadvertently misinterpreted or misrepresented Hvorslev's work. Figure 4-12 and Figure 4-13 from Hvorslev's paper are presented on the following pages. These figures are essential to the reanalysis discussion.

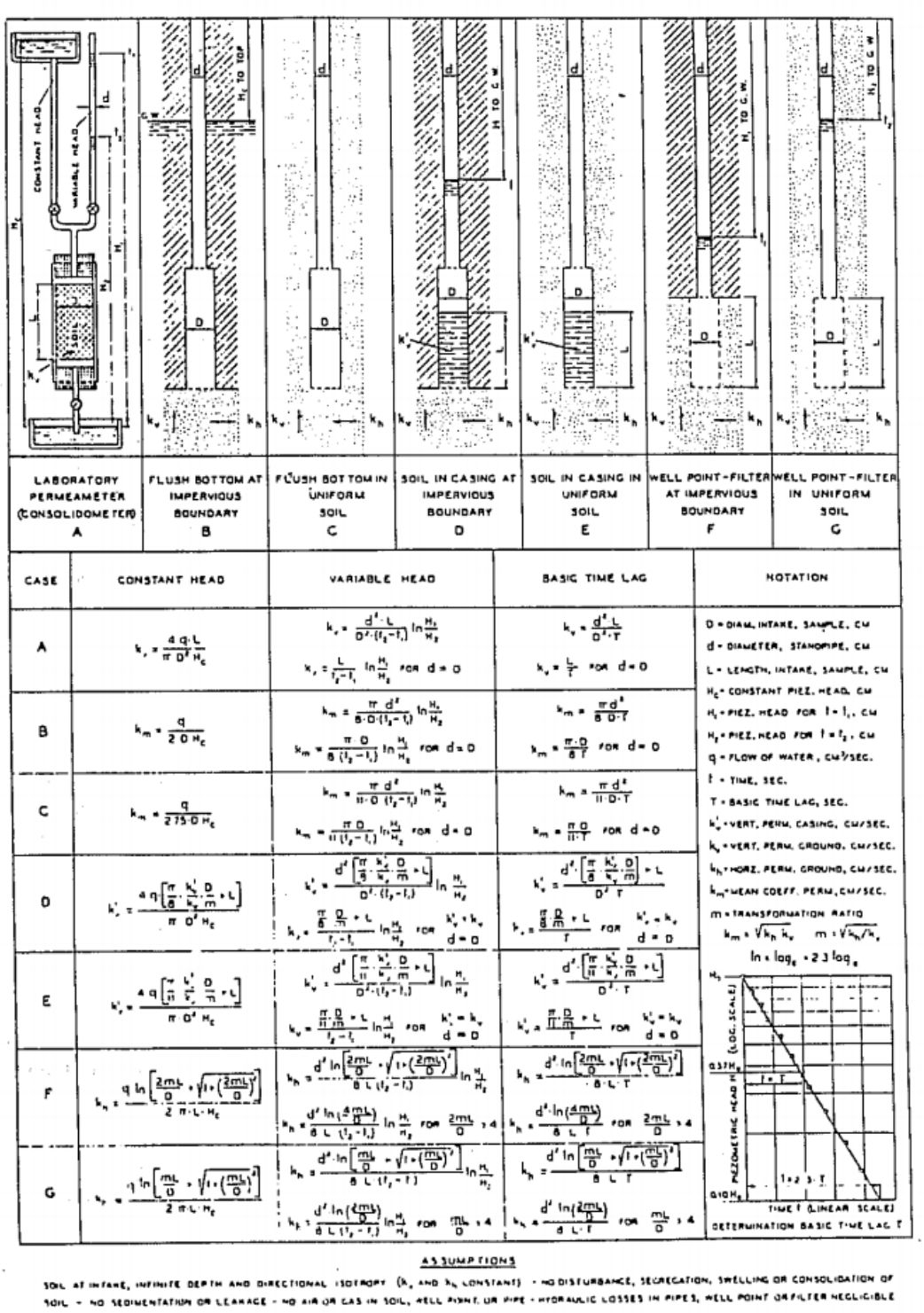

Figure 4-12. Chart from Hvorslev (1951) showing permeability for different well-point configurations

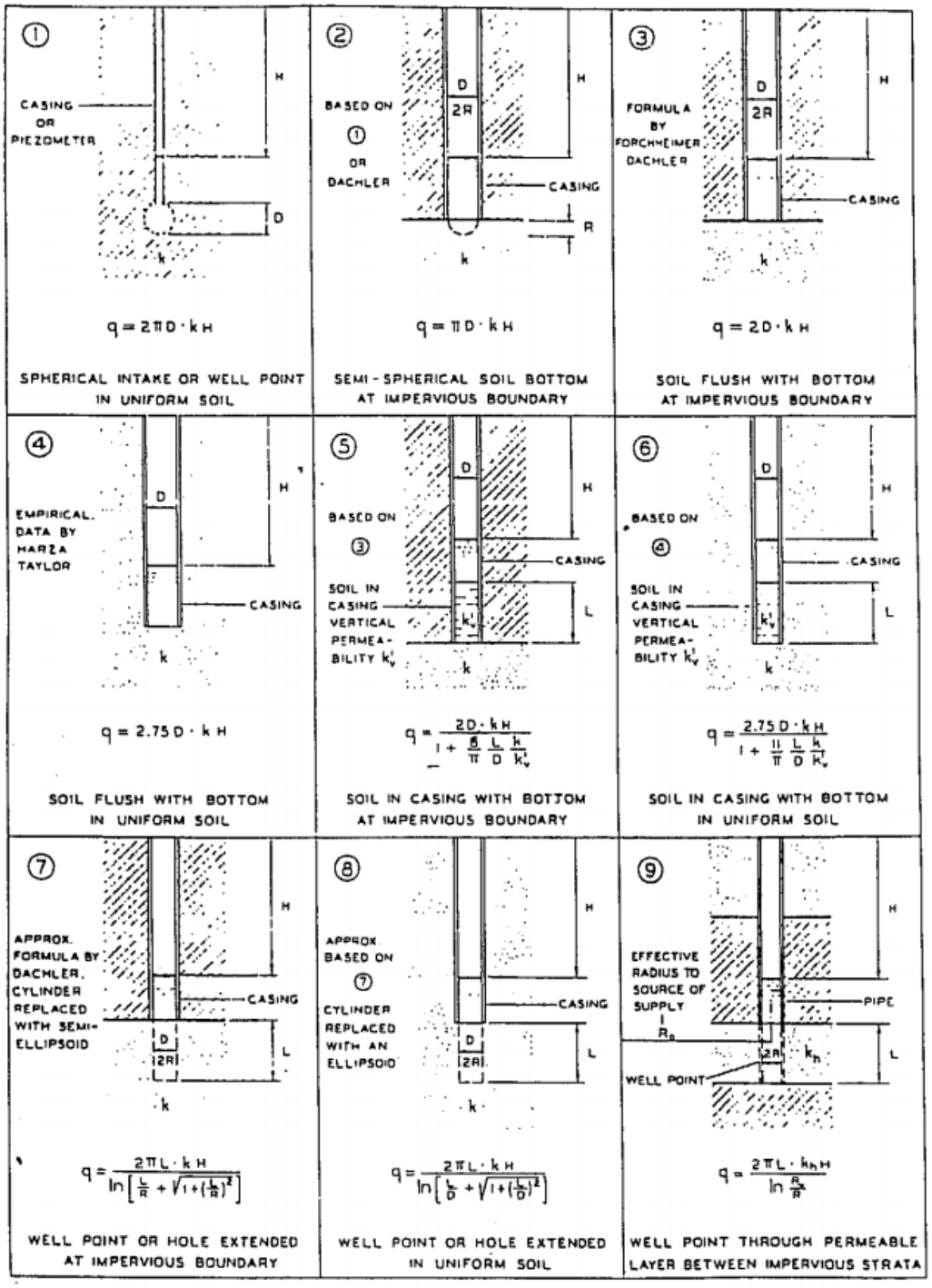

Figure 4-13. Chart from Hvorslev (1951) showing shape factors for different well configurations

Equation 4-3 is simply Case C in Figure 4-12 for a variable head test. However, in the 2007 report, the permeability coefficient, *k*, in Equation 4-2 was incorrectly misinterpreted as the vertical permeability coefficient. This error was probably caused by the fact that the original paper was retrieved on microfilm; and the screenshot of Figure 4-12 in the 2007 report was of poor resolution. A higher resolution copy of Hvorslev's paper was obtained that clearly shows that Equation 4-3 should be rewritten as:

$$k_m = \frac{\pi a^2}{11 D_v \Delta t} \ln\left(\frac{H_{1v}}{H_{2v}}\right) \tag{4-4}$$

where k_m is defined as:

$$k_m = m k_v = \frac{k_h}{m} = \sqrt{k_h k_v} \tag{4-5}$$

where k_v is the vertical permeability coefficient; k_h is the horizontal permeability coefficient; and *m* is the anisotropy coefficient. Note that a subscripted *v* has been added to all orientation-dependent terms to signify that this equation is for vertical flow only. Hvorslev's paper indicates that these equations should be used when conditions are not isotropic while Equation 4-2 and Equation 4-3 are for isotropic conditions only. When conditions are isotropic, *m* = 1, and Equation 4-4 becomes Equation 4-3.

Similar to the 2007 report, to determine the shape factor, *F*, first assume a constant head and subtract Case 4 from Case 8 in illustrated in Figure 4-13. However, unlike before, these equations should be written with the correct permeability coefficient orientations. From Hvorslev, Case 8 becomes:

$$q = \frac{2\pi L k_h H}{\ln\left(\frac{mL}{D_h} + \sqrt{1 + \left(\frac{mL}{D_h}\right)^2}\right)} \tag{4-6}$$

And Case 4 becomes:

$$q = 2.75 D_v k_m H \tag{4-7}$$

Note that subscripts have been added to denote vertical and horizontal VAHIP dimensions. Subtracting and rearranging gives:

$$q = \left(\frac{2\pi L k_h}{\ln\left(\frac{mL}{D_h} + \sqrt{1 + \left(\frac{mL}{D_h}\right)^2}\right)} - 2.75 D_v k_m \right) H \tag{4-8}$$

Since by definition, $q = kHF$ and $k_m = k_h/m$, Equation 4-8 may be rewritten:

$$q = \left(\frac{2\pi L}{\ln\left(\frac{mL}{D_h} + \sqrt{1 + \left(\frac{mL}{D_h}\right)^2}\right)} - \frac{2.75 D_v}{m} \right) H k_h \tag{4-9}$$

And the shape coefficient, F must be:

$$F = \left(\frac{2\pi L}{\ln\left(\frac{mL}{D_h} + \sqrt{1 + \left(\frac{mL}{D_h}\right)^2}\right)} - \frac{2.75 D_v}{m} \right) \tag{4-10}$$

For a falling head test, the horizontal permeability coefficient would be given by:

$$k_h = \frac{\frac{\pi}{4} d^2}{F \Delta t} \ln\left(\frac{H_{ih}}{H_{fh}}\right) = m k_m \tag{4-11}$$

This may be rewritten as:

$$\frac{\frac{\pi}{4}d^2}{mF\Delta t}\ln\left(\frac{H_{ab}}{H_{2b}}\right) = k_m \tag{4-12}$$

Substituting into Equation 4-4 gives:

$$\frac{\pi d^2}{11D_v\Delta t_v}\ln\left(\frac{H_{av}}{H_{2v}}\right) - \frac{\pi d^2}{4mF\Delta t_h}\ln\left(\frac{H_{ab}}{H_{2b}}\right) \tag{4-13}$$

This is an implicit equation for *m*.

It should be possible to solve Equation 4-13 for *m*. However, for both VAHIP sand-barrel data and field data collected during this study, investigators were unable to get Equation 4-13 to converge. It was unclear why this occurred, although there are several possibilities. First, Hvorslev's original equations were written for situations with a long screen length. Because the effective screen length of the VAHIP is relatively short (1.75 inch), this would appear to violate his assumption. Secondly, Case 4 from Hvorslev is an empirical expression where there is no known analytical solution. Conditions where the empirical expression in Case 4 was developed may have been different than the VAHIP. Third, Hvorslev assumed infinite soil around his well point. For the case of the sand barrel, this condition was clearly violated. While in the field, this assumption is valid, there are too little data to definitively dismiss Equation 4-13. Especially because if the *2.75D/m* term were eliminated in Equation 4-10, Equation 4-11 would precisely become Case G from Figure 4-12; and if the first term in Equation 4-10 is eliminated, it becomes Case C.

Regardless, the Equations from the 2007 report should not be used to obtain orientation-dependent permeability coefficients. Instead, the analysis in this report should be used, and the vertical flow condition (Equation 4-4) should be used to solve

for average permeability coefficient, k_m. While the VAHIP does provide for flow into the ground both horizontally and vertically, as of this date, there is no known method to convert these flow rates into orientation-dependent permeability coefficients.

CHAPTER 5
TEST RESULTS AND ANALYSIS

5.1 Test Results

Testing of the 2012 VAHIP probe consisted of the following types:

- Probe Permeability Tests
- Sand-barrel Tests (2 Methods)
- Lab Permeability Tests
- Field Tests

The first three test-types listed are implemented to observe how the VAHIP performs in various soil conditions and to determine its permeability limits. All testing results were used to determine the shape factors required for field analysis. Sand-Barrel tests were compared with results from field permeability probe testing.

5.1.1 Probe Permeability Tests

These tests were performed to determine the permeability of the probe itself and were conducted by the hanging the probe in the air so that its flow was not restricted. These results represent the value of the maximum permeability the VAHIP can be used to measure. Permeability through poorly graded sands and gravels can be very high relative to other types of soils, and if voided areas within the soil mass are greater than the area of the VAHIP's flow ports, the flow ports may be unable to deliver enough volume of water to measure the permeability accurately. The resistance to flow in the soil would be less than the resistance of the probe, and hence the data collected would reflect the permeability of the probe rather than that of the soil (Bloomquist, 2007). Results appear to indicate that the probe's permeability is on the order of magnitude of 10^1 cm/sec.

5.1.2 Sand-Barrel Tests

These tests (Figure 5-1 and Figure 5-2) were performed to determine if the VAHIP functions as intended and to produce test results which can be compared to conventional laboratory test methods. Two types of sand-barrel tests were performed:

- Back Fill
- Push Technique

Each method provided a different soil compaction setting and is performed using a 55-gallon barrel testing both horizontal and vertical permeabilities for each trial. Two soil types were tested – AASHTO A-2-4-type soil and 8/30 (Figure 5-3) to represent "coarse" and "fine" conditions. Gradation curves for these soils are presented in Figure 5-4 and Figure 5-5.

Figure 5-1. Sand-barrel testing

Figure 5-2. Probe embedded in soil

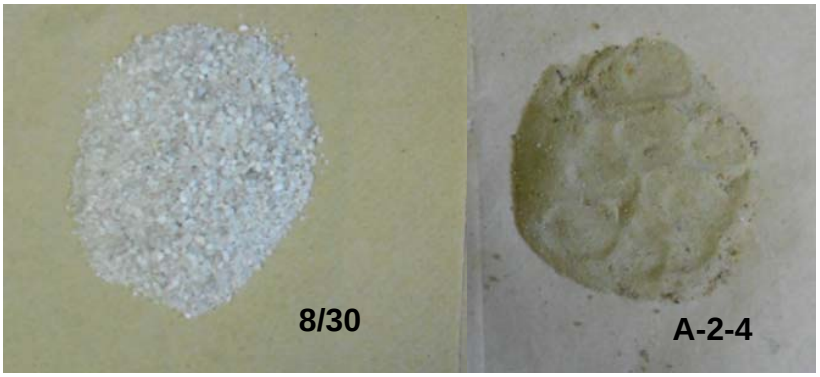

Figure 5-3. Sand-barrel soil types showing 8/30 soil (left) and A-2-4 soil (right)

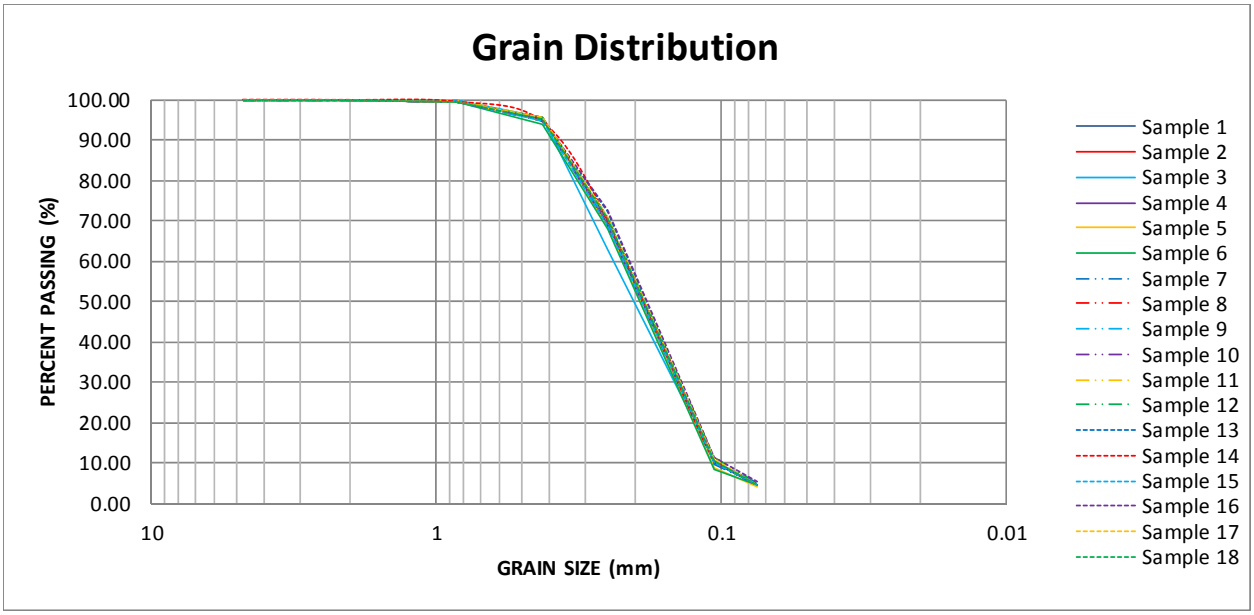

Figure 5-4. Gradation curve for A-2-4 soil

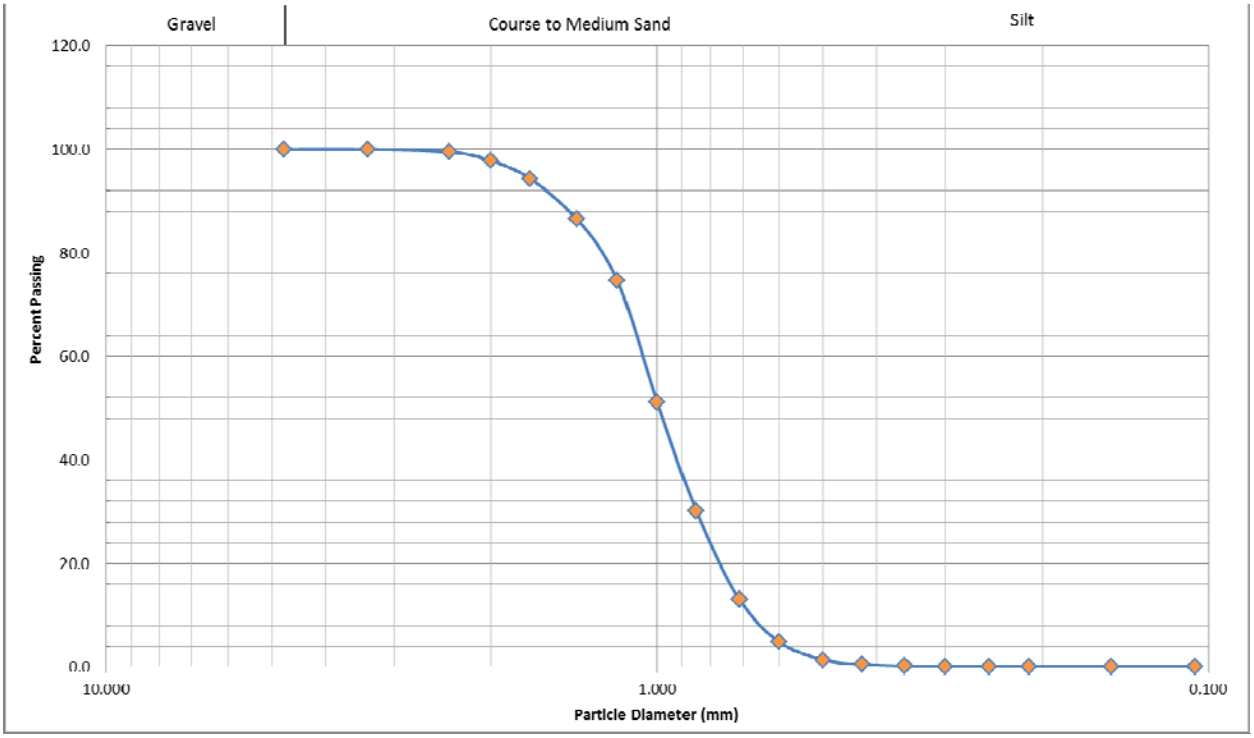

Figure 5-5. Gradation curves for 8/30 soil

Back fill testing, push technique testing, and vibration testing (a method discussed in this project's original scope) are discussed below:

- **Back Fill Testing.** For this round of tests, soil was added to the barrel in six inch lifts that were pre-weighed, recorded and compacted. After twelve inches of soil was placed, the probe was then held in the center of the barrel and back filling continued until the probe was fully buried.

- **Push Technique.** For the push technique testing, soil was filled, recorded and compacted in the same manner as back fill testing. However, the barrel was first filled completely before the probe was introduced. Once all layers had been compacted the probe was pushed into the center of the soil formation using a forklift.

  This technique did not function as intended. Steel plates were stacked onto the forklift's legs to function as a level pushing surface, but the soil was often too compacted for the probe to penetrate – especially with the A-2-4 soil. Instead, the plates would be lifted off the forklift's legs. Investigators stopped stacking steel plates when 12 plates were used because of safety concerns.

  In response, the forklift's legs were used to push downward on the probe directly. However, it was not possible to guarantee that the forklift's legs were completely level with the ground surface. As a result, the probe was pushed at a slight angle. This created a void alongside the probe, which rendered the test unusable. Two failed attempts were made to push the probe into the A-2-4 sand barrel, and each test failed. The probe was able to penetrate the 8/30 soil using the forklift technique.

- **Vibration.** While originally vibration tests were planned, these tests were ultimately abandoned because of the A-2-4 push technique failure. Vibration would make the soil matrix more compact. Therefore, investigators logically assumed that if push technique tests were impossible, vibration tests would be impossible as well. While in the future it may be beneficial to conduct vibration tests with 8/30 soil, these tests were not conducted as part of this project due to time constraints.

Push technique tests with the 8/30 soil appear to indicate that the VAHIP was effective at moving from one stage to another. During each fill test and each successful push technique test, the probe was able to be opened horizontally, opened vertically, flushed, and reclosed without any of its internal mechanisms "binding up." This appears

to indicate that sediment intrusion was reduced when compared to previous incarnations of the device.

Testing was conducted before the analysis discussed in Chapter 4 was performed. Since there does not appear to be a way to use horizontal flow rates to back-calculate horizontal permeability, only average permeability results were computed (i.e., k_m) and converted to permeability at 20 degrees Celsius (Table 5-1).

Table 5-1. VAHIP sand-barrel results

Test Number	Sand Barrel Technique	Soil Type	k_m (cm/sec)
1	Fill	8/30	1.10e-2
2	Fill	8/30	8.48e-2
3	Push	8/30	1.58e-2
4	Push	8/30	3.64e-2
5	Fill	A-2-4	2.96e-3
6	Fill	A-2-4	1.52e-3
7	Push	A-2-4	2.29e-3
8	Push	A-2-4	2.41e-3
9	Fill	A-2-4	3.67e-3

5.1.3 Lab Permeability Tests

Lab permeability tests (Figure 5-6) were performed on all soils tested in sand-barrel trials. Results from lab permeability testing were used to compare with sand-barrel test results. Both falling head and constant head tests were performed. All tests were performed in accordance with ASTM D5084. Results are presented in Table 5-2.

Figure 5-6. Lab permeameter testing permeability

Table 5-2. Permeability bench test results

Test Number	Soil Type	Falling Head Permeability (cm/s)	Constant Head Permeability(cm/s)
1	8/30	1.95e-2	2.61e-2
2	8/30	1.00e-2	1.28e-2
3	A-2-4	3.84e-3	3.49e-3
4	A-2-4	3.27e-3	3.73e-3

5.1.4 Field Tests

Due to the availability of a drill rig, only limited field tests could be conducted. On November 28, 2012, a team of researchers conducted two series of tests at the SMO. These tests are discussed in the following sections.

5.1.4.1 VIP Tests

First, the VIP discussed in Section 3.9.7 was tested. All previous testing with VAHIP-type devices was conducted using strictly a "surface-push-technique" whereby the probe was pushed into the ground without a predrilled borehole. As discussed in Section 4.2, Bloomquist (2007) speculated that predrilling may be used to reduce stress on the probe and the drill rig's hydraulics. However, Bloomquist (2007) also indicated that he did not test this procedure in the field.

Testing with the VIP appears to indicate that if any of the previous VAHIP-style devices were tested using a predrilled borehole, they would have failed. The earlier probes were attached to the drill rods via their inner shafts while their outer casings essentially "hung" from the inner rods. As a result, if a borehole had been predrilled, it would have been possible to prevent the outer casing from contacting the soil surface before the probe's tip. This is illustrated in Figure 5-7.

Three trials were conducted with the VIP to try to get its outer casing to stay closed. However, none were successful, and sand consistently intruded into the device's tip. As a result, it was impossible to pull "up" on the inner rod to initiate vertical flow. In the future, a locking mechanism similar to the VAHIP's must be added to the VIP to prevent similar failures. Alternatively, the VIP may be used as-is without a predrilled borehole.

Figure 5-7. Illustration of the VIP's "hanging" outer casing

5.1.4.2 VAHIP tests

VAHIP tests were more successful. Because of the device's "locking" mechanism, it remained closed until investigators topside initiated flow. The probe was successfully moved through both its vertical and horizontal flow stages at two depths (approximately 7 feet and 18 feet). "Flushing" between stages appears to successfully prevent sediment intrusion into the device. Data were recorded for both horizontal and vertical flow rates. At the second depth, the device encountered a clay layer and flow both horizontally and vertically appeared to be negligible. Results at the first depth appear to indicate that the average permeability coefficient was 7.51e-4 cm/s.

5.2 Analysis

Average permeability during VAHIP sand-barrel tests for 8/30 soil was computed to be 3.70e-2; and during laboratory permeability tests, it was computed as 1.71e-2. However, during the second VAHIP sand-barrel test, the permeability reading was

unusually high. If this reading is eliminated, VAHIP average permeability is 2.10e-2. While the sample size is small, this does appear to indicate that readings are within the same approximate ranges. Results from "push" tests and "fill" tests were approximately consistent for 8/30 soil. For A-2-4 soil, average VAHIP permeability was 2.57e-3; and average bench-test permeability was 3.58e-3. In all cases, the sample size was small, but as shown, computed permeabilities appear to be of the same order of magnitude. In general, VAHIP A-2-4 tests showed slightly lower permeabilities when compared to bench test results.

However, one should be careful when analyzing results. As discussed, the equation for vertical flow is empirical, and it was derived for wide casings with long effective screen lengths. The VAHIP has small casings and screen lengths. As shown, application of the Hvorslev equations for exclusive horizontal flow appears to fail, and one of the possible explanations is the empirical equation for vertical flow – i.e., "Case C" – in Figure 4-11. Case C simply comes from Case 4 in Figure 4-12 through substitution of a shape factor similar to the analysis discussed in Chapter 4. The "11" in the denominator of the Equation 4-4 is obtained simply by dividing a $\pi d^2/4$ term by 2.75 (i.e., 2.75*4 = 11). While this analysis appears to give somewhat accurate results for vertical flow, it should be pointed out that if it were "correct," Equation 4-13 would converge. To properly ensure accuracy during a vertical flow test, an empirical relationship should be developed specifically for a VAHIP-sized probe. Results presented here are therefore approximate.

As discussed, while the VAHIP does appear to be smear-proof, and it does appear to move through both horizontal and vertical flow stages as designed, it is

unclear how to correctly use horizontal flow rate values to back-solve for orientation-dependent permeability. Furthermore, the VAHIP is very mechanically complicated, and very expensive to fabricate. Conversely, the VIP is much more cost effective and much simpler mechanically. In addition, there is some question in terms of analyzing the flow rates to develop vertical permeability. Therefore, it appears that the next logical step should be to focus on vertical flow only using a VIP-style device.

Although the VIP failed during its only day in the field, it can be retrofitted to include a tracking system. Other than that, no significant modifications should be required to induce a vertical point source of water. It should be emphasized that the VIP still has significant advantages when compared with other in situ permeability measuring techniques. Unlike other devices, because of the VIP's retractable tip, the device still should be "smear-proof" and "sediment intrusion proof."

During future research with the VIP, more analytical analysis should be conducted to determine if it would be possible to use a VAHIP-style device to back-calculate orientation-dependent permeability coefficients. Alternatively, an empirical study could be conducted. Using a small soil box, a series of "wet-dry sensors," or small wires, could be set up in a soil matrix around the VAHIP. Flow could be made to run through the device, and the wires' resistivities could be measured. As water touches the wires, their resistivities should significantly decrease. This technology has been shown to work in previous FDOT projects (project BD545-58 for example); and it is how many commercially-available sprinkler systems operate. Not only might this type of analysis give investigators the tools they would need to determine orientation-specific permeability coefficients; it would also determine whether or not a VAHIP-style probe

can induce orientation-specific flow. As discussed in Chapter 1, some believe that as soon as water leaves the VAHIP, it will necessarily travel along the path of least resistance. Until either of these analyses is conducted, full-scale deployment of the VAHIP is not recommended. Instead, as discussed, the VIP should be FDOT's focus for production-type testing.

CHAPTER 6
SUMMARY AND RECOMMENDATIONS

The following is a bulleted list of key points and recommendations from this report:

- Several VAHIP-style devices were designed, built, and tested.
- The final version of the VAHIP was tested both in sand barrels and in the field. Results were compared to bench permeability test results. Data appear to indicate that average in situ permeability coefficients from the VAHIP are reasonably close to permeability coefficients measured during bench permeability tests. However, this analysis should be seen as only a rough approximation.
- A vertical-only, VIP probe was also designed and developed. It was tested in the field, but because a hole was pre-drilled, the device failed. The device should be redesigned with an internal tracking system similar to the VAHIP. Or, in lieu of a tracking system, predrilled boreholes should not be used during future VIP tests.
- Analysis was conducted on Hvorslev's equations that appears to indicate that the previous methods for using VAHIP data were incorrect. The new analysis appears to indicate that while the final version of the VAHIP may induce flow rates as intended, it is unclear how to use the horizontal flow rate to back-calculate the horizontal permeability.
- Some have argued that as soon as water leaves the VAHIP, it will follow the path of least resistance. A study should be conducted with the VAHIP and a series of wet-dry sensors to determine how/if horizontal flow is initiated; and if this data can be used to empirically solve for the horizontal permeability coefficient.
- Until more analysis is conducted with the VAHIP, FDOT's focus should be on the VIP. The device should be redesigned to include a tracking system; and several tests should be conducted so that an accurate shape factor can be used for analysis.

LIST OF REFERENCES

ASTM D4044-96 (1998). Standard test method (field procedure) for instantaneous change in head (slug) test for determining hydraulic properties of aquifers. West Conshohocken, PA: American Society for Testing of Materials.

ASTM D5084-10 (2010). Standard test methods for measurement of hydraulic conductivity of saturated porous materials using a flexible wall permeameter. West Conshohocken, PA: American Society for Testing of Materials.

Andreyev, N. E. and Wiseman, L. P. (1989). *Stormwater retention pond infiltration analyses in unconfined aquifers*. New York: Jamal and Associates.

Aravin, V. I. and Numerov, S. N. (1953). *Theory of motion of liquids and gases in undeformable porous media* (in Russian). Moscow : Gostekhizdat, English translation by A. Moscona, Israel, Prog. For Scientific Trans., 1965, referenced in Bear, 1979.

Bear, J. (1979). *Dynamics of fluids in porous media*. New York: Dover.

Birgisson, B. and Solseng, P. B. (1996). *An evaluation of methods/devices for measuring in-situ drainage characteristics of aggregate base and granular subgrade materials, phase I*, Minnesota: Barr Engineering Company.

Bloomquist, D. (2007). Development of a field permeability apparatus. *FDOT Final Report, Project No. BD-545, RPWO #15,* Tallahassee, FL: Florida Department of Transportation.

Bouwer, H. and Rice, R. C. (1976). A slug test for determining hydraulic conductivity of unconfined aquifers with completely or partially penetrating wells. *Water Resources Research*, 12 (3), pp. 424-428.

Butler, J. J. Jr. (1998). *The Design, performance, and analysis of slug tests*. New York: Lewis Publishers.

Carrier, W. D. (2003). Goodbye Hazen; hello, Kozeny-Carman. *Journal of Geotechnical and Geoenvironmental Engineering*, 129 (11), 1054-1056.

Chertousov, M. D. (1949). *A specialized hydraulics course* (in Russian). Moscow: Gosenergouzdat, referenced in Bear, 1979.

Chertousov, M. D. (1962). *Hydraulics* (in Russian). Moscow: Gosenergouzdat, referenced in Bear, 1979.

Chu, L. and Grader, A. S. (1991). Transient-pressure analysis for an interference slug test. SPE Paper 23444, presented at the SPE Eastern Regional Meeting, Lexington, KY, Oct. 22-25.

Cooper, H. H., Bredehoeft, H. D., and Papadopulos, I. S. (1967). Response of a finite-diameter well to an instantaneous charge of water. *Water Resources J.*, 1, 263-269.

Dagan, G. (1967). A method of determining the permeability and effective porosity of unconfined anisotropic aquifers. *Water Resources. Research*, 3 (4), 1059-1071.

Darcy, H. (1856). *The public fountains of the city of Dijon: appendix – note D*. English translation by P. Bobeck: Dubuque, Iowa: Kendall/Hunt Publishing Co., 2004.

Das, B. M. (2002). *Principles of geotechnical engineering 5th edition*. Pacific Grove, CA: Wadsworth Group.

Das, B. M. (2004). *Principles of foundation Engineering 5th edition.* Pacific Grove, CA: Brooks/Cole.

Davidson, J. L. (2002). *Soil mechanics laboratory manual*. Gainesville, FL: University of Florida course materials.

Domenico, P. A. and Schwartz, F. W. (1990). *Physical and chemical hydrogeology*. New York: John Wiley and Sons.

Fancher, G. H., Lewis, J. A. and Barnes, K. B. (1933). Some physical characteristics of oil sands. Pa. State College, Min. Ind. Exp. Sta. Bull. 12, p. 141, referenced in Leonards, 1962.

Grim, R. E. (1953). *Clay mineralogy.* New York: McGraw-Hill.

Hvorslev, M. J. (1951). Time lag and soil permeability in groundwater observations. *Bulletin no.36,* Vicksburg, MS: U.S. Army Engineer Waterways Experiment Station.

Lambe, T. S. and Whitman, R. (1969). *Soil mechanics*. New York: John Wiley & Sons.

Leonards, G. A. (1962). *Foundation engineering.* New York: McGraw-Hill.

Murthy V. N. S. (2003). *Geotechnical engineering principles and practices of soil mechanics and foundation engineering*. New York: Marcel Dekker.

Peres, A. M. M., Onur, M., and Reynolds, A. C. (1989). A new analysis procedure for determining aquifer properties from slug test data. *Water Resources Research,* 25 (7), 1597-1602.

Reynolds, O. (1883). An experimental investigation of the circumstances which determine whether the motion of water shall be direct or sinuous and of the law of resistance of parallel channels. *Phil. Trans. Roy. Soc. London*, vol. 174., referenced in Leonards 1962.

Shroff, A. V., and Shah., D. L. (2003). *Soil mechanics and geotechnical engineering*. New York: Taylor and Francis.

Terzaghi, I. and Peck, R. G. (1969). *Soil mechanics in engineering practice*. New York: John Wiley and Sons.

Yoshikuni, H., Moriwaki, T., Ikegami, S., and Xo, T. (1995). Direct determination of permeability of clay from constant rate of strain consolidation tests. *Proc. Int. Symp. On Compression and Consolidation of Clayey Soils*, vol. 1, 609-614.

APPENDIX A

VAHIP EQUIPMENT CHECKLIST

Table A-1. VAHIP equipment checklist

Quantity	Part	Check
1	Probe	
1	Water Vessel w/ Cap	
1	Support Stand	
1	Flexible Tubing	
1	AWJ Connection – Female	
1	AWJ Connection – Male	
1	Air Tank w/ Quick Connection Hose	
1	Air Compressor	
1	Coordinate Dial	
1	Reference Stake	
1	Tape Measure	
*	Data Sheet	
1	Pen/Pencil	
1	Chalk	
1	Allen Key	
1	Wire Brush	
1	Stopwatch	
**	AWJ Rod O-rings	
1	Grease Sealant	
***	AWJ Rods	

*Bring enough data sheets to record the intended number of test plus a few for backup.
**Bring enough to seal the number of rod connections to be used plus extras.
***Should be supplied on SPT rig

APPENDIX B

SAND BARREL RAW DATA

Table B-1. Raw data from VAHIP sand-barrel test 1

Vertical Flow

Inputs		Units	
Description	Symbol	Inches	cm
Probe Diameter	D	0.75	1.905
Piezometer Diameter	d	6.065	15.4051
Length of Rod	L_{r1}	39.25	99.695
# of Rods	N/A	1	
Total Rod Length	L_{rtotal}	39.25	99.695
Water Temperature	T (˚C)	23	
Water Density	ρ (kg/m^3)	998	
Viscosity	μ (N-s/m^2)	0.000934	
Viscosity@20˚C	μ (N-s/m^2)	0.001002	
Roughness Coef.	ε	0.0045	
Rod Diameter	D_{rod}	1.625	4.1275

Test No.	Time 1 (s)	Time 2 (s)	L_{rtotal} (in)	L_{rtotal} (cm)	H_{1Tank} (in)	H_{2Tank} (in)	ΔH_{Tank} (in)	H_{1Total} (cm)	H_{2Total} (cm)	Re	Flow Type	$f_{laminar}$	$f_{turbulent}$	olebrook E	f	H_{loss}	$H_1 - H_{loss}$)/ H
1	30	60	39.25	99.695	19.25	18.625	0.625	148.59	147.0025	23.34544	Laminar	2.74143	0.40785	0.40785	2.74143	0.00009	1.01080
2	60	90	39.25	99.695	18.625	18.125	0.5	147.0025	145.7325	18.67635	Laminar	3.42679	0.35911	0.35911	3.42679	0.00008	1.00871
3	90	120	39.25	99.695	18.125	17.5	0.625	145.7325	144.145	23.34544	Laminar	2.74143	0.35911	0.35911	2.74143	0.00009	1.01101
4	120	150	39.25	99.695	17.5	17	0.5	144.145	142.875	18.67635	Laminar	3.42679	0.40785	0.40785	3.42679	0.00008	1.00889
5	150	180	39.25	99.695	17	16.375	0.625	142.875	141.2875	23.34544	Laminar	2.74143	0.48017	0.48017	2.74143	0.00009	1.01124
6	180	210	39.25	99.695	16.375	15.875	0.5	141.2875	140.0175	18.67635	Laminar	3.42679	0.35911	0.35911	3.42679	0.00008	1.00907
7	210	240	39.25	99.695	15.875	15.25	0.625	140.0175	138.43	23.34544	Laminar	2.74143	0.38135	0.38135	2.74143	0.00009	1.01147
8	240	270	39.25	99.695	15.25	14.375	0.875	138.43	136.2075	32.68361	Laminar	1.95817	0.44007	0.44007	1.95817	0.00013	1.01632
9	270	300	39.25	99.695	14.375	14.25	0.125	136.2075	135.89	4.66909	Laminar	13.70717	0.44007	0.44007	13.70717	0.00002	1.00234

Results

Test No.	Permeability K_v (cm/s)	Permeability $K_{v@20˚C}$ (cm/s)	Likely Soil Type	Drainage Conditions	Degree of Permeability
1	1.27E-02	1.19E-02	Clean Sand and Gravel Mix	Good	Medium
2	1.03E-02	9.59E-03	Clean Sand and Gravel Mix	Good	Medium
3	1.30E-02	1.21E-02	Clean Sand and Gravel Mix	Good	Medium
4	1.05E-02	9.78E-03	Clean Sand and Gravel Mix	Good	Medium
5	1.33E-02	1.23E-02	Clean Sand and Gravel Mix	Good	Medium
6	1.07E-02	9.98E-03	Clean Sand and Gravel Mix	Good	Medium
7	1.35E-02	1.26E-02	Clean Sand and Gravel Mix	Good	Medium
8	1.92E-02	1.79E-02	Clean Sand and Gravel Mix	Good	Medium
9	2.77E-03	2.58E-03	Clean Sand and Gravel Mix	Good	Medium
	AVG	1.10E-02	Clean Sand and Gravel Mix	Good	Medium

Table B-2. Raw data from VAHIP sand-barrel test 2

Vertical Flow

Inputs		Units	
Description	Symbol	Inches	cm
Probe Diameter	D	0.75	1.905
Piezometer Diameter	d	6.065	15.4051
Length of Rod	L_{r1}	39.25	99.695
# of Rods	N/A	1	
Total Rod Length	L_{rtotal}	39.25	99.695
Water Temperature	T (°C)	25	
Water Density	ρ (kg/m^3)	998	
Viscosity	μ (N-s/m^2)	0.000892	
Viscosity@20°C	μ (N-s/m^2)	0.001002	
Roughness Coef.	ε	0.0045	
Rod Diameter	D_{rod}	1.625	4.1275

Test No.	Time 1 (s)	Time 2 (s)	L_{rtotal} (in)	L_{rtotal} (cm)	H_{1Tank} (in)	H_{2Tank} (in)	ΔH_{Tank} (in)	H_{1Total} (cm)	H_{2Total} (cm)	Re	Flow Type	$f_{laminar}$	$f_{turbulent}$	Colebrook EQ	f	H_{loss}	$(H_1 - H_{loss})/ H_2$
1	30	60	39.25	99.695	17.125	12.75	4.375	143.1925	132.08	170.99467	Laminar	0.37428	0.40785	0.40785	0.37428	0.00063	1.08413
2	60	90	39.25	99.695	12.75	8.5	4.25	132.08	121.285	166.10911	Laminar	0.38529	0.35911	0.35911	0.38529	0.00061	1.08900
3	90	120	39.25	99.695	8.5	4.625	3.875	121.285	111.4425	151.45242	Laminar	0.42257	0.35911	0.35911	0.42257	0.00056	1.08831
4	120	150	39.25	99.695	4.625	1	3.625	111.4425	102.235	141.68130	Laminar	0.45172	0.40785	0.40785	0.45172	0.00052	1.09006
5	150	180	39.25	99.695	19.625	15.25	4.375	149.5425	138.43	170.99467	Laminar	0.37428	0.48017	0.48017	0.37428	0.00063	1.08027
6	180	210	39.25	99.695	15.25	11.375	3.875	138.43	128.5875	151.45242	Laminar	0.42257	0.35911	0.35911	0.42257	0.00056	1.07654
7	210	240	39.25	99.695	11.375	7.75	3.625	128.5875	119.38	141.68130	Laminar	0.45172	0.38135	0.38135	0.45172	0.00052	1.07712
8	240	270	39.25	99.695	7.75	4.125	3.625	119.38	110.1725	141.68130	Laminar	0.45172	0.44007	0.44007	0.45172	0.00052	1.08357

Results

Test No.	Permeability K_v (cm/s)	Permeability $K_{v@20°C}$ (cm/s)	Likely Soil Type	Drainage Conditions	Degree of Permeability
1	9.58E-02	8.53E-02	Clean Sand and Gravel Mix	Good	Medium
2	1.01E-01	9.00E-02	Clean Sand and Gravel Mix	Good	Medium
3	1.00E-01	8.94E-02	Clean Sand and Gravel Mix	Good	Medium
4	1.02E-01	9.11E-02	Clean Sand and Gravel Mix	Good	Medium
5	9.16E-02	8.15E-02	Clean Sand and Gravel Mix	Good	Medium
6	8.75E-02	7.79E-02	Clean Sand and Gravel Mix	Good	Medium
7	8.81E-02	7.85E-02	Clean Sand and Gravel Mix	Good	Medium
8	9.52E-02	8.48E-02	Clean Sand and Gravel Mix	Good	Medium
	AVG	8.48E-02	Clean Sand and Gravel Mix	Good	Medium

Table B-3. Raw data from VAHIP sand-barrel test 3

Inputs		Units	
Description	Symbol	Inches	cm
Probe Diameter	D	0.75	1.905
Piezometer Diameter	d	6.065	15.4051
Length of Rod	L_{r1}	39.25	99.695
# of Rods	N/A	1	
Total Rod Length	L_{rtotal}	39.25	99.695
Water Temperature	T (°C)	22	
Water Density	ρ (kg/m^3)	998	
Viscosity	μ (N-s/m^2)	0.000956	
Viscosity@20°C	μ (N-s/m^2)	0.001002	
Roughness Coef.	ε	0.0045	
Rod Diameter	D_{rod}	1.625	4.1275

Test No.	Time 1 (s)	Time 2 (s)	L_{rtotal} (in)	L_{rtotal} (cm)	H_{1Tank} (in)	H_{2Tank} (in)	ΔH_{Tank} (in)	H_{1Total} (cm)	H_{2Total} (cm)	Re	Flow Type	$f_{laminar}$	$f_{turbulent}$	olebrook E	f	H_{loss}	$H_1 - H_{loss})/ H$
1	30	60	39.25	99.695	20.875	20	0.875	152.7175	150.495	31.93458	Laminar	2.00410	0.40785	0.40785	2.00410	0.00014	1.01477
2	60	90	39.25	99.695	20	19.125	0.875	150.495	148.2725	31.93458	Laminar	2.00410	0.35911	0.35911	2.00410	0.00014	1.01499
3	90	120	39.25	99.695	19.125	18.25	0.875	148.2725	146.05	31.93458	Laminar	2.00410	0.35911	0.35911	2.00410	0.00014	1.01522
4	120	150	39.25	99.695	18.25	17.4375	0.8125	146.05	143.98625	29.65354	Laminar	2.15826	0.40785	0.40785	2.15826	0.00013	1.01433
5	150	180	39.25	99.695	17.4375	16.625	0.8125	143.98625	141.9225	29.65354	Laminar	2.15826	0.48017	0.48017	2.15826	0.00013	1.01454
6	180	210	39.25	99.695	16.625	15.875	0.75	141.9225	140.0175	27.37250	Laminar	2.33811	0.35911	0.35911	2.33811	0.00012	1.01360
7	210	240	39.25	99.695	15.875	15.125	0.75	140.0175	138.1125	27.37250	Laminar	2.33811	0.38135	0.38135	2.33811	0.00012	1.01379
8	240	270	39.25	99.695	15.125	14.4375	0.6875	138.1125	136.36625	25.09146	Laminar	2.55067	0.44007	0.44007	2.55067	0.00011	1.01280
9	300	330	39.25	99.695	14.4375	13.75	0.6875	136.36625	134.62	25.09146	Laminar	2.55067	0.44007	0.44007	2.55067	0.00011	1.01297

Results

Test No.	Permeability K_v (cm/s)	Permeability $K_{v@20°C}$ (cm/s)	Likely Soil Type	Drainage Conditions	Degree of Permeability
1	1.74E-02	1.66E-02	Clean Sand and Gravel Mix	Good	Medium
2	1.76E-02	1.68E-02	Clean Sand and Gravel Mix	Good	Medium
3	1.79E-02	1.71E-02	Clean Sand and Gravel Mix	Good	Medium
4	1.69E-02	1.61E-02	Clean Sand and Gravel Mix	Good	Medium
5	1.71E-02	1.63E-02	Clean Sand and Gravel Mix	Good	Medium
6	1.60E-02	1.53E-02	Clean Sand and Gravel Mix	Good	Medium
7	1.62E-02	1.55E-02	Clean Sand and Gravel Mix	Good	Medium
8	1.51E-02	1.44E-02	Clean Sand and Gravel Mix	Good	Medium
9	1.53E-02	1.46E-02	Clean Sand and Gravel Mix	Good	Medium
	AVG	1.58E-02	Clean Sand and Gravel Mix	Good	Medium

Table B-4. Raw data from VAHIP sand-barrel test 4

Vertical Flow

Inputs		Units	
Description	Symbol	Inches	cm
Probe Diameter	D	0.75	1.905
Piezometer Diameter	d	6.065	15.4051
Length of Rod	L_{r1}	39.25	99.695
# of Rods	N/A	1	
Total Rod Length	L_{rtotal}	39.25	99.695
Water Temperature	T (˚C)	22	
Water Density	ρ (kg/m^3)	998	
Viscosity	μ (N-s/m^2)	0.000956	
Viscosity@20˚C	μ (N-s/m^2)	0.001002	
Roughness Coef.	ε	0.0045	
Rod Diameter	D_{rod}	1.625	4.1275

Test No.	Time 1 (s)	Time 2 (s)	L_{rtotal} (in)	L_{rtotal} (cm)	H_{1Tank} (in)	H_{2Tank} (in)	ΔH_{Tank} (in)	H_{1Total} (cm)	H_{2Total} (cm)	Re	Flow Type	$f_{laminar}$	$f_{turbulent}$	plebrook E	f	H_{loss}	H_1 - H_{loss})/ H
1	30	60	39.25	99.695	20.875	19.0625	1.8125	152.7175	148.11375	66.15020	Laminar	0.96750	0.40785	0.40785	0.96750	0.00028	1.03108
2	60	90	39.25	99.695	19.0625	17.625	1.4375	148.11375	144.4625	52.46395	Laminar	1.21989	0.35911	0.35911	1.21989	0.00022	1.02527
3	90	120	39.25	99.695	17.625	15.875	1.75	144.4625	140.0175	63.86916	Laminar	1.00205	0.35911	0.35911	1.00205	0.00027	1.03174
4	120	150	39.25	99.695	15.875	14	1.875	140.0175	135.255	68.43124	Laminar	0.93525	0.40785	0.40785	0.93525	0.00029	1.03521
5	150	180	39.25	99.695	14	12.25	1.75	135.255	130.81	63.86916	Laminar	1.00205	0.48017	0.48017	1.00205	0.00027	1.03398
6	180	210	39.25	99.695	12.25	10.625	1.625	130.81	126.6825	59.30708	Laminar	1.07913	0.35911	0.35911	1.07913	0.00025	1.03258
7	210	240	39.25	99.695	10.625	8.125	2.5	126.6825	120.3325	91.24166	Laminar	0.70143	0.38135	0.38135	0.70143	0.00039	1.05277
8	240	270	39.25	99.695	8.125	7.375	0.75	120.3325	118.4275	27.37250	Laminar	2.33811	0.44007	0.44007	2.33811	0.00012	1.01608
9	300	330	39.25	99.695	7.375	5.75	1.625	118.4275	114.3	59.30708	Laminar	1.07913	0.44007	0.44007	1.07913	0.00025	1.03611

Results

Test No.	Permeability K_v (cm/s)	Permeability $K_{v@20˚C}$ (cm/s)	Likely Soil Type	Drainage Conditions	Degree of Permeability
1	3.63E-02	3.46E-02	Clean Sand and Gravel Mix	Good	Medium
2	2.96E-02	2.82E-02	Clean Sand and Gravel Mix	Good	Medium
3	3.71E-02	3.53E-02	Clean Sand and Gravel Mix	Good	Medium
4	4.10E-02	3.91E-02	Clean Sand and Gravel Mix	Good	Medium
5	3.96E-02	3.78E-02	Clean Sand and Gravel Mix	Good	Medium
6	3.80E-02	3.63E-02	Clean Sand and Gravel Mix	Good	Medium
7	6.10E-02	5.82E-02	Clean Sand and Gravel Mix	Good	Medium
8	1.89E-02	1.80E-02	Clean Sand and Gravel Mix	Good	Medium
9	4.21E-02	4.01E-02	Clean Sand and Gravel Mix	Good	Medium
	AVG	3.64E-02	Clean Sand and Gravel Mix	Good	Medium

Table B-5. Raw data from VAHIP sand-barrel test 5

Vertical Flow

Inputs		Units	
Description	Symbol	Inches	cm
Probe Diameter	D	0.75	1.905
Piezometer Diameter	d	6.065	15.4051
Length of Rod	L_{r1}	39.25	99.695
# of Rods	N/A	1	
Total Rod Length	L_{rtotal}	39.25	99.695
Water Temperature	T (˚C)	24	
Water Density	ρ (kg/m^3)	998	
Viscosity	μ (N-s/m^2)	0.000913	
Viscosity@20˚C	μ (N-s/m^2)	0.001002	
Roughness Coef.	ε	0.0045	
Rod Diameter	D_{rod}	1.625	4.1275

Test No.	Time 1 (s)	Time 2 (s)	L_{rtotal} (in)	L_{rtotal} (cm)	H_{1Tank} (in)	H_{2Tank} (in)	ΔH_{Tank} (in)	H_{1Total} (cm)	H_{2Total} (cm)	Re	Flow Type	$f_{laminar}$	$f_{turbulent}$	olebrook E	f	H_{loss}	$H_1 - H_{loss})/ H$
1	30	60	39.25	99.695	22.25	22	0.25	156.21	155.575	9.55383	Laminar	6.69888	0.40785	0.40785	6.69888	0.00004	1.00408
2	60	90	39.25	99.695	22	21.875	0.125	155.575	155.2575	4.77692	Laminar	13.39777	0.35911	0.35911	13.39777	0.00002	1.00204
3	90	120	39.25	99.695	21.875	21.75	0.125	155.2575	154.94	4.77692	Laminar	13.39777	0.35911	0.35911	13.39777	0.00002	1.00205
4	120	150	39.25	99.695	21.75	21.5	0.25	154.94	154.305	9.55383	Laminar	6.69888	0.40785	0.40785	6.69888	0.00004	1.00411
5	150	180	39.25	99.695	21.5	21.375	0.125	154.305	153.9875	4.77692	Laminar	13.39777	0.48017	0.48017	13.39777	0.00002	1.00206
6	180	210	39.25	99.695	21.375	21.1875	0.1875	153.9875	153.51125	7.16537	Laminar	8.93184	0.35911	0.35911	8.93184	0.00003	1.00310
7	210	240	39.25	99.695	21.1875	21	0.1875	153.51125	153.035	7.16537	Laminar	8.93184	0.38135	0.38135	8.93184	0.00003	1.00311
8	240	270	39.25	99.695	21	20.875	0.125	153.035	152.7175	4.77692	Laminar	13.39777	0.44007	0.44007	13.39777	0.00002	1.00208
9	270	300	39.25	99.695	20.875	20.75	0.125	152.7175	152.4	4.77692	Laminar	13.39777	0.44007	0.44007	13.39777	0.00002	1.00208

Results

Test No.	Permeability K_v (cm/s)	Permeability $K_{v@20˚C}$ (cm/s)	Likely Soil Type	Drainage Conditions	Degree of Permeability
1	4.83E-03	4.40E-03	Clean Sand and Gravel Mix	Good	Medium
2	2.42E-03	2.21E-03	Clean Sand and Gravel Mix	Good	Medium
3	2.43E-03	2.21E-03	Clean Sand and Gravel Mix	Good	Medium
4	4.87E-03	4.44E-03	Clean Sand and Gravel Mix	Good	Medium
5	2.44E-03	2.22E-03	Clean Sand and Gravel Mix	Good	Medium
6	3.67E-03	3.35E-03	Clean Sand and Gravel Mix	Good	Medium
7	3.68E-03	3.36E-03	Clean Sand and Gravel Mix	Good	Medium
8	2.46E-03	2.24E-03	Clean Sand and Gravel Mix	Good	Medium
9	2.47E-03	2.25E-03	Clean Sand and Gravel Mix	Good	Medium
	AVG	2.96E-03	Clean Sand and Gravel Mix	Good	Medium

Table B-6. Raw data from VAHIP sand-barrel test 6

Vertical Flow

Inputs		Units	
Description	Symbol	Inches	cm
Probe Diameter	D	0.75	1.905
Piezometer Diameter	d	6.065	15.4051
Length of Rod	L_{r1}	39.25	99.695
# of Rods	N/A	1	
Total Rod Length	L_{rtotal}	39.25	99.695
Water Temperature	T (˚C)	23	
Water Density	ρ (kg/m^3)	998	
Viscosity	μ (N-s/m^2)	0.000934	
Viscosity@20˚C	μ (N-s/m^2)	0.001002	
Roughness Coef.	ε	0.0045	
Rod Diameter	D_{rod}	1.625	4.1275

Test No.	Time 1 (s)	Time 2 (s)	L_{rtotal} (in)	L_{rtotal} (cm)	H_{1Tank} (in)	H_{2Tank} (in)	ΔH_{Tank} (in)	H_{1Total} (cm)	H_{2Total} (cm)	Re	Flow Type	$f_{laminar}$	$f_{turbulent}$	olebrook E	f	H_{loss}	$H_1 - H_{loss}$)/ H
1	30	60	39.25	99.695	21.6875	21.625	0.0625	154.78125	154.6225	2.33454	Laminar	27.41435	0.40785	0.40785	27.41435	0.00001	1.00103
2	60	90	39.25	99.695	21.625	21.5625	0.0625	154.6225	154.46375	2.33454	Laminar	27.41435	0.35911	0.35911	27.41435	0.00001	1.00103
3	90	120	39.25	99.695	21.5625	21.5	0.0625	154.46375	154.305	2.33454	Laminar	27.41435	0.35911	0.35911	27.41435	0.00001	1.00103
4	120	150	39.25	99.695	21.5	21.375	0.125	154.305	153.9875	4.66909	Laminar	13.70717	0.40785	0.40785	13.70717	0.00002	1.00206
5	150	180	39.25	99.695	21.375	21.3125	0.0625	153.9875	153.82875	2.33454	Laminar	27.41435	0.48017	0.48017	27.41435	0.00001	1.00103
6	180	210	39.25	99.695	21.3125	21.1875	0.125	153.82875	153.51125	4.66909	Laminar	13.70717	0.35911	0.35911	13.70717	0.00002	1.00207
7	210	240	39.25	99.695	21.1875	21.125	0.0625	153.51125	153.3525	2.33454	Laminar	27.41435	0.38135	0.38135	27.41435	0.00001	1.00104
8	240	270	39.25	99.695	21.125	21.0625	0.0625	153.3525	153.19375	2.33454	Laminar	27.41435	0.44007	0.44007	27.41435	0.00001	1.00104
9	270	300	39.25	99.695	21.0625	20.9375	0.125	153.19375	152.87625	4.66909	Laminar	13.70717	0.44007	0.44007	13.70717	0.00002	1.00208

Results

Test No.	Permeability K_v (cm/s)	Permeability $K_{v@20˚C}$ (cm/s)	Likely Soil Type	Drainage Conditions	Degree of Permeability
1	1.22E-03	1.13E-03	Clean Sand and Gravel Mix	Good	Medium
2	1.22E-03	1.14E-03	Clean Sand and Gravel Mix	Good	Medium
3	1.22E-03	1.14E-03	Clean Sand and Gravel Mix	Good	Medium
4	2.44E-03	2.28E-03	Clean Sand and Gravel Mix	Good	Medium
5	1.22E-03	1.14E-03	Clean Sand and Gravel Mix	Good	Medium
6	2.45E-03	2.28E-03	Clean Sand and Gravel Mix	Good	Medium
7	1.23E-03	1.14E-03	Clean Sand and Gravel Mix	Good	Medium
8	1.23E-03	1.14E-03	Clean Sand and Gravel Mix	Good	Medium
9	2.46E-03	2.29E-03	Clean Sand and Gravel Mix	Good	Medium
	AVG	1.52E-03	Clean Sand and Gravel Mix	Good	Medium

Table B-7. Raw data from VAHIP sand-barrel test 7

Vertical Flow

Inputs		Units	
Description	Symbol	Inches	cm
Probe Diameter	D	0.75	1.905
Piezometer Diameter	d	6.065	15.4051
Effective Screen Length	L	0.75	1.905
Shape Factor	F	3.284141935	8.341720514
Length of Rod	L_{r1}	39.25	99.695
# of Rods	N/A	1	
Total Rod Length	L_{rtotal}	39.25	99.695
Water Temperature	T (°C)	23	
Water Density	ρ (kg/m^3)	998	
Viscosity	μ (N-s/m^2)	0.000934	
Viscosity@20°C	μ (N-s/m^2)	0.001002	
Roughness Coef.	ε	0.0045	
Rod Diameter	D_{rod}	1.625	4.1275

Test No.	Time 1 (s)	Time 2 (s)	L_{rtotal} (in)	L_{rtotal} (cm)	H_{1Tank} (in)	H_{2Tank} (in)	ΔH_{Tank} (in)	H_{1Total} (cm)	H_{2Total} (cm)	Re	Flow Type	$f_{laminar}$	$f_{turbulent}$	Colebrook EQ	f	H_{loss}	$(H_1 - H_{loss})/ H_2$
1	30	60	39.25	99.695	21.5625	21.4375	0.125	154.46375	154.14625	4.66909	Laminar	13.70717	0.40785	0.40785	13.70717	0.00002	1.00206
2	60	90	39.25	99.695	21.4375	21.3125	0.125	154.14625	153.82875	4.66909	Laminar	13.70717	0.35911	0.35911	13.70717	0.00002	1.00206
3	90	120	39.25	99.695	21.3125	21.1875	0.125	153.82875	153.51125	4.66909	Laminar	13.70717	0.35911	0.35911	13.70717	0.00002	1.00207
4	120	150	39.25	99.695	21.1875	21.0625	0.125	153.51125	153.19375	4.66909	Laminar	13.70717	0.40785	0.40785	13.70717	0.00002	1.00207
5	150	180	39.25	99.695	21.0625	20.9375	0.125	153.19375	152.87625	4.66909	Laminar	13.70717	0.48017	0.48017	13.70717	0.00002	1.00208
6	180	210	39.25	99.695	20.9375	20.8125	0.125	152.87625	152.55875	4.66909	Laminar	13.70717	0.35911	0.35911	13.70717	0.00002	1.00208
7	210	240	39.25	99.695	20.8125	20.6875	0.125	152.55875	152.24125	4.66909	Laminar	13.70717	0.38135	0.38135	13.70717	0.00002	1.00209
8	240	270	39.25	99.695	20.6875	20.5625	0.125	152.24125	151.92375	4.66909	Laminar	13.70717	0.44007	0.44007	13.70717	0.00002	1.00209
9	270	300	39.25	99.695	20.5625	20.4375	0.125	151.92375	151.60625	4.66909	Laminar	13.70717	0.44007	0.44007	13.70717	0.00002	1.00209

Results

Test No.	Permeability K_v (cm/s)	Permeability $K_{v@20°C}$ (cm/s)	Likely Soil Type	Drainage Conditions	Degree of Permeability
1	2.44E-03	2.27E-03	Clean Sand and Gravel Mix	Good	Medium
2	2.45E-03	2.28E-03	Clean Sand and Gravel Mix	Good	Medium
3	2.45E-03	2.28E-03	Clean Sand and Gravel Mix	Good	Medium
4	2.46E-03	2.29E-03	Clean Sand and Gravel Mix	Good	Medium
5	2.46E-03	2.29E-03	Clean Sand and Gravel Mix	Good	Medium
6	2.47E-03	2.30E-03	Clean Sand and Gravel Mix	Good	Medium
7	2.47E-03	2.30E-03	Clean Sand and Gravel Mix	Good	Medium
8	2.48E-03	2.31E-03	Clean Sand and Gravel Mix	Good	Medium
9	2.48E-03	2.31E-03	Clean Sand and Gravel Mix	Good	Medium
	AVG	2.29E-03	Clean Sand and Gravel Mix	Good	Medium

Table B-8. Raw data from VAHIP sand-barrel test 8

Vertical Flow

Inputs		Units	
Description	Symbol	Inches	cm
Probe Diameter	D	0.75	1.905
Piezometer Diameter	d	6.065	15.4051
Effective Screen Length	L	0.75	1.905
Shape Factor	F	3.284141935	8.341720514
Length of Rod	L_{r1}	39.25	99.695
# of Rods	N/A	1	
Total Rod Length	L_{rtotal}	39.25	99.695
Water Temperature	T (˚C)	23	
Water Density	ρ (kg/m^3)	998	
Viscosity	μ (N-s/m^2)	0.000934	
Viscosity@20˚C	μ (N-s/m^2)	0.001002	
Roughness Coef.	ε	0.0045	
Rod Diameter	D_{rod}	1.625	4.1275

Test No.	Time 1 (s)	Time 2 (s)	L_{rtotal} (in)	L_{rtotal} (cm)	H_{1Tank} (in)	H_{2Tank} (in)	ΔH_{Tank} (in)	H_{1Total} (cm)	H_{2Total} (cm)	Re	Flow Type	$f_{laminar}$	$f_{turbulent}$	Colebrook EQ	f	H_{loss}	$(H_1 - H_{loss})/ H_2$
1	30	60	39.25	99.695	21.875	21.75	0.125	155.2575	154.94	4.66909	Laminar	13.70717	0.40785	0.40785	13.70717	0.00002	1.00205
2	60	90	39.25	99.695	21.75	21.625	0.125	154.94	154.6225	4.66909	Laminar	13.70717	0.35911	0.35911	13.70717	0.00002	1.00205
3	90	120	39.25	99.695	21.625	21.4375	0.1875	154.6225	154.14625	7.00363	Laminar	9.13812	0.35911	0.35911	9.13812	0.00003	1.00309
4	120	150	39.25	99.695	21.4375	21.3125	0.125	154.14625	153.82875	4.66909	Laminar	13.70717	0.40785	0.40785	13.70717	0.00002	1.00206
5	150	180	39.25	99.695	21.3125	21.1875	0.125	153.82875	153.51125	4.66909	Laminar	13.70717	0.48017	0.48017	13.70717	0.00002	1.00207
6	180	210	39.25	99.695	21.1875	21.0625	0.125	153.51125	153.19375	4.66909	Laminar	13.70717	0.35911	0.35911	13.70717	0.00002	1.00207
7	210	240	39.25	99.695	21.0625	20.9375	0.125	153.19375	152.87625	4.66909	Laminar	13.70717	0.38135	0.38135	13.70717	0.00002	1.00208
8	240	270	39.25	99.695	20.9375	20.8125	0.125	152.87625	152.55875	4.66909	Laminar	13.70717	0.44007	0.44007	13.70717	0.00002	1.00208
9	270	300	39.25	99.695	20.8125	20.6875	0.125	152.55875	152.24125	4.66909	Laminar	13.70717	0.44007	0.44007	13.70717	0.00002	1.00209

Results

Test No.	Permeability K_v (cm/s)	Permeability $K_{v@20˚C}$ (cm/s)	Likely Soil Type	Drainage Conditions	Degree of Permeability
1	2.43E-03	2.26E-03	Clean Sand and Gravel Mix	Good	Medium
2	2.43E-03	2.27E-03	Clean Sand and Gravel Mix	Good	Medium
3	3.66E-03	3.41E-03	Clean Sand and Gravel Mix	Good	Medium
4	2.45E-03	2.28E-03	Clean Sand and Gravel Mix	Good	Medium
5	2.45E-03	2.28E-03	Clean Sand and Gravel Mix	Good	Medium
6	2.46E-03	2.29E-03	Clean Sand and Gravel Mix	Good	Medium
7	2.46E-03	2.29E-03	Clean Sand and Gravel Mix	Good	Medium
8	2.47E-03	2.30E-03	Clean Sand and Gravel Mix	Good	Medium
9	2.47E-03	2.30E-03	Clean Sand and Gravel Mix	Good	Medium
	AVG	2.41E-03	Clean Sand and Gravel Mix	Good	Medium

APPENDIX C

RAW FIELD DATA

Table C-1. Raw Data from VAHIP Field Test

Vertical Flow

Inputs		Units	
Description	Symbol	Inches	cm
Probe Diameter	D	0.75	1.905
Piezometer Diameter	d	6.065	15.4051
Length of Rod	L_{r1}	113	287.02
# of Rods	N/A	1	
Total Rod Length	L_{rtotal}	113	287.02
Water Temperature	T (˚C)	22	
Water Density	ρ (kg/m^3)	998	
Viscosity	μ (N-s/m^2)	0.000956	
Viscosity@20˚C	μ (N-s/m^2)	0.001002	
Roughness Coef.	ε	0.0045	
Rod Diameter	D_{rod}	1.625	4.1275

Test No.	Time 1 (s)	Time 2 (s)	L_{rtotal} (in)	L_{rtotal} (cm)	H_{1Tank} (in)	H_{2Tank} (in)	ΔH_{Tank} (in)	H_{1Total} (cm)	H_{2Total} (cm)	Re	Flow Type	$f_{laminar}$	$f_{turbulent}$	Colebrook EQ	f	H_{loss}	$(H_1 - H_{loss})/ H_2$
1	30	60	113	287.02	19.125	19.0625	0.0625	335.5975	335.43875	2.28104	Laminar	28.05736	0.40785	0.40785	28.05736	0.00003	1.00047
2	60	90	113	287.02	19.0625	19	0.0625	335.43875	335.28	2.28104	Laminar	28.05736	0.35911	0.35911	28.05736	0.00003	1.00047
3	90	120	113	287.02	19	18.9375	0.0625	335.28	335.12125	2.28104	Laminar	28.05736	0.35911	0.35911	28.05736	0.00003	1.00047
4	120	150	113	287.02	18.9375	18.875	0.0625	335.12125	334.9625	2.28104	Laminar	28.05736	0.40785	0.40785	28.05736	0.00003	1.00047
5	150	180	113	287.02	18.875	18.8125	0.0625	334.9625	334.80375	2.28104	Laminar	28.05736	0.48017	0.48017	28.05736	0.00003	1.00047
6	180	210	113	287.02	18.8125	18.75	0.0625	334.80375	334.645	2.28104	Laminar	28.05736	0.35911	0.35911	28.05736	0.00003	1.00047
7	210	240	113	287.02	18.75	18.6875	0.0625	334.645	334.48625	2.28104	Laminar	28.05736	0.38135	0.38135	28.05736	0.00003	1.00047
8	240	270	113	287.02	18.6875	18.625	0.0625	334.48625	334.3275	2.28104	Laminar	28.05736	0.44007	0.44007	28.05736	0.00003	1.00047
9	270	300	113	287.02	18.625	18.4375	0.1875	334.3275	333.85125	6.84312	Laminar	9.35245	0.44007	0.44007	9.35245	0.00008	1.00143
10	300	330	113	287.02	18.4375	18.25	0.1875	333.85125	333.375	6.84312	Laminar	9.35245	0.44007	0.44007	9.35245	0.00008	1.00143

Results

Test No.	Permeability K_v (cm/s)	Permeability $K_{v@20˚C}$ (cm/s)	Likely Soil Type	Drainage Conditions	Degree of Permeability
1	5.61E-04	5.35E-04	Clean Sand and Gravel Mix	Good	Low
2	5.61E-04	5.35E-04	Clean Sand and Gravel Mix	Good	Low
3	5.62E-04	5.36E-04	Clean Sand and Gravel Mix	Good	Low
4	5.62E-04	5.36E-04	Clean Sand and Gravel Mix	Good	Low
5	5.62E-04	5.36E-04	Clean Sand and Gravel Mix	Good	Low
6	5.62E-04	5.36E-04	Clean Sand and Gravel Mix	Good	Low
7	5.63E-04	5.37E-04	Clean Sand and Gravel Mix	Good	Low
8	5.63E-04	5.37E-04	Clean Sand and Gravel Mix	Good	Low
9	1.69E-03	1.61E-03	Clean Sand and Gravel Mix	Good	Medium
10	1.69E-03	1.61E-03	Clean Sand and Gravel Mix	Good	Medium
	AVG	7.51E-04	Clean Sand and Gravel Mix	Good	Low

APPENDIX D

USERS' MANUAL FOR THE 2012 VAHIP

D.1 Description of the 2012 VAHIP Permeameter

The 2012 VAHIP permeameter is designed to be robust and capable of quick and convenient field assembly/disassembly. Used with SPT/CPT rigs, the probe is advanced to a desired depth and tests both the vertical and horizontal permeability in two separate stages. Unlike the previous designs, the probe's inner rod is designed for rotational and axial movement. This allows the probe to use an internal expandable system of retractable "keys" that close the probe's exterior during hole advancement and prevent smearing throughout testing. The probe is designed with a closing/flushing drop-down stage that is used with a pressurized flushing technique to rid any debris that enters the probe during testing. A friction reducer with "wings" has been added to the 2012 VAHIP design. By adding the friction reducer, the probe is now restricted from unwanted underground rotation. Additionally, the friction reducer creates a void larger than the AWJ rods used to advance it down the hole. By creating this void, AWJ rods are now easier to maneuver as the skin friction between the rods and soil stratum are reduced. The probe is used with a falling head water vessel that sits atop a support stand providing a more user-friendly testing environment. A coordinate dial has also been developed to track the probe's underground movement at the surface of the hole.

D.2 VAHIP Design Properties

- Constructed using 304 stainless steel
- 21 inch closed length
- 24 inch open length
- 2 inch O.D.
- 2 ¼ inch O.D. friction reducer with ¼ inch wings extending outward
- ¾ inch diameter vertical tip opening
- 12 - 1 ½ inch x ¼ inch vertically oriented horizontal vents in 30 degree increments

- Approximately 16.5 lb. in weight

Figure D-1. Probe components

Figure D-2. Fully assembled probe with AWJ female connection attached

D.3 Description of Water Vessel and Support Stand

The water vessel is constructed from a 2 foot section of 6 inch O.D. schedule 40 clear PVC and capped with two 0.25 inch thick, 7 inch by 7 inch steel plates held in place by water a water-proof sealant and four threaded steel structural rods. The water vessel is designed to be rugged for the field and easily broken down for transport. The attached unit scale provides a simplistic method for tracking flow. A new flow port with a removable cap was added atop the water tank. This allows the user to fill and refill the tank quickly with a standard hose. A quick connect has also been placed atop the water vessel to provide an open atmosphere system capable of being pressurized.

The support stand was developed to provide a stationary testing environment where the falling head vessel would not move with the probe and AWJ rods during stage lifting. The legs of the support stand can be folded for transport. The support stand is also equipped with an aluminum support plate that provides a stabilized platform for the water vessel to sit upon. Flexible tubing is used to transport water from the water vessel to the probe. The flexible tubing is equipped with quick connects on both ends for convenient breakdown of system.

Figure D-3. Water vessel and support stand

Figure D-4. Top plate of water vessel with removable cap and quick connect

D.4 Recommended Procedure for Field Use of VAHIP

The following field permeability testing procedure is recommended when using the 2012 VAHIP.

D.4.1 Probe Assembly

The following procedure is provided to instruct new VAHIP users in proper assembly of the device. Images of assembly have been included to better illustrate the process. An Allen key will be needed to tighten set screws into the probe. The total process should take 3 – 5 minutes depending on the experience of the user.

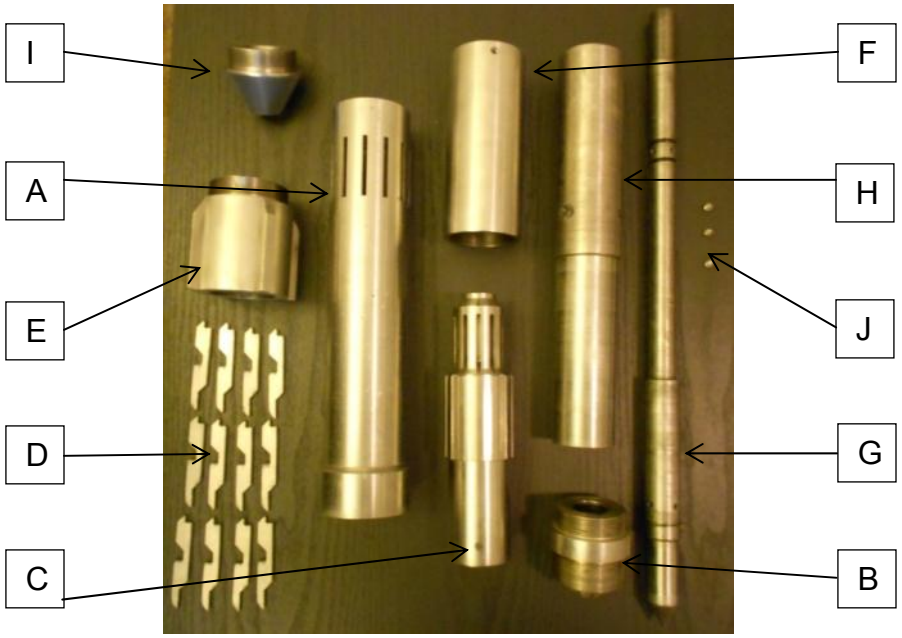

Key:
1. Upper chamber/outer shell (A)
2. Ramped connection (B)
3. Tracked male inner core (C)
4. 12 Keys (D)
5. Friction reducer with wings (E)
6. Tracked lower chamber (F)
7. Inner rod with knob (G)
8. AWJ connection (H)
9. Cone shaped tip (I)
10. 3 set screws (J)

Figure D-5. VAHIP components

D.4.2 Assembly Steps

1. Attach piece A to B by threading the ramped end of piece B into the smaller diameter end of piece A.

Figure D-6. VAHIP assembly step 1

2. Grip piece C with one hand and place the keys (the 12 pieces labeled D), into the designated slots. Remember to keep a good grip on piece C and the keys when proceeding to step 3.

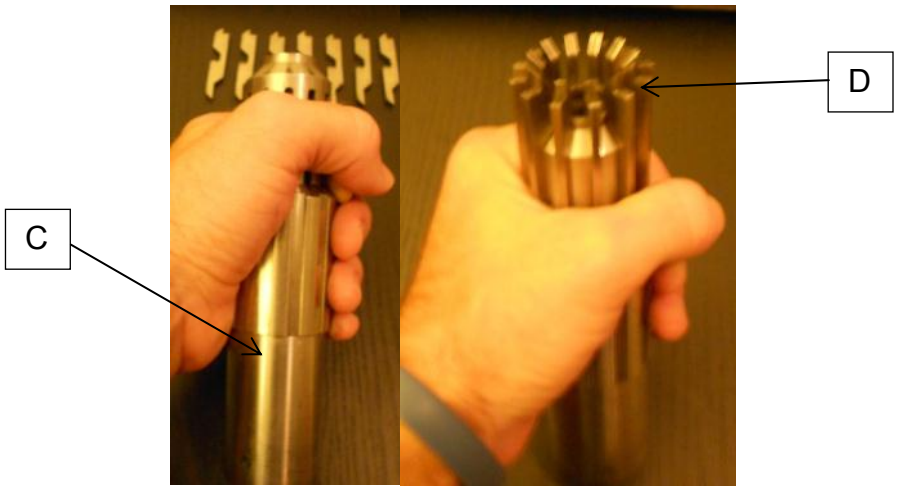

Figure D-7. VAHIP assembly step 2

3. Place piece C with the keys lodged in their designated positions into the larger diameter opening of piece A. Push piece C into piece A until the keys engage and can be seen in the openings of piece A.

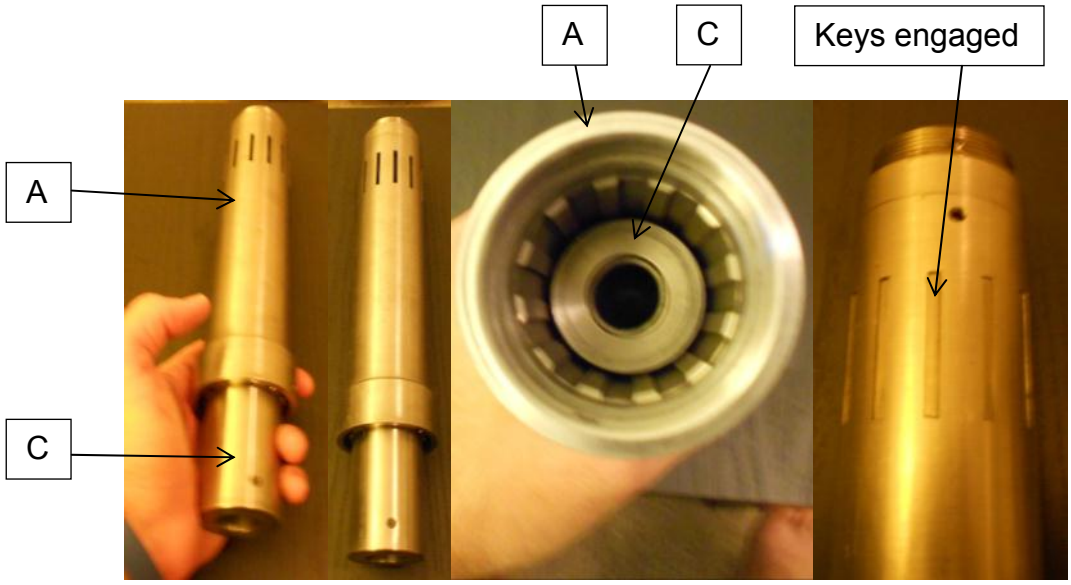

Figure D-8. VAHIP assembly step 3

4. Thread piece E into the larger diameter opening of piece A.

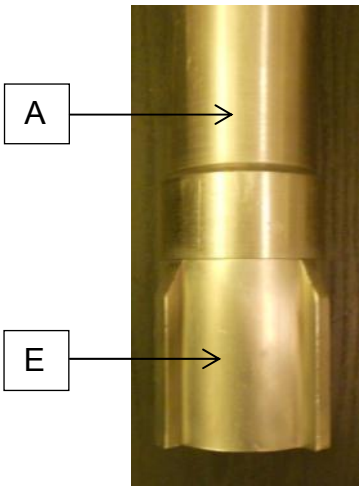

Figure D-9. VAHIP assembly step 4

5. Thread piece F onto piece B.

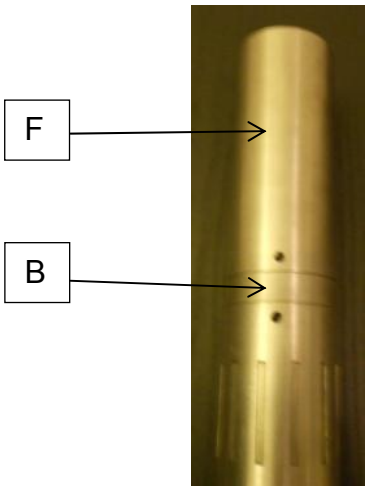

Figure D-10. VAHIP assembly step 5

6. Place the threaded end of piece G through pieces F, B and C contained within piece A. Make sure the knob of piece G is placed into the larger drop down-slot of piece F.

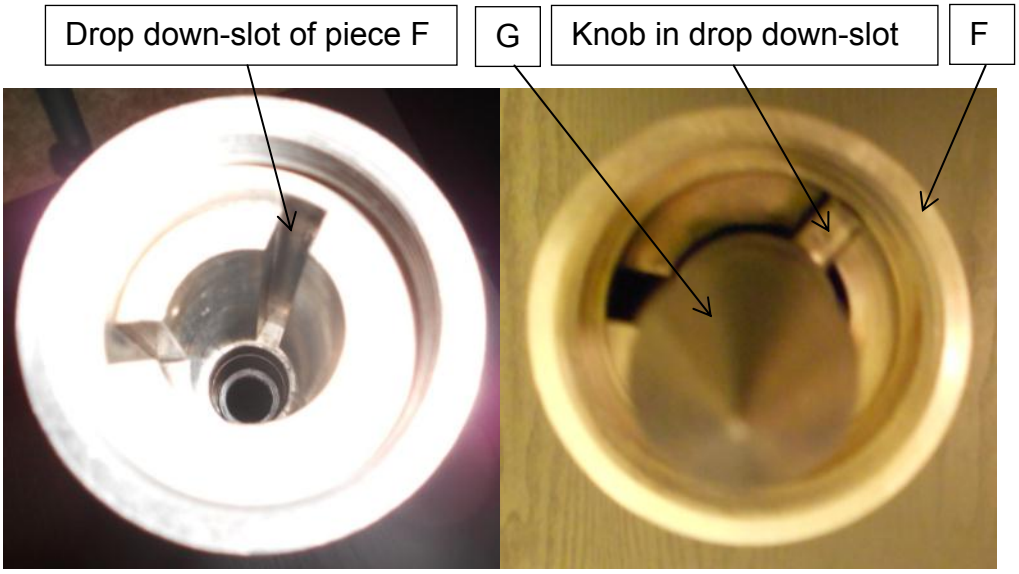

Figure D-11. VAHIP assembly step 6

7. Insert and push the smaller diameter end of piece H into piece E until piece E comes in contact with the threading of piece G. Once the two pieces are in contact, turn piece H in a clockwise direction. This threads piece E into piece H. Once threading is complete, push piece H until the knob of piece G is exposed in piece F. Rotate piece H slightly so the knob is no longer in the drop-down slot of piece F and proceed to step 8. Make sure not to over tighten the threading performed in step 7.

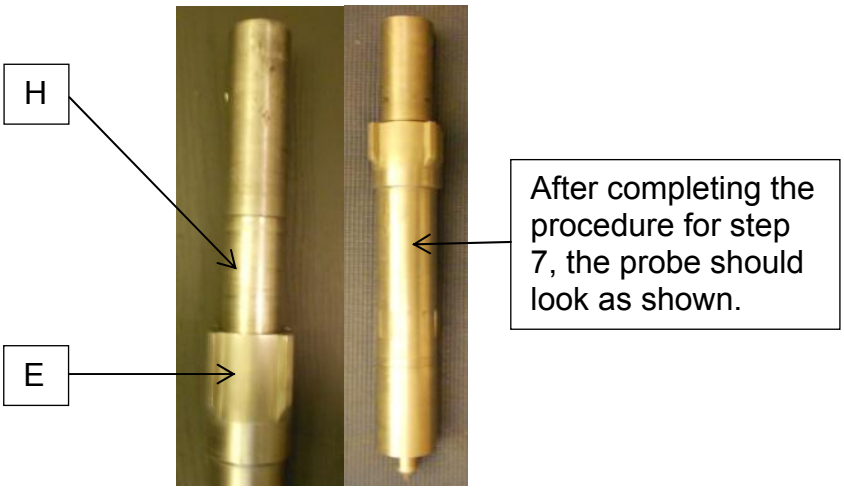

Figure D-12. VAHIP assembly step 7

8. Thread piece I into piece F.

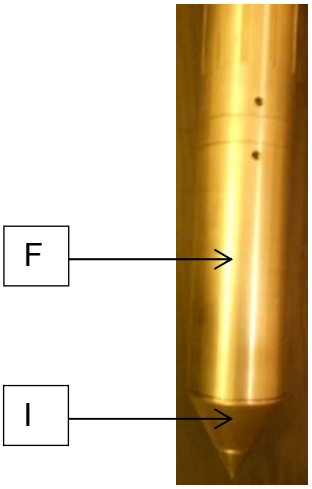

Figure D-13. VAHIP assembly step 8

9. Thread the three J pieces into the threaded openings of pieces A and F. The probe is now fully assembled.

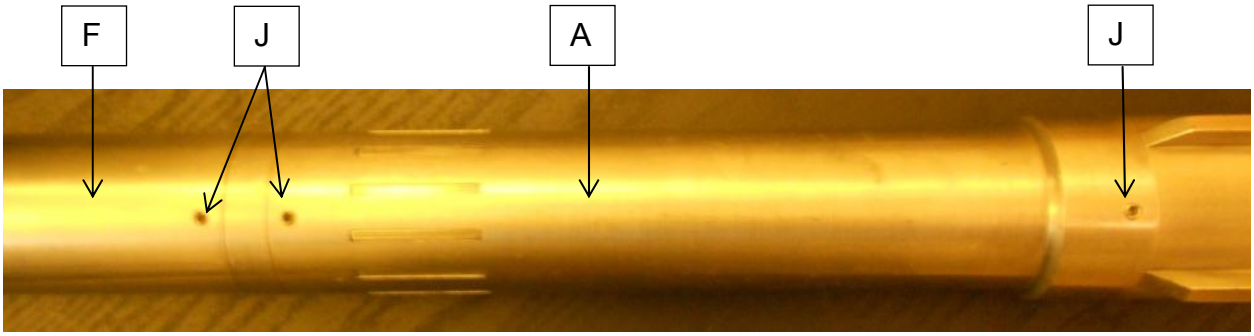

Figure D-14. VAHIP assembly step 9

10. Inspect the probe to ensure everything is installed and functioning correctly.

Figure D-15. VAHIP assembly step 10

D.4.3 Water Vessel and Support Stand Assembly

1. Place the support stand in the upright position with the legs locked in place.
2. Run the quick connect end of the flexible tubing through the support plate opening on the support stand.
3. Attach the quick connect end of the flexible wall tubing to the bottom plate quick connect of the water vessel.
4. Carefully place the water vessel onto the support plate of the support stand. Pull the excess flexible wall tubing through the opening of the support plate. Ensure that all four steel rod ends of the water vessel fit securely into the four respective holes of the support plate. The water vessel and support stand assembly is now complete.

D.4.4 Pre-field Preparation

1. The VAHIP must be cleaned and rid of any foreign material that would hinder water flow. Refrain from adding lubricants to the probe as they may cause unwanted debris to adhere to the inner components of the probe and cause malfunction.
2. Prepare all materials and tools listed in the equipment check list in Appendix A.

D.4.4.1 Field Test Procedure

1. Fully assemble the probe and ensure that it is in the closed stage discussed above.

2. Fully assemble the water vessel and support stand; and place in an area that will not hinder the SPT rig pushing the probe into the ground. Try to find a location with level ground.

3. Place an O-ring between the probe's AWJ female connection and the male end of the SPT rig's AWJ rod. Tighten the probe onto the AWJ rod ready for insertion on the SPT rig.

4. Advance the probe to the desired test depth using the SPT rig's push technique.

5. Disconnect the drive head of the SPT rig and slide the coordinate dial over the AWJ rod extending out of the ground. Ensure the dial is placed at ground-level, tighten the set screws and place the reference stake in its respective position.

6. Attach the water vessel's AWJ connection to the AWJ rod extending out of the ground placing an O-ring between the connections.

7. Remove the cap of the water vessel, attach SPT water hose and add water until the water vessel is filled and stabilizes.

8. Rotate the AWJ rod extending out of the ground approximately 60 degrees clockwise, lift 1.75 inches, and rotate an additional 60 degrees clockwise. Track the probe's rotation and lift using the coordinate dial.

9. When the probe is lifted 1.75 inches water is released in the vertical direction. The final 60 degree rotation locks the probe into the vertical position. This signifies that time and measurement recordings may now begin.

10. After vertical testing has been completed, quickly rotate the AWJ rods 60 degrees clockwise, lift 1.75 inches, and rotate an additional 60 degrees clockwise to lock the probe into the horizontal flow position. Track the probe's rotation and lift with the coordinate dial.

11. Attach the SPT rig water hose to the water vessel cap again, and refill the water vessel. There will be no restriction of flow as soon as the water vessel is filled completely, time and measurement recordings for horizontal testing can begin.

12. When horizontal testing is complete, refill the water vessel attach water vessel cap and pressure tank quick connect. Allow the water vessel to drain until it is approximately three-quarter full, and slowly bleed compressed air from the air tank into the system to flush.

13. While the system is flushing, rotate the AWJ rod 60 degrees clockwise, push downward 3.5 inches, and rotate a final 60 degrees clockwise. Track the probe's

rotation and lift with the coordinate dial. If the probe is unable to be closed, lift the AWJ rods upward 3.5 inches, and allow flushing to resume until the probe can be closed. More water may need to be added to the water vessel and the air tank may need to be refilled to increase the pressure.

14. After the probe has been flushed and rotated the final 60 degrees, lock it into the closed stage. It is ready to be pushed to the next test depth. The coordinate dial should now be back at the original position and needs to be removed before adding more AWJ rods and proceeding to deeper testing.

D.4.4.2 2012 VAHIP Falling Head Test Instructions

The previous probes incorporated both falling head and constant head testing. However, 2012 VAHIP testing methods have been simplified and only the falling head technique is used.

1. Use a stop watch, the unit scale attached to the water vessel and data sheet for recording the data.
2. Take an initial reading of the water level in the water vessel and start the stop watch at the same time.
3. Take a reading every 30 seconds recording it on the data sheet.
4. Repeat steps 2 and 3 as many times as needed. Use average readings in the data analysis and disregard any outlying values.
5. Enter recorded data into the respective test type, vertical or horizontal, computer analysis program to determine permeability.

D.5 Data Reduction

Data should be collected in the field using data sheets. The spreadsheet developed for the 2012 VAHIP should then be used to calculate permeability from testing. Probe and tank dimensions have been preloaded in to the spreadsheet. However, these dimensions can be quickly changed if future designs are different from the current model.

D.6 VAHIP Maintenance

- **Cleanup.** Disassemble the probe and wash with clean water and wire brush removing all soil particles from flow ports and connecting parts.

- **Routine Inspections.** The probe should be inspected after each cleanup for deformed and/or worn parts. Note deformities and replace parts as needed.

- **Storage.** The VAHIP and water vessel components should be stored in a cool dry place to prevent oxidation to steel components.